1990

Design Of Stabilizers For Static Var Compensators

Sumrit Hungsasutra

DESIGN OF STABILIZERS FOR STATIC VAR COMPENSATORS

by

HUNGSASUTRA, Sumrit

Department of Electrical Engineering

Submitted in partial fulfilment
of the requirements for the degree of
Doctor of Philosophy

Faculty of Graduate Studies
The University of Western Ontario
London, Ontario
April 1990

ISBN 0-315-55297-2

ABSTRACT

Steady-state stability of power systems has long been one of the major concerns for all electric utilities. Power system stabilizers (PSS) are frequently employed for adding system damping. However, in an interconnected power system, the most effective generator for deploying a PSS may lie outside the control of the utility or PSS may not be available on that generator. Static Var Compensator (SVC) is a new fast-acting reactive power control device. It has found many applications in power systems.

Although a SVC is primarily designed to regulate the voltage of the bus on which it is connected, it can also provide damping to the system if a proper stabilizing supplementary control is added to it. Application of SVCs for improving system stability is carried out in this thesis. The research has two major objectives ;

(i) development of a criterion for selecting the most effective location of a SVC, and

(ii) design of an optimal stabilizer for the selected SVC to provide maximum damping for the network.

Locally available signals and the application of supplementary control of SVCs are shown to be very effective in improving the system damping. At first, damping effectiveness is demonstrated on a single machine infinite bus (SMIB) system and later the usefulness of the developed techniques is applied on a complex power system of the Electricity Generating Authority of Thailand (EGAT).

ACKNOWLEDGEMENTS

The author would like to express his sincere gratitude to Dr. R.M. Mathur, his supervisor, for his valuable guidance, encouragement and endorsement. He also thanks the advisory and examining committees for their evaluations of the thesis. He has gained a lot of experiences in the area of power system during his association with Dr. M.V. Hariharan and Dr. Sachchidanand, visiting professors from IIT Bombay and IIT Kanpur, India respectively. As well, he appreciates all informative suggestions obtained from his discussions with Dr. J.F. Eggleston and fellow graduate students.

He is indebted to his advisor, the University of Western Ontario and the Department of Electrical Engineering for granting research and teaching assistantships, fee waivers and scholarships through out his study.

He also likes to thank the Electricity Generating Authority of Thailand (EGAT) for providing the needed system data for a more detailed test system. He acknowledges with gratitude the opportunity to use the Small Signal Stability (S^3) program developed by Mr. M.S. Moorty.

He would like to thank the University of Khon Kaen, Thailand for granting him leave of absence to undertake his Ph.D. work in Canada. Finally he thanks his beloved wife for her patience and understanding over the lengthy period of his study in Canada.

TABLE OF CONTENTS

Page

CERTIFICATE OF EXAMINATION ... ii

ABSTRACT ... iii

ACKNOWLEDGEMENTS ... iv

TABLE OF CONTENTS ... v

LIST OF TABLES ... ix

LIST OF FIGURES ... x

NOMENCLATURE ... xiv

CHAPTER I INTRODUCTION ... 1

1.1 General background ... 1
1.2 Practical problems in power systems ... 2
1.3 Traditional remedies ... 3
1.3.1 Solutions to the voltage problems ... 3
1.3.1.1 Switched Reactors/Capacitors ... 3
1.3.1.2 Load Tap Changers (LTC) on Transformer ... 4
1.3.1.3 Synchronous Condensers (SC) ... 4
1.3.1.4 Static Var Compensators (SVC) ... 4
1.3.2 Solutions for stability problem ... 5
1.3.2.1 Series compensation ... 6
1.3.2.2 New parallel lines ... 6
1.3.2.3 Power system stabilizers (PSS) ... 6
1.3.2.4 Static Var Compensators (SVC) ... 7
1.4 Research Objectives of the Thesis ... 7
1.5 Contribution of the thesis ... 8
1.6 Scope of the thesis ... 8

CHAPTER II STATIC VAR COMPENSATOR 10

2.1 General 10

2.2 Types of static var compensators 11
2.2.1 Thyristor Controlled Reactor (TCR) 11
2.2.2 Thyristor Switched Capacitor (TSC) 11
2.2.3 Thyristor Controlled Reactor and Fixed Capacitor (TCR+FC) 12
2.2.4 Thyristor Controlled Reactor and Thyristor Switched Capacitor (TCR+TSC) 12
2.2.5 Saturated Reactor 12
2.2.6 Thyristor Controlled Transformer (TCT) 13
2.2.7 Other types of compensator 13
2.3 Harmonics and losses 13
2.4 Operating characteristics 14
2.5 Applications of static var compensator 17
2.5.1 Industrial load compensation 18
2.5.2 Power system application 18
2.6 Power system studies 18
2.6.1 Early planning stage 19
2.6.2 Detailed planning stage 19
2.6.3 Design stage 20
2.6.4 Operating stage 20
2.7 Modelling of SVC for power system studies 21
2.7.1 Models for load flow studies 21
2.7.2 SVC models for steady-state studies 22
2.8 The choices of strategic locations 25

CHAPTER III THE CONTROL OF SVC 26

3.1 Control objectives 26
3.2 Types of controller 27
3.3 Power system representation 29
3.3.1 Power system representation for voltage control 29
3.3.2 Power system representation for a steady-state stability study 30
3.4 SVC models 31
3.4.1 Non-linear model 32
3.4.1.1 The TCR model 32
3.4.1.2 TSC model 34
3.4.1.3 The TCR+TSC model 35
3.4.2 Linearized model 36
3.4.2.1 Closed-loop transfer function 38
3.5 Main regulator 39
3.5.1 Proportional controller 39

3.5.2 Integral controller. 41
3.5.3 Proportional-Integral controller. 41
3.6 Effects of system dynamics. 42
3.7 Supplementary control. 43
3.7.1 The choices of damping signal .43
3.7.2 Damping control 44
3.7.2.1 Modal control 45
3.7.2.2 Frequency response technique 47

CHAPTER IV APPLICATION OF SVC IN A SMIB SYSTEM. 50

4.1 System configuration. 50
4.2 Small signal dynamic model. 52
4.2.1 Small signal equations 52
4.2.2 Small signal quantities 57
4.2.2.1 Electrical torque 57
4.2.2.2 Terminal voltage 58
4.2.2.3 Field voltage 58
4.2.2.4 Mid-point voltage 59
4.2.2.5 Small signal model-block diagram. 60
4.2.3 Damping signals for the SVC. .61
4.2.3.1 Line current 61
4.2.3.1 Line active-power. 62
4.2.3.1 Line reactive-power. 62
4.2.4 Summary of small signal quantities 63
4.3 Model parameters. 63
4.4 System dynamics 77
4.4.1 Optimal control parameters 78
4.4.1.1 Exciter control parameters 78
4.4.1.2 SVC control parameters 79
4.4.2 Step responses. 82
4.5 System damping improvement 83

CHAPTER V APPLICATION OF SVCs IN A COMPLEX SYSTEM 90

5.1 The EGAT system. 90
5.2 Objectives of the studies 93
5.3 System representation. 94
5.4 Load flow study 94
5.5 SVC control parameters. 96
5.6 Eigenvalue analysis. 98
5.6.1 System modelling 98
5.6.2 Eigenvalue analysis. 99

5.6.3 System eigenvalues 100
5.6.4 Large disturbance study 104
5.7 Steady-state stability improvement
using the existing SVCs 108
5.7.1 Tentatively improved oscillation modes 109
5.7.2 Design of damping control. 109
5.7.3 Design steps 112
5.7.4 Illustration of the design. 112
5.8 Further system dynamic improvement. 119
5.8.1 Suitable SVC location. 119
5.8.2 SVC rating 122
5.8.3 Damping improvement through KK SVC 125

CHAPTER VI CONCLUSIONS. 133

6.1 Summary 133
6.2 Discussions 136
6.3 Conclusions. 138

APPENDICES

APPENDIX A Optimal proportional controller 140
APPENDIX B Optimal integral controller 141
APPENDIX C Optimal PI controller 142
APPENDIX D Bus and line data of the EGAT system. 143
APPENDIX E Machine parameters. 146

REFERENCES 146

VITA. 154

LIST OF TABLES

Table	Description	Page
4.1	Calculated gain K_c and T_2 of the supplementary control at the SVC of the SMIB system	84
5.1	Load flow results	95
5.2	SVC's bus quantities (p.u.)	97
5.3	System eigenvalues	101
5.4	System eigenvalues and participations of all machines	103
5.5	System eigenvalues and eigenvectors of all inertial modes	105
5.6	System gain and phase at TTK bus	111
5.7	Phase compensation requirements	113
5.8	Calculated poles and zeroes	113
5.9	Calculated values of TTK compensating network	115
5.10	System eigenvalues and participations of all machines with damping control at TTK SVC	117
5.11	Short-circuit levels at various buses in Region 2	120
5.12	Voltage participations at various buses in Region 2	121
5.13	System eigenvalues and participations of all machines with damping control at TTK SVC and additional SVC at KK	124
5.14	Frequency response data of line KK-UD1	128
5.15	System eigenvalues and participations of all machines with damping control at TTK and KK SVCs KK	131
6.1	System damping improvement of the EGAT system	135

LIST OF FIGURES

Figure	Description	Page
2.1	Typical voltage-current characteristics of a TCR+FC type compensator	15
2.2	Typical voltage-current characteristics of a TCR+TSC type compensator	17
2.3	SVC models for load flow studies	23
2.4	Illustration of the basic SVC model under overloading conditions	23
2.5	Basic SVC model for steady-state and transient stability studies	24
3.1	Power system representation for a SVC operating in voltage control	29
3.2	Variation of $f(\alpha)_{TCR}$	33
3.3	TCR model interfaced to the system as a voltage behind a reactance	34
3.4	Thévenin equivalence of power system with a SVC as voltage control	36
3.5	Non-linear control block diagram of the SVC	37
3.6	Linearized model of the SVC	38
3.7	Proportional controller with lead/lag compensation	39
3.8	Integral controller for SVC	41
3.9	Proportional-Integral controller for SVC	42
3.10	Conceptual control system	48
3.11	Conceptual unity feedback system	48

4.1 Single machine infinite bus system with SVC compensated line 51

4.2 Small signal dynamic model of a SMIB system with a SVC 60

4.3(a) Constant K_1 65

4.3(b) Constant K_2 65

4.3(c) Constant K_3 66

4.3(d) Constant K_4 66

4.3(e) Constant K_5 67

4.3(f) Constant K_6 67

4.3(g) Constant K_7 68

4.3(h) Constant K_8 68

4.3(i) Constant K_9 69

4.3(j) Constant K_{10}. 69

4.3(k) Constant K_{11}. 70

4.3(l) Constant K_{12}. 70

4.3(m) Constant K_{13}. 71

4.3(n) Constant K_{14}. 71

4.3(o) Constant K_{15}. 72

4.3(p) Constant K_{16}. 72

4.3(q) Constant K_{17}. 73

4.3(r) Constant K_{18}. 73

4.3(s) Constant K_{19}. 74

4.3(t) Constant K_{20}. 74

4.3(u) Constant K_{21}. 75

4.3(v) Constant K_{22} 75

4.3(w) Constant K_{23} 76

4.3(x) Constant K_{24} 76

4.4 Dynamic models of the exciter and the SVC 77

4.5(a) Optimal value K_F of the exciter 79

4.5(b) Optimal value T_F of the exciter 80

4.6(a) Optimal value of T_i for the SVC 81

4.6(b) Optimal value K_p for the SVC 81

4.7(a) Rotor angle response to a 5% step change in the mechanical power of the SMIB system with SVC 82

4.7(b) Voltage responses to a 5% step change in the mechanical power of the SMIB system with SVC 82

4.8 Inertial mode damping improvement of the SMIB system through the supplementary control of the SVC. 84

4.9(a) Generator's power responses to a 5% increase in the mechanical power of the SMIB system with damping control at the SVC. 86

4.9(b) Mid-point voltage responses to a 5% increase in the mechanical power of the SMIB system with damping control at the SVC. 86

4.10(a) Rotor angle response of the SMIB system to a temporyry increase in local load (0.2 pu resistance) for P=0.7 pu 87

4.10(b) Mid-point voltage response of the SMIB system to a temporyry increase in local load (0.2 pu resistance) for P= 0.7 p. u 87

4.10(c) Response of Q_{svc} of the SMIB system to a temporyry increase in local load (0.2 pu resistance)for P=0.7 pu 88

5.1 Simplified EGAT system 91

5.2(a) Rotor angle responses of the simplified EGAT system to a temporary increase in local load (0.1 pu resistance) at LS without damping control 104

5.2(b) Voltage responses of the simplified EGAT system to a temporary increase in local load (0.1 pu resistance) at LS without damping control 105

5.3(a) Magnitude response of line currents taken at TTK bus of the EGAT system without damping control 108

5.3(b) Phase response of line currents taken at TTK bus of the EGAT system without damping control 108

5.4 Poles and zeroes location 112

5.5(a) Rotor angle responses of the simplified EGAT system to a temporary increase in local load (0.1 pu resistance) at LS with damping controlat TTK SVC 116

5.5(b) Voltage responses of the simplified EGAT system to a temporary increase in local load (0.1 pu resistance) at LS with damping control at TTK SVC 117

5.6(a) Rotor angle responses of the simplified EGAT system to a temporary increase in local load (0.1 pu resistance) at LS with damping control at TTK and an additional SVC at KK . . 123

5.6(b) Voltage responses of the simplified EGAT system to a temporary increase in local load (0.1 pu resistance) at LS with damping control at TTK and an additional SVC at KK . . 124

5.7(a) Magnitude response of line currents taken at KK bus of the EGAT system 125

5.7(b) Phase response of line currents taken at KK bus of the EGAT system 125

5.8(a) Rotor angle responses of the simplified EGAT system to a temporary increase in local load (0.1 pu resistance) at LS with damping control at TTK and KK SVCs 127

5.8(b) Voltage responses of the simplified EGAT system to a temporary increase in local load (0.1 pu resistance) at LS with damping control at TTK and KK SVCs 128

NOMENCLATURE
(Principal symbols)

x_d	direct axis synchronous reactance
x_d'	direct axis transient reactance
x_q	quadrature axis synchronous reactance
T_{do}'	direct axis open circuit field time constant
M,H	Inertia constant
e_q'	voltage behind transient reactance
δ	torque angle
Δ	small changes
s	time unit, Laplace operator
i,v	instantenous current, voltage
i_d,i_q,v_d,v_q	d-q components of current, voltage (time domain)
I,V	scalar quantities of current, voltage
$\mathbf{I},\mathbf{V}$	current, voltage phasors
A,B,C,D,E..	matrices
T	time constant
T_y	thyristor time constant
T_m	measuring time constant
K_i	current droop
Φ_c	compensated phase
P_c	compensated pole
Z_c	compensated zero
α	pole-zero separation
P_s	system pole
λ	eigenvalue

NOMENCLATUE (CONTINUED)

ω_n eigenfrequency

SVC static var compensator

TCR thyristor controlled reactor

TSC thyristor switched capacitor

FC fixed capacitor

SMIB single machine infinite bus

SR saturated reactor

SC synchronous condenser

TCT thyristor controlled transformer

LCT load tap changer transformer

PSS power system stabilizer

Note : Other symbols are defined in the text before used.

CHAPTER I

INTRODUCTION

1.1 General background

Electricity has become the most convenient and vital source of energy for industrial and residential consumers. Power system utilities are coping with the increasing demands by adding new transmission lines and installing new generating power plants. Unfortunately, as the energy production continues to grow new natural energy resources are often found remote from the load centre. Also large nuclear power plants have to be sited far away from the populated residential areas due to their environmental risk. Therefore longer transmission lines are built to transport electrical energy to the customers.

In electrical systems, generators and important load buses are invariably interconnected through multiple paths forming complex electrical networks. Furthermore the networks of one utility are connected to other neighbouring utilities to permit economic exchange of power and to add to the system security. Interconnected systems reduce the spinning reserves required for peak loads in each of the connected utilities. Operation of an interconnected system occasionally presents stability problems. Stability of a system depends on a multitude of factors. Weaker ac systems, having long transmission lines, experience greater stability problems and therefore require special provision to operate stably. This thesis examines the steady-state stability problems of a power system and explores the effectiveness of using Static Var Compensator (SVC) to add to the system damping. It is not intended to show that the SVCs are the best or the only tools. Instead, the objective is to develop procedures for the design of supplementary controls if SVCs, new or existing, should be used.

1.2 Practical problems in power systems

Many problems are encountered in the satisfactory operation of a power system. To satisfy the customer expectations, the quality as well as the security of electrical power has to be very high. Electrical utilities, in addition to satisfying the customer expectations, must operate a system in the most economical manner. Therefore, the electrical utilities attempt to fully load generating sites which produce the least expensive power first and thereafter add on relatively more expensive generation to the power pool. This practice results in loading economical generators close to their stability limits. Load variations and system disturbances present a stability risk for the units which may be operating close to their stability limits. Hence the control of electric power system plays a vital role on the stability of the system.

Power systems are frequently subjected to unexpected disturbances. At times, the severity and the location of a disturbance in combination with certain system configurations may lead to collapse of the system if protective actions are not successful in withholding the system. And in some cases even when the system recovery is achieved the system voltages at some points in the system may turn out to be too low, too high or oscillatory for a long period of time. Some form of reactive power compensation is needed for correcting such voltage deviations. The stability of the system may be lost if some generators suffer from uncontrollable power or voltage oscillations.

Subsequent to major disturbances, system restoration is critical. Due to the loss of synchronism of the severely affected generators a system breakup may take place. This situation is known as "islanding". If the key generators in a system are tripped out and corrective measures are not taken in time, voltage collapse or system black out may ensue. Therefore stability of the system and voltage control are the prominent concerns for the power system utilities. Static Reactive Power Compensators of one form or another are increasingly being employed on systems to address the voltage regulation and increasing the transmission capacity of the existing lines.

1.3 Traditional remedies

1.3.1 Solutions to the voltage problems

Voltage problems are commonly alleviated by many techniques as described in this Section.

1.3.1.1 Switched Reactors/Capacitors

Switched inductors or capacitors are located at buses which otherwise experience wide voltage variations. Based on the known loading characteristics, the appropriate time and duration for which the inductors or capacitors should be switched in or out can be determined. However, there are limitations on the performance improvement as the control is discrete and the action is very slow. Also high maintenance is required as the contacts of the mechanical switches tend to wear out with increased number of operations.

1.3.1.2 Load Tap Changers (LTC) on Transformer

Load tap changers on connecting transformers are used to control the voltage at selected buses in the system. The limitation of LTC is similar to that of switched reactors/capacitors although the control step may be much smaller.

1.3.1.3 Synchronous Condensers (SC)

Synchronous Condensers (synchronous machine with no active power exchange) are employed at some strategic buses to continuously control the bus voltage through reactive power absorbtion or generation by the machine. It is accomplished by the excitation of the SC. The disadvantage of a SC is that it is expensive to install and maintain.

1.3.1.4 Static Var Compensators (SVC)

SVC is a modern voltage controlled device and has been used in many utilities for years. The main advantage of a SVC over other types of voltage controlled devices is that it can be continuously controlled and it exhibits a fast response. However, the operating characteristic and control of a SVC are totally different from a SC. Thus a special attention must be paid for the control of a SVC.

1.3.2 Solutions for stability problem

Power system engineers identify two types of stable behavior of a power system and its stability limits as [53]

Steady-state stability :

A power system is steady-state stable for a particular steady-state operating condition if, following any small disturbance, it reaches a steady-state operating condition which is identical or close to the pre-disturbance operating condition. This is also known as small disturbance stability of a power system.

Transient stability :

A power system is transiently stable for a particular steady-state operating condition and for a particular disturbance if, following that disturbance, it reaches an acceptable steady-state operating condition.

Steady-state stability limit :

The steady-state stability limit is a steady-state operating condition for which the power system is steady-state stable but for which an arbitrarily small change in any of the operating quantities in an unfavorable direction causes the power system to lose stability. This is also known as the small disturbance stability limit.

Transient stability limit:

The transient stability limit for a particular disturbance is the steady-state operating condition for which the power system is transiently stable but for which an arbitrarily small change in any of the operating quantities in an unfavorable direction causes the power system to lose stability for that disturbance.

Many practical measures are taken to improve the steady-state and transient stabilities of the system.

1.3.2.1 Series compensation

In systems which have long transmission lines, series compensation of the long lines may be employed. Series compensation increases the power transfer capability of the line. Consequently, the steady-state and transient stability limits of the system are significantly increased. However series compensation also increases the fault level and the risk of subsynchronous resonance if the degree of compensation is high [49,50] and the system employs turbo generators.

1.3.2.2 New parallel lines

Addition of new parallel lines increases the amount of power that can be transferred. These additions increase the steady-state instability limit and improve the transient stability as well as enhance the system reliability. However new lines require a large investment. New parallel lines are added only when they become necessary.

1.3.2.3 Power system stabilizers (PSS)

PSSs are employed at some key generators to damp the inertial modes of oscillations associated with a system. Tuning of the PSS parameters, in a complex system, is always difficult. In an interconnected system, the most effective generator on which a PSS should be utilized may lie outside the jurisdiction of the utility.

1.3.2.4 Static Var Compensators (SVC)

For a radial system having long transmission lines, placement of SVCs at some intermediate buses on a line not only improves the voltage profile of the line but it also increases the power transfer capability, steady-state instability limit and transient stability [3-6,10]. Addition of SVCs on a line may reduce the urgency to add a new parallel line. In addition to the increase of the steady-state stability limit, the application of SVCs can also improve the transient stability of the system if stabilizers are employed in the SVC controls.

1.4 Research Objectives of the Thesis

Selection of optimal locations for the application of SVCs and design of their controls for improving the system stability is the goal of this research. To achieve this goal, procedures for selecting suitable locations, and for determining the size of the SVCs must be developed. As well, procedure for the design of controls for the SVCs must be developed. Finally the validity of these procedures must be demonstrated by tests (simulations) on sample systems. The tests should clearly show the improvements of voltage profiles and addition of damping for selected modes. The stabilizers designed for steady-state stability enhancement should also be useful for damping systems which have suffered a major disturbance.

1.5 Contributions of the thesis

The research work described in this thesis adds to the basic understanding of the damping capabilities of SVCs. It presents a new system model for a simple system and choices for damping signals. The thesis introd :es design procedures for the main and auxiliary controls of SVCs for both voltage control and damping control. The thesis also presents procedures to determine the optimal location and size of SVCs with a view to selectively damp inertial modes of oscillations present in a complex system.

1.6 Scope of the thesis

For completeness fundamental types, characteristics, applications and modelling techniques of SVCs are very briefly described in Chapter 2. In Chapter 3 control philosophy is developed. At first control models of TCR, TSC and TCR+TSC are developed. Then a linearized model is chosen and parameters of optimal controllers are determined. This chapter also develops techniques for the design of supplementary controls of the SVCs for enhancing system performance. The pertinent classical and modern control theories and eigenvalue analysis are also included.

A procedure for the design of the SVC controls when employed in a single machine infinite bus (SMIB) system, for increasing the power transfer capability of the line, voltage control and damping enhancement is embodied in Chapter 4. A new dynamic model of the SMIB system is developed and used to determined the optimal controller parameters of the main and supplementary controls. Numerical results from eigenvalue analysis and time domain simulations are also included.

Having gained the confidence in the design of the controls of a SVC in a simple system, the technique is tested in a multi-machine system of EGAT.

In Chapter 5 eigenvalue analysis is used to identify lightly damped modes. Pole placement technique is used to design the supplementary controls for an existing SVC in the system. Selective damping of some modes is sought. The effectiveness of the SVC stabilizer is shown by changes in the eigenvalues. Also the system is subjected to a fault and the effectiveness of adding a stabilizer on an existing SVC is demonstrated. In the latter part of the Chapter the question of adding a new SVC is addressed. A suitable location is selected by taking into account several considerations. Voltage Participation Factors [52] in influencing selected eigenvalues is shown to be a useful quantity to determine an effective location from the view point of damping enhancement by a SVC. The effectiveness of adding a new SVC (± 50 Mvar) is shown on the test EGAT system.

Chapter 6 presents a summary, discussions and conclusions of the research contained in this thesis.

CHAPTER II

STATIC VAR COMPENSATOR

2.1 General

The use of mechanically switched inductors/capacitors for controlling the voltage profile in a transmission system has long been practiced by the power system utilities. System planners have to determine the size and location of these switched elements and system operators have to determine the frequency of switching and appropriate voltage levels at which switching must occur.

Reactive power compensators employing switched elements are quite suitable for slow daily load changes. However subsequent to major disturbances, the voltage variation is normally large and rapid. Under such conditions, switched devices must be replaced by fast reactive power compensators. In the recent past, high powered thyristors have been successfully developed and extensively employed in hvdc transmission systems. Gradually, these thyristors have also been utilized as fast controlled switches for controlling current in inductors and switching capacitors. These controlled elements in combination with fixed elements or the two together are known as Static Var Compensators (SVC). By employing feedback control techniques, a continuous control of reactive power to regulate the voltage at the connected bus (or elsewhere) is achieved. Indeed the control of the thyristor switches can be exercised within a cycle. Basic types, operating characteristics and applications of SVCs in power systems are briefly reviewed in the following Sections.

2.2 Types of static var compensators

Several types of SVC configurations are commercially available. They differ from one another depending upon the combination of switched, controlled or fixed inductors/capacitors.

2.2.1 Thyristor Controlled Reactor (TCR)

A thyristor controlled reactor (TCR) consists of a linear reactor connected in series with an anti-parallel combination of thyristors. By controlling the onset of conduction the effective current through the inductor is controlled. Consequently, the reactive power absorption can be varied from zero to its full absorption limit in a continuous fashion. TCR acts as a nonlinear load and therefore in addition to a fundamental frequency current component generates odd harmonic frequencies of currents.

2.2.2 Thyristor Switched Capacitor (TSC)

Capacitor banks are switched in or out by series connected anti-parallel thyristors. The switching speed is very fast, however, the reactive power is discretely controlled and a special firing control technique is required to minimize switching transients. TSC does not generate current harmonics.

2.2.3 Thyristor Controlled Reactor and Fixed Capacitor (TCR+FC)

A fixed capacitor bank is added in parallel with a TCR. If the Mvar rating of the inductor is chosen to be greater than that of the capacitor, the net reactive power can be adjusted smoothly from generation to absorption. This combination results in power losses in the elements even when no net reactive power is exchanged by the TCR with the network.

2.2.4 Thyristor Controlled Reactor and Thyristor Switched Capacitor (TCR+TSC)

The combination of TCR and TSC reduces the reactor ratings and therefore harmonics for the same operating range as a TCR+FC. Also the net power losses for low settings of reactive power are minimized [4,12,13]. The reactive power can be smoothly controlled from full absorption to full generation limits. In this configuration, many thyristors and co-ordinated controls are required. However, TCR+TSC offers better technical performance.

2.2.5 Saturated Reactor (SR)

Saturated reactor has only an inherent control ability. As the voltage across the reactor exceeds a design limit, it leads to the saturation of the reactor's magnetic core. Thereby reducing its effective reactance. Under saturated state the SR acts as a lower value linear reactor and absorbs higher reactive power. This action controls the voltage of the connected bus. SR may be combined with a FC to cover the entire range of var generation to absorption.

2.2.6 Thyristor Controlled Transformer (TCT)

This configuration employs a very high leakage reactance transformer. Anti-parallel thyristor valves are used to exercise controlled short circuiting of the secondary winding of the reactance transformer. Thus, the inductive reactance of the transformer as seen from the system is controlled. Additional fixed capacitor banks facilitate the compensator to span the entire range of reactive power exchange.

2.2.7 Other types of compensators

For economic reasons, mechanical switches may still be used in conjunction with all of the above types of compensators. For example the resulting combination of mechanically switched reactor (MSR) with TCR provides a reduction in size, cost and harmonics generated by the compensator [4,10]. As well, mechanically switched capacitors (MSC) cut down the number of thyristors required, loss and the compensator cost. The operating speed of these combinations does not suffer appreciably as the fast control action may still be accomplished by thyristors.

2.3 Harmonics and losses

Thyristor controlled reactor generates harmonic currents. The magnitude and frequency of the harmonic currents depend on TCR's rating, conduction angle of the thyristors and the configuration of multiphase TCR's. Harmonic generation is considered to be an important problem for the system. Harmonic current injection in the system can lead to an uncontrollable voltage oscillation at another point in the system due to the system resonance at a harmonic frequency. Therefore, the best remedy to this problem is to eliminate or minimize the harmonic injection in the system. Therefore all types of SVCs utilizing TCRs are equipped with tuned harmonic filters. Practically the three elements of TCRs for a 3-phase system are connected in delta and operated in 6 or 12 pulse mode to eliminate triplen harmonic and generating only $np\pm1$ harmonic orders (p=pulse no., n=integer).

All types of compensators have associated losses. They include losses due to the quality factors of the inductors/capacitors, transformers, the auxiliary circuits and the thyristors. The TCR+FC type compensator possesses high losses in the absorption range while the TCR+TSC type has high losses in the production range [4,12].

2.4 Operating characteristics

Regardless of the compensator type, the operating characteristic is generally similar for all SVCs except TSC. TCR, SR, and TCT types of SVC are confined to operate in the var absorption range. A combination of the controlled inductors with FC or TSC results in a SVC which operates in the full range of var absorption to generation. The typical voltage-current characteristics of a TCR+FC type compensator is shown in Fig. 2.1 .

At the point of connection, a power system can be represented by its Thévenin equivalent circuit, the parameters of which (E_s and X_s) depend on the line loading and the system strength from the point of observation. Without any compensation, the voltage at the connecting bus will vary between points 1 and 2 (in Fig. 2.1) when the system loading is changed from light load to heavy load respectively. With the application of the compensator, under the same conditions, the voltage can be regulated between points 3 and 4 .

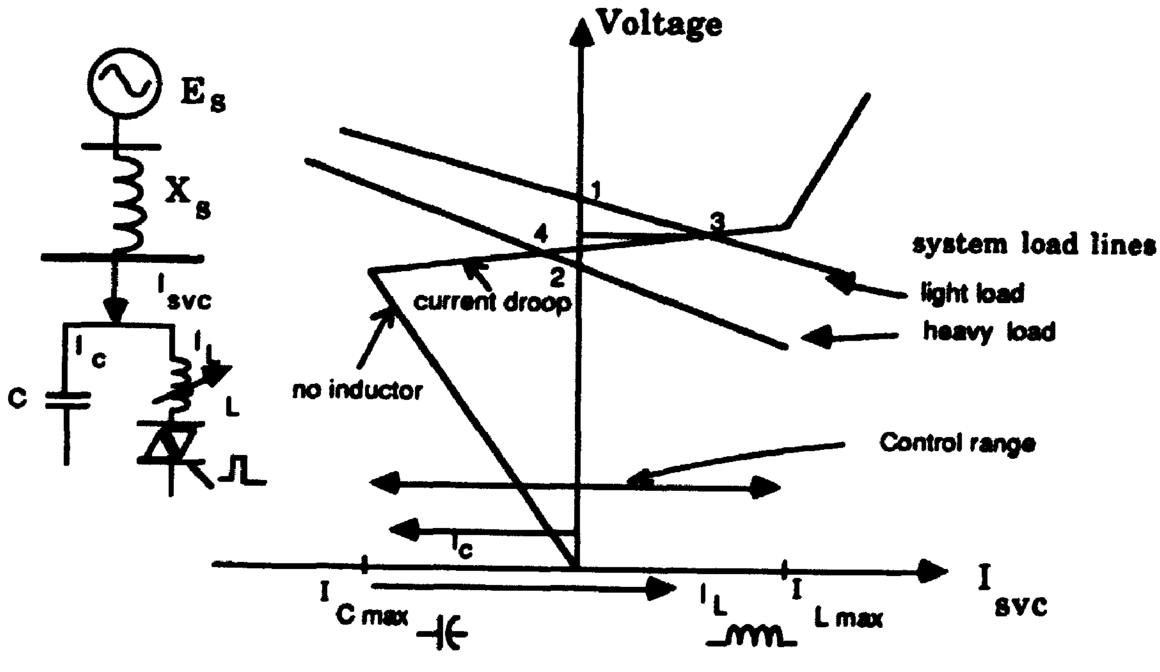

Fig. 2.1 : Typical voltage-current characteristics of a TCR+FC type compensator.

The controlled voltage is achieved through the control of the compensator which causes a change in the susceptance of the SVC. At point 3, the net current of the compensator is inductive, thus reactive power is absorbed as the connected bus voltage tends to be above the nominal (ref) voltage. On the other hand, the net current of the SVC operating at point 4 is capacitive, by the capacitor, as the connected bus voltage drops below the nominal value. The voltage variation due to loading variation can be limited by reducing the slope of the V-I characteristics (current droop).

Generally, it is unnecessary to restrict the voltage variation within very tight limits. In practice the voltage is allowed to vary within acceptable limits. The advantage of providing the current droop characteristics is that the rating of the required compensator is reduced and if other var sources exist at the same bus, better var sharing is accomplished.

As the rating of the TCR has to overcome the capacitor rating, reactive power generated by the capacitor is partially consumed by the reactor. Only the difference between reactive power generated by the capacitor and absorbed by the reactor is effective for controlling the voltage. Thus the TCR+FC type is not economically efficient. In the TCR+TSC scheme, the capacitor bank is split into many small capacitor banks controlled either by thyristors or a combination with mechanical switches. The required rating of the TCR can then be chosen to be slightly greater than that of one small capacitor bank.

The control range is continuously maintained by switching the capacitor banks in or out just before the control of the TCR reaches its limits. The operating characteristic of the TCR+TSC type compensator is illustrated in Fig. 2.2 . The operation of other types of compensators is similar in concept and is therefore not discussed.

2.5 Applications of static var compensator

The application of static var compensators falls into two areas namely, industrial load compensation and power system application. The purposes of employing SVCs in these areas depends on the problems encountered in the system.

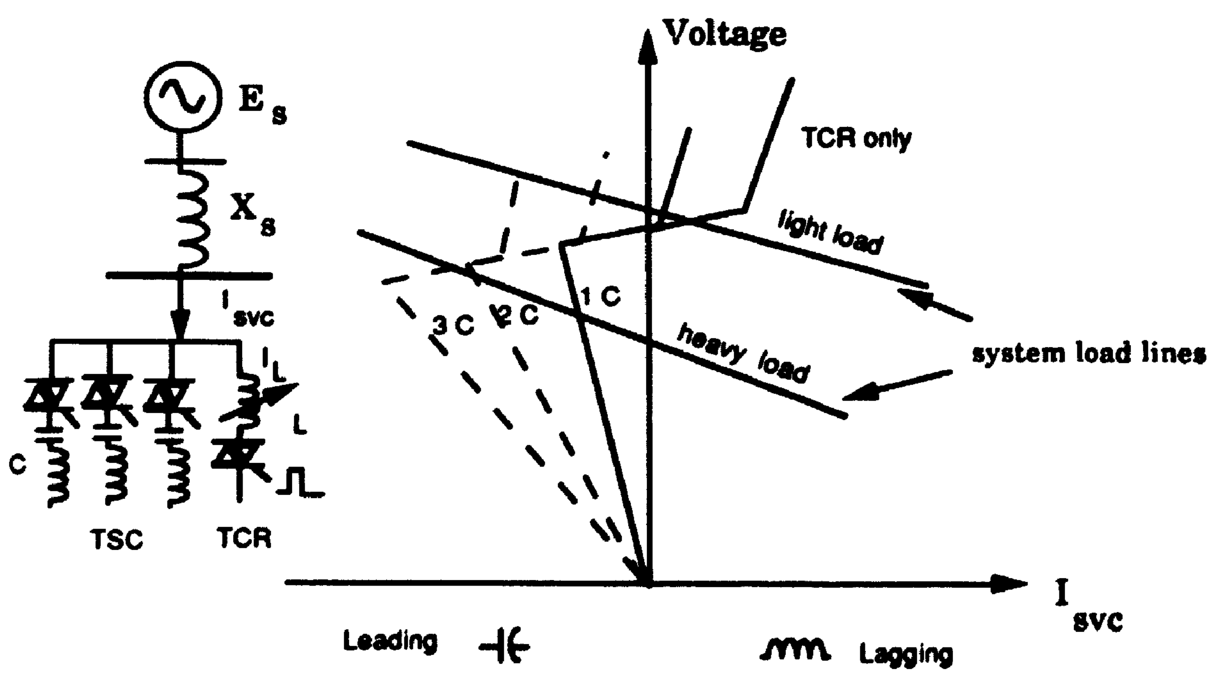

Fig. 2.2 : Typical voltage-current characteristics of a TCR+TSC type compensator.

2.5.1 Industrial load compensation

For industrial applications SVCs can be used for balancing asymmetrical loads, regulating the voltage within the desired limits or for improving power factor of the loads. Static var compensators are very effective in controlling fast voltage fluctuation caused by rapid changing loads such as arc furnaces [12,13].

2.5.2 Power system application

Transmission of electric power from remote generators to load centres exhibits many limitations. The maximum power transfer capability of a line is limited below the thermal limit, as well the voltage profile of a line may vary beyond accepted tolerances as a result of line loads. The system must be stable or recover satisfactorily following small or severe disturbances. Application of SVCs are recommended to address the above limitations. Lately they have also been employed to enhance the dynamic performance of the system through appropriate controls. This thesis undertakes a systematic study of the design aspects of the contribution of SVCs for steady-state stability enhancement.

2.6 Power system studies

Power system studies are needed when static var compensators are to be employed to improve the performance of the system. The purpose of various studies are ;

a) to identify the problem to be solved by the SVCs,

b) to determine the rating and operating characteristics of the SVCs,

c) to establish economic and technical requirements and

d) to evaluate the use and benefits of SVCs in comparison with other alternatives.

The type of power system study to be used depends specifically on the desired objectives and the stages of the system development such as early planning, detailed planning, design, operation etc. Power system studies in these stages are briefly described in the subsequent subsections.

2.6.1 Early planning stage

In this stage, reactive power requirements and the appropriate locations are determined based on a wide range of system loading, generations and network configuration. Iterative studies are necessary as the configuration and the development strategy of the power system can be affected by the application of the SVCs. The approximate ratings as well as the first selection of locations of the SVCs can be obtained from load flow studies. Over and under voltage buses are prime locations. Transient stability studies are necessary follow up to generate additional information on SVCs' ratings for maintaining satisfactory system stability under different system contingencies.

2.6.2 Detailed planning stage

Power system performance is evaluated in detail to achieve the necessary SVCs' performance specifications. Considerations are based on system demand variations, fault levels, contingencies, voltage criteria, loss evaluation and stability criteria. The results of the studies lead to the finalization of

a) steady-state operating characteristics,
b) appropriate operating techniques to meet system requirements under abnormal conditions,
c) continuous and short term over load capabilities,
d) control and protection requirements,
e) step-down transformer and tap-changer requirements and
f) harmonic performance requirements.

2.6.3 Design stage

The selection of an appropriate SVC to meet the performance specifications can be placed with the manufacturer in this stage. In some cases, utilities may prefer to select SVC type based on their previous experience or in close co-operation with a manufacturer to ensure that the final design fully meets the performance specifications.

2.6.4 Operating stage

The operating regimes at different system contingencies and constraints must be verified. Various tools available for power system studies related to SVC's applications are time domain and frequency domain simulation programs. Physical model simulator is also a very useful tool for the design of SVC's control. In frequency domain, eigenvalue analysis and frequency response techniques are very useful for evaluating system stability and designing the control of the SVCs. Time domain simulations and, if possible, field tests are performed to verify the performance of the system under small and large disturbances.

2.7 Modelling of SVC for power system studies

The appropriate model of a SVC depends on the objective of the power system study. The model must satisfy basic characteristics of SVC, it should be simple in concept and it should be possible to integrate it in the available tools without significant difficulty. The models used in power system studies such as load flow and steady-state stability are reviewed in the following subsections.

2.7.1 Models for load flow studies

The SVC models for load flow studies represent the steady-state fundamental frequency characteristics of a SVC under balanced conditions. The voltage-current characteristics of the SVC including its limits can be considered as a voltage-controlled reactive power source in the linear operating region. Outside the control range, it can be represented by a fixed capacitor or a fixed inductor depending on the deviation of the voltage at the SVC bus beyond the control range about the reference voltage. Typical representation of the SVC in load flow studies is to treat it as a reactive power source with limits.

If the slope of the V-I characteristics (droop) of the SVC is zero, it can be modelled as a PV bus in the load flow studies. The power P is set to zero and the magnitude of V is set to be the desired voltage of that bus. Otherwise the slope of the characteristics in the control range S_L must be included in the model by representing the SVC as a PV bus connected in series with an impedance $X_{svs} = S_L$, normally in per unit value, to the system. Thus the point of connection to the system is treated as a PQ bus where both P and Q are zero.

The models of the SVC for load flow studies are depicted in Fig. 2.3 [10]. These basic models are sufficient to determine the required SVC's rating irrespective of its type. These models are used for load flow to determine the effect of the SVC without considering transformer saturation. It should be noted that the basic models with Q limits are not appropriate for representing the SVC under overload conditions because the characteristics of the SVC under such conditions is incorrect. As the value of Q is set constant, the V-I characteristics of the SVC outside the control range assumes hyperbolic curves as illustrated in Fig. 2.4 [10]. Modifications in the basic models can be made to correct this problem. The SVC can be represented as a variable susceptance or voltage-controlled reactive power model. In these models the susceptance of the SVC, real and reactive power and representation of the SVC can be controlled corresponding to the operating point of the SVC [9,10].

2.7.2 SVC models for steady-state studies

The variable susceptance model is generally adopted to represent a SVC for steady-state and transient stability studies. It represents the positive sequence impedance of the SVC with control actions. Normally, the

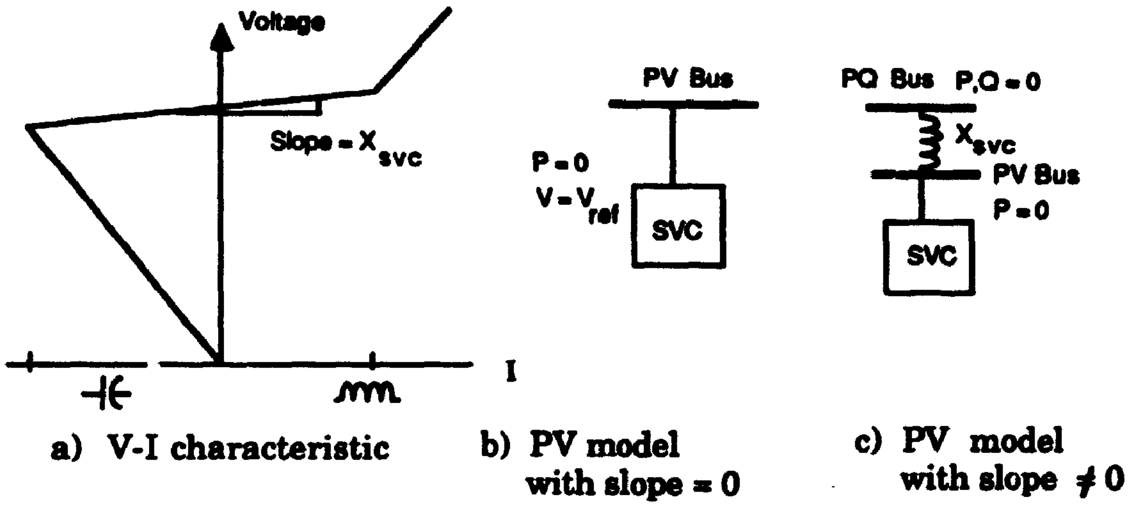

Fig. 2.3 : SVC models for load flow studies.

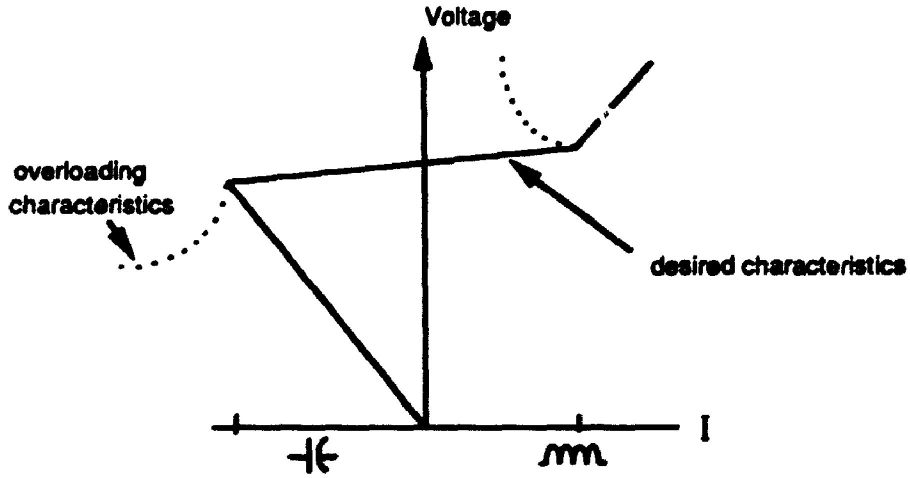

Fig. 2.4 : Illustration of basic SVC model under overloading conditions.

electromagnetic transients in the network and SVC's components can be ignored as long as the performance being evaluated deals with electromechanical oscillations. SVC models for subsynchronous resonance studies must accurately establish the SVC characteristics under steady-state and transient conditions. In general, the functional feature of a SVC can be illustrated as in Fig. 2.5. In Fig. 2.5, the system voltage is compared with the reference voltage of the SVC and the error signal is

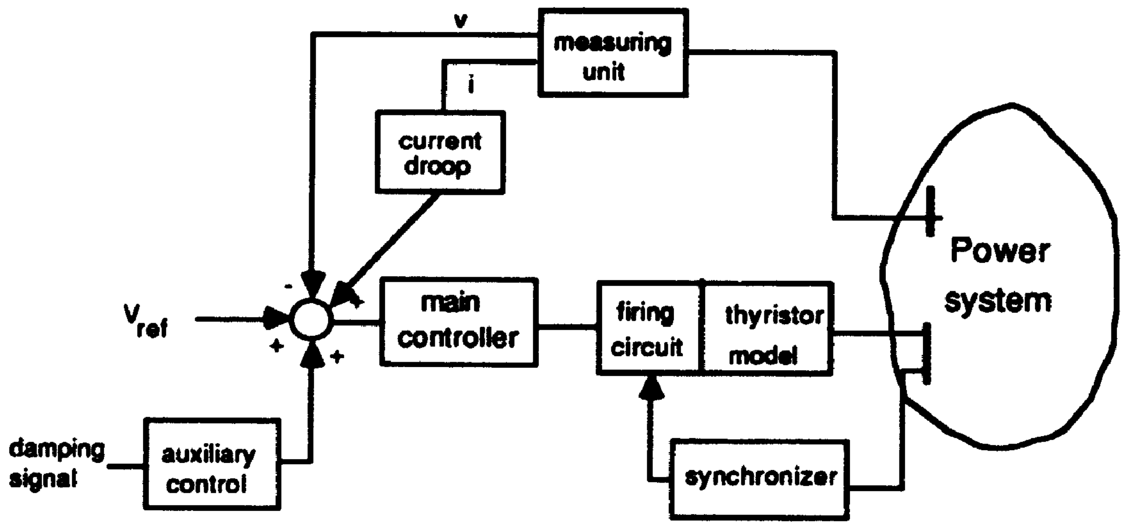

Fig. 2.5 : Basic SVC model for steady-state and transient stability studies.

passed to the main controller. The output of the main controller adjusts the firing of the thyristors which, consequently, changes the susceptance of the SVC in order to correct the error signal. The current droop characteristics can be accomplished through the use of current feedback in the model. The auxiliary control of the SVC is employed to enhance the system performance. The details of the SVC's control including the determination of proper control parameters are covered in Chapter 3.

2.8 The choices of strategic locations

The suitable locations of SVCs are dictated by the required objectives, economy and technical considerations. Practically the following locations are considered ;

a) the point of largest voltage variation or maximum system damping for a given dynamic control range,

b) the existence of a step-down transformer in the system with a suitable secondary or tertiary voltage,

c) the location of voltage sensitive loads or hvdc terminals, and

d) the point of variable industrial loads.

CHAPTER III

THE CONTROL OF SVC

Proper control of a SVC is very essential in obtaining the desired characteristics to improve the performance of the power system. In the past, classical and modern control theories have been extensively applied to design and evaluate the performance of a SVC. As power systems are becoming increasingly complex, effective control techniques are also being refined. Recent researches are focused on computer aided control in which new control strategies such as adaptive control, non-linear control and the combination of linear and non-linear controls can be implemented [10,21-23, 29-31].

3.1 Control objectives

A static var compensator is primarily designed for regulating the voltage at the bus of its connection in a system. Nowadays in addition to being applied as a voltage regulator it is also applied to improve both the transient and the dynamic performance of the system. Therefore its control objectives may be multiple and these may be different from one system to another. Control objectives of a SVC are classified as :

a) to control the voltage at the connected point,

b) to increase the system damping,

c) to control reactive power flow,

d) to minimize system losses,

e) to control subsynchronous resonance and

f) a combination of several of the above objectives.

In a radial system, the control of voltages at intermediate points not only improves the voltage profile of the line but it also enhances the transient stability of the system [3,12-14,35,43]. Damping control is required in relatively poorly damped systems.

The combination of voltage and damping control is a multi-purpose objective and has gained attention from many utilities. Reactive power flow, loss minimization and subsynchronous resonance are specific applications for certain systems.

3.2 Types of controller

Three major types of SVC controllers are ;

a) linear controller,

b) non-linear controller and

c) adaptive controller.

Linear controller is the most common type employed in a time-invariant system. The design of this controller is based on the well-known classical or modern control theories. Since the system is generally non-linear, therefore, it is linearized about its operation point for control design. The control so designed remains very effective so long as the system operates at or near the designed point. As the operating point changes, retuning of controller parameters becomes necessary. This leads to the application of non-linear type of controllers in which non-linear properties of the control are employed. A non-linear controller is rather complex and it usually employs a digital processor(s). In reality, power system characteristics randomly change with time. Small and large disturbances occur from time to time anywhere in the system. Under severe disturbances, even a well-designed linear or non-linear controller may not be able to maintain the desired control objectives. To cope with the changing system characteristics, researches in adaptive controller are currently very active [29-31].

An adaptive controller requires the information of all states which are very difficult to measure and turn out to be inaccurate if they are reproduced from a state estimator. Thus the application of an adaptive controller may need to be studied for a long time before it can be applied to a complex system.

The main objectives for the control of a SVC in this thesis is to control the system voltage and to improve the dynamic performance of a system. Because of the simplicity and robustness of a linear controller it is considered in the subsequent Sections.

3.3 Power system representation

The behaviour of a power system can be reasonably well predicted when its major components are accurately modelled. Because of the complex interconnections, a power system is generally approximated. Depending upon the desired control objective one can further simplify the model by neglecting detailed representation of many components. The models of a power system used for the voltage control and steady-state stability studies are discussed in the following subsections.

3.3.1 Power system representation for voltage control

In the simplest case the system can be represented by the Thévenin equivalence at the point of connection of a SVC for voltage control as shown in Fig. 3.1. This representation is fairly adequate for the analysis of the system voltage at the SVC location. However information of the voltage elsewhere in the system is lost. Since the components of a power system are mainly inductive and the system losses are usually low, the

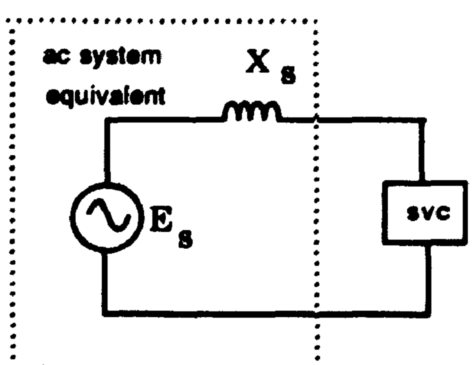

Fig. 3.1 : Power system representation for a SVC operating in voltage control.

equivalent system impedance can be approximated by an inductive reactance X_s. The magnitudes of E_s and X_s are neither known in advance nor they are constant. They depend on the power system operating conditions and vary from one system configuration to another. The value of E_s is the open-circuit voltage at the SVC bus while X_s is the reciprocal of the short-circuit MVA at that bus (in pu values). Load flow and short-circuit studies are employed to determine E_s and X_s.

3.3.2 Power system representation for a steady-state stability study

Typically, steady-state stability of a system is related to the low frequency inertial oscillations of the generators. For studies, where some machines may be represented by classical models, other machines should be represented with their excitation regulators. In any case if power system stabilizers are employed on the generator exciters and supplementary controls for steady-state stability exist in the SVCs it is necessary that these be represented in detail.

Since the dynamic performance of a system is dominated by synchronous machines, appropriate machine models are to be used. In linear control systems generator models are based on the linearization of Park's equations. Transmission lines and loads are normally treated as lumped impedances at nominal frequency. The interactions of the generators with other controlled devices are either expressed in the form of state-space equations or block diagrams containing appropriate transfer functions [15-18]. Block diagram approach gives a clear insight into the interaction of generators with other controlled devices. However this approach can be employed only on a simple system. For a complex system, linearized state-variable approach is normally adopted which takes the general form

$$\dot{x} = Ax + Bu$$

$$y = Cx + Du$$

where x = system state variables,

y = output vector of the system,

u = control vector and

A,B,C,D = system matrices with appropriate dimensions.

The state-variable approach is the best technique as each device can be modelled separately and then combined together to form the entire system model [47]. The behaviour of the entire system can be closely investigated by using modern control theories.

3.4 SVC models

The performance of a system incorporating SVCs can be accurately determined if the models representing the SVCs are proper. Various types of SVC models are reported in publications [9-11,21-23,26-28]. These are classified into two types namely :

a) non-linear model and

b) linearized model.

The output of the SVC in these models is considered as a variable susceptance or a variable voltage behind a fixed reactance.

3.4.1 Non-linear model

This type of model is employed in digital simulations. The characteristics of a SVC are expressed by equations interacting with the system. The models of TCR, TCR+FC and TCR+TSC are discussed in the next subsections.

3.4.1.1 The TCR model

The fundamental current component of a TCR having a conduction angle σ connected to an ac bus of magnitude V can be expressed as [12]

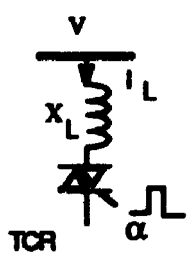

$$I_L = \frac{(\sigma - \sin\sigma)}{\pi} \cdot \frac{V}{X_L} \tag{3.1}$$

where σ = conduction angle of thyristors

X_L = rated TCR reactance.

With $\alpha = \pi - \sigma/2$, Eqn.(3.1) can be rewritten as

$$I_L = \frac{[2\pi - 2\alpha + \sin(2\alpha)]}{\pi} \cdot \frac{V}{X_L}$$

$$= V \cdot \left[\frac{f(\alpha)_{TCR}}{X_L}\right] \tag{3.2}$$

As the firing angle changes within the limits $\pi/2$ to π, the value of $f(\alpha)$ lies between 1 and 0 as shown in Fig. 3.2.

Therefore, the behaviour of a TCR in the control range can be modelled as a controllable susceptance. For load flow and transient stability studies, this model is not appropriate as the admittance matrix

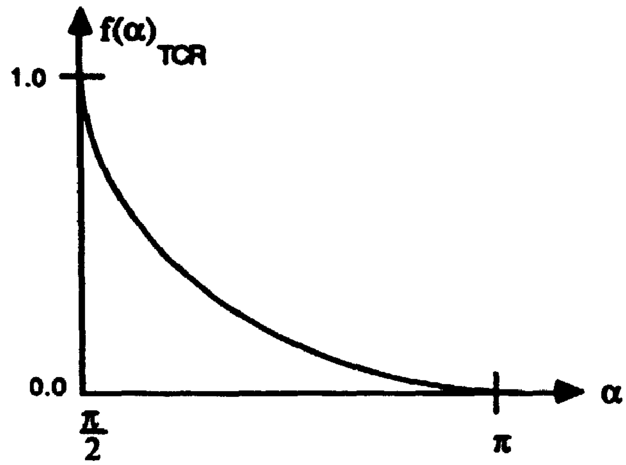

Fig. 3.2 : Variation of $f(\alpha)_{TCR}$

of the system needs to be recalculated in every step. To avoid this computational inefficiency the TCR may be considered to be a controlled voltage source behind a reactance. This model is derived from Eqn.(3.2) as shown below.

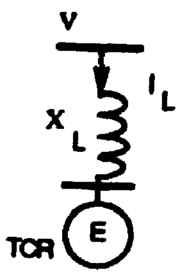

The TCR is represented by an inphase controlled voltage E connected to the ac bus of magnitude V through its rated reactance X_L. The fundamental current drawn by the TCR is thus expressed as

$$I_L = \frac{V - E}{X_L} \tag{3.3}$$

Thus from Eqns. (3.2) and (3.3)

$$\frac{V - E}{X_L} = f(\alpha)_{TCR} \frac{V}{X_L}$$

or

$$E = V(1 - f(\alpha)_{TCR}) \tag{3.4}$$

In order to continuously control the voltage of a bus by a SVC, a closed-loop control system must be employed on the SVC. The control block diagram for controlling the voltage using a SVC, known as the CIGRÉ

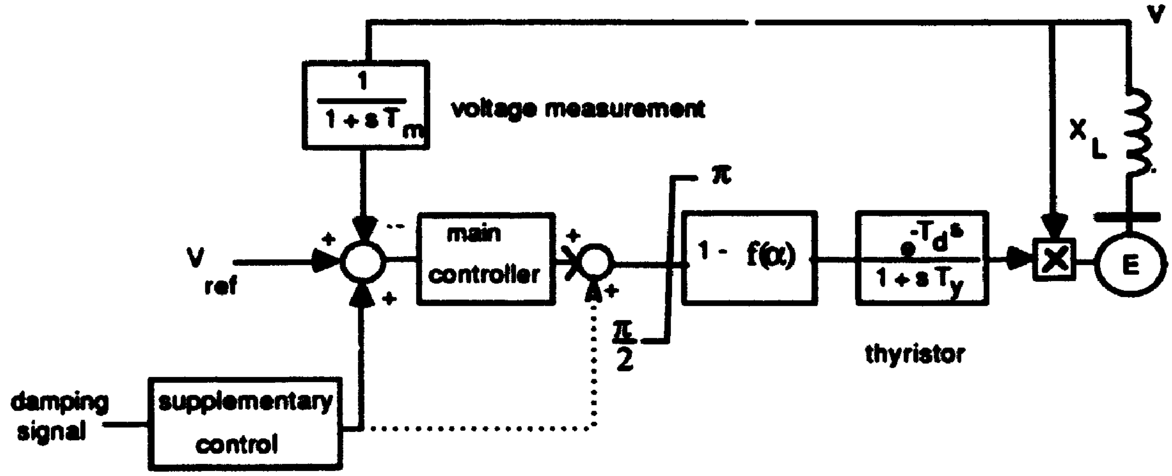

Fig. 3.3 : TCR model interfaced to the system as a voltage behind a reactance.

model [9], is shown in Fig. 3.3. The main controller in Fig. 3.3 can be of any type, i.e. proportional, integral or their combination. The time delay associated with the voltage measurement unit and the inherent delay in the conduction of the thyristors are included. A supplementary control signal can be added to the V_{ref} signal or in some cases, to the output of the main controller of the SVC. This model is obviously non-linear and is normally used in time domain simulations.

3.4.1.2 The TSC model

In order to obtain a model for TSC a technique similar to that applied for a TCR type compensator is used. The only difference for the TSC model is on the non-linear function f(α). From the voltage behind reactance representation, the injected current I_C is given by

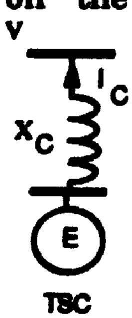

$$I_C = \frac{E - V}{X_C} \qquad (3.5)$$

where X_C = rated reactance of the TSC.

As the parallel capacitor banks of the TSC are discretely controlled by the thyristors, the current injected into the system can be defined as

$$I_C = \frac{N_{co}}{N_{cmax}} \cdot \frac{V}{X_C} \tag{3.6}$$

where N_{co} = number of capacitor banks in service,

and N_{cmax} = maximum number of capacitor banks.

Equating Eqns.(3.5) and (3.6) yields

$$E = V(1 + \frac{N_{co}}{N_{cmax}}) \tag{3.7}$$

Comparing Eqns(3.7) and (3.4) one gets

$$f(\alpha)_{TSC} = - \frac{N_{co}}{N_{cmax}} \tag{3.8}$$

3.4.1.3 The TCR+TSC model

The model for a TCR+TSC type compensator is a little more complex as the capacitor and the reactor are simultaneously controlled. If the rated reactance of the TCR is chosen to interface with the system, the value of E can be calculated. Eqn.(3.4) is still valid in the case that no capacitor bank is in service. But the Eqn.(3.6) must be modified as the value of the interfacing reactance is different.

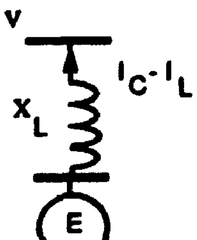

TCR+TSC, TCR+FC

From Eqn.(3.6) one can write

$$I_C = \frac{N_{co}}{N_{cmax}} \cdot \frac{V}{X_L} \cdot \frac{X_L}{X_C}$$

$$= \frac{N_{c}}{N_{cmax}} \cdot \frac{V}{X_L} \cdot \frac{Q_C}{Q_L} \qquad (3.9)$$

where $Q_C =$ the rating of the TSC

and $Q_L =$ the rating of the TCR

Since $I_C - I_L = \frac{E - V}{X_L}$

hence the magnitude of the voltage E can be expressed as

$$E = V(1 - f(\alpha)_{TCR} + \frac{N_c}{N_{cmax}} \cdot \frac{Q_C}{Q_L})$$

$$= V(1 - f(\alpha)_{TCR} - f(\alpha)_{TSC} \cdot \frac{Q_C}{Q_L}) \qquad (3.10)$$

It must be noted here that Eqn.(3.10) is also valid for a TCR+FC type compensator in which $N_c = N_{cmax} = 1$.

3.4.2 Linearized model

The linearized model of a SVC is developed from the equivalent system shown in Fig. 3.4. The magnitude of V at the SVC bus is governed by

$$V = E_s - X_s I_{svc} \qquad (3.11)$$

and $I_{svc} = B_{svc} V. \qquad (3.12)$

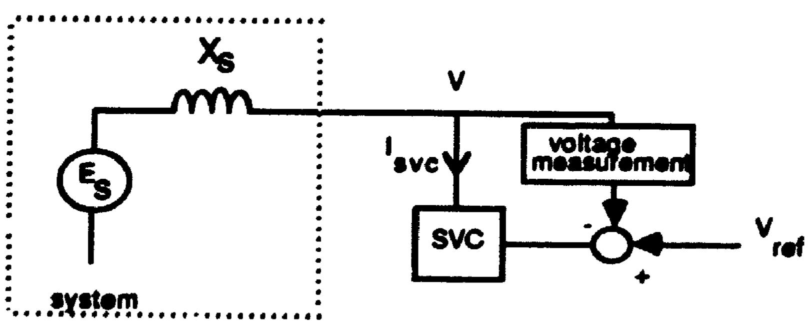

Fig. 3.4 : Thévenin equivalence of power system with a SVC as voltage control.

As the SVC control is a closed-loop system, the output B_{svc} of the SVC is a function of the error signal and its controls. Assume that the non-linear function $f(\alpha)$ is compensated by a non-linear network containing opposite characteristics, the control of the SVC can be simply represented by a linear transfer function G. If H represents the transfer function of the voltage measuring unit, the control block diagram of the system can be developed from Eqns.(3.11) and (3.12) as shown in Fig. 3.5.

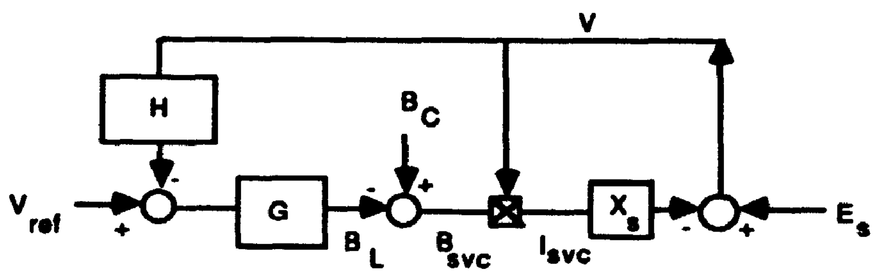

Fig. 3.5 : Non-linear control block diagram of the SVC.

The bock diagram in Fig. 3.5 can be applied to a TCR+FC or a TCR+TSC as well since for small analysis only the reactor is controlled thus capacitor switching can be ignored. The linearized forms of Eqns.(3.11) and (3.12) at an operating point can be expressed as

$$\Delta V = \Delta E_s - X_s \Delta I_{svc} \tag{3.13}$$

and

$$\Delta I_{svc} = B_o \Delta V + V_o \Delta B_{svc} \tag{3.14}$$

where the subscript "o" denotes the values at the operating point. The linearized model of the system is indicated in Fig. 3.6.

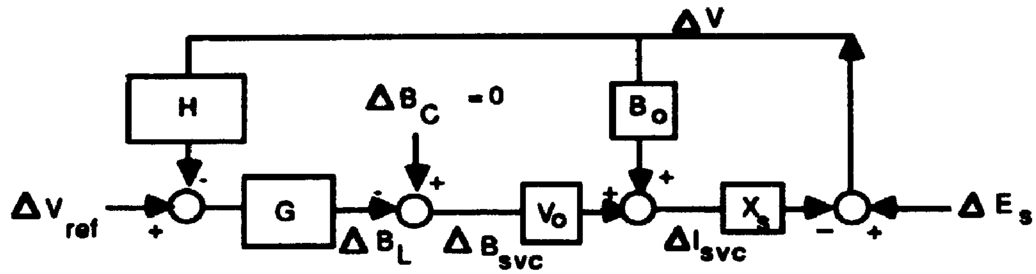

Fig. 3.6 : Linearized model of the SVC.

3.4.2.1 Closed-loop transfer function

The closed-loop transfer function of the linearized model as shown in Fig. 3.6 can be derived form the block diagram as follows :

$$\Delta B_L = G(\Delta V_{ref} - H\,\Delta V)$$

$$\Delta I_{svc} = B_o\,\Delta V - V_o\,\Delta B_L$$

$$= B_o\,\Delta V - (G\,\Delta V_{ref} - GH\,\Delta V)\,V_o$$

$$\Delta V = \Delta E_s - \Delta I_{svc}.X_s$$

$$= \Delta E_s - (B_o\,\Delta V - (G\,\Delta V_{ref} - GH\,\Delta V)\,V_o\,)X_s$$

$$= \Delta E_s + V_o X_s G\,\Delta V_{ref} - (GHV_o + B_o)X_s\,\Delta V$$

therefore,

$$\Delta V = \frac{\Delta E_s + V_o X_s G\,\Delta V_{ref}}{1 + X_s(GHV_o + B_o)} \qquad (3.15)$$

if $\Delta E_s = 0$,

$$\frac{\Delta V}{\Delta V_{ref}} = \frac{V_o\,X_s\,G}{1 + X_s(GHV_o + B_o)} \qquad (3.16)$$

or if $\Delta V_{ref} = 0$,

$$\frac{\Delta V}{\Delta E_s} = \frac{1}{1 + X_s(GHV_o + B_o)}. \qquad (3.17)$$

These transfer functions depend on the initial operating condition, the system reactance and the control of the SVC. Therefore, the appropriate control has to be determined to satisfy the required performance and to insure system stability.

3.5 Main regulator

Regulators for SVC control are not unique but they fall into four basic types namely : proportional (P), integral (I), derivative (D) and the combination PI or PD or PID. The usage of derivative control is very rare as it is very sensitive to the system noise.

Since the system reactance X_s and the operating condition V_o and B_o are explicitly involved in the closed-loop transfer functions, the design of the regulator is system-dependent. In some cases, lead or lag compensation must be utilized to improve the stability of the voltage controlled-loop.

3.5.1 Proportional controller

Assume that the measuring unit H in Fig. 3.6 can be represented by a first order delay of time constant T_m. The steady-state gain of the regulator G must satisfy the current droop characteristics of the SVC, which is the reciprocal of the slope S_L in per unit. A lead or lag network can be added in series with the regulator G to improve the transient and steady-state response of the voltage. The SVC model with a proportional controller and lead/lag compensation is shown in Fig. 3.7.

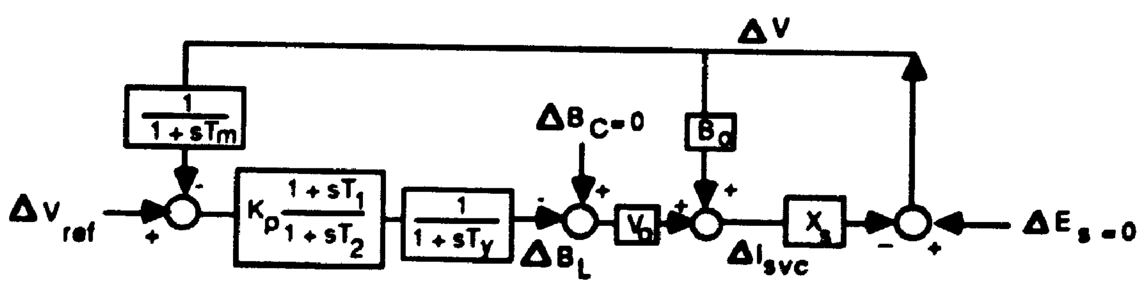

Fig. 3.7 : Proportional controller with lead/lag compensation.

The time constants T_1 and T_2 of the lead/lag compensator can be determined by using the classical control theory. The characteristic equation of the system obtained from Eqn.(3.16) or (3.17) is

$$1 + X_s\,(GHV_o + B_o) = 0. \qquad (3.18)$$

Substituting for G and H, Eqn. (3.18) yields

$$\frac{1}{X_s} + K_pV_o\frac{1 + sT_1}{1 + sT_2}\cdot\frac{1}{(1+sT_m)(1+sT_y)} + B_o = 0$$

and since T_m and T_y are practically small, further simplification can be made by [24]

$$\frac{1}{(1+sT_m)(1+sT_y)} \approx \frac{1}{1+s(T_m+T_y)} = \frac{1}{1+sT_y^*}.$$

Hence the characteristic equation becomes

$$(B_o+S_c)(1+sT_2)(1+sT_y^*) + K_pV_o(1+sT_1) = 0,\ S_c = 1/X_s\ .$$

The Appendix A shows the approximate value of the time constant T_1 to be

$$T_1 = \frac{[2(B_o+S_c)(B_o+S_c+K_pV_o)\,T_2T_y^*]^{1/2} - (B_o+S_c)(T_2+T_y^*)}{K_p\,V_o}. \qquad (3.19)$$

The lead and lag time constants T_1 and T_2 must be selected to satisfy the condition in Eqn.(3.19). Typically T_1 is less than T_2 and the compensator is a phase lag network. The frequency response technique, based on phase and gain margins, is also applicable for the determination of the compensator parameters. The compensator may not be required if these margins are within the typical values of 30-60 degrees and 4-12 dB respectively.

3.5.2 Integral controller

Integral controllers are also used for controlling SVCs. In order to produce the desired current-droop characteristics, SVC's current is fed back through a drooping control unit as illustrated in Fig. 3.8.

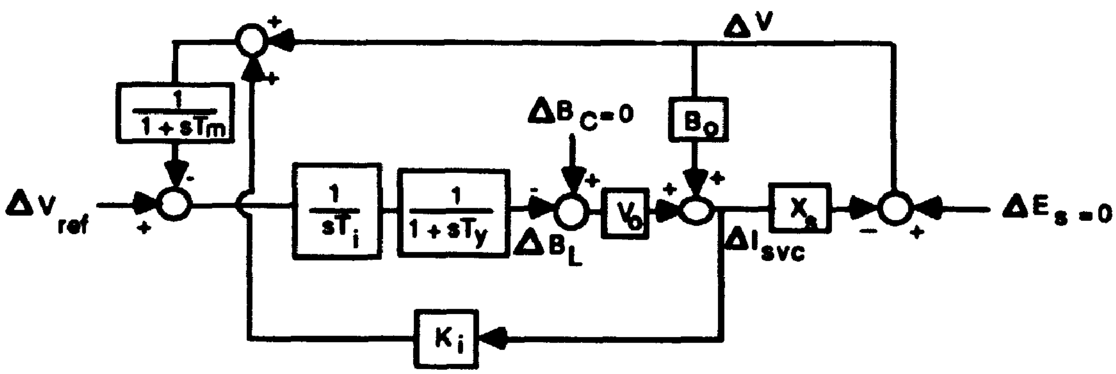

Fig. 3.8 : Integral controller for SVC.

The time delay associated with current measurement is accounted for through the delay of the voltage measuring unit to simplify the block diagram. The only unknown for this case is the integral time T_i which can be approximately calculated. The Appendix B gives the approximate value of T_i to be

$$T_i \quad = \quad 2V_o(1+B_oX_s)\cdot(X_s-K_i)\cdot(T_m+T_y) \qquad (3.20)$$

3.5.3 Proportional-Integral controller

PI controller combines the favourable characteristics of the proportional and integral controllers. The speed of the response is considerably faster and the steady-state error is eliminated. Similar to the integral controller, current feedback is necessary to establish the desired current-droop characteristics of the SVC. The control block diagram of the SVC using PI controller is shown in Fig. 3.9 .

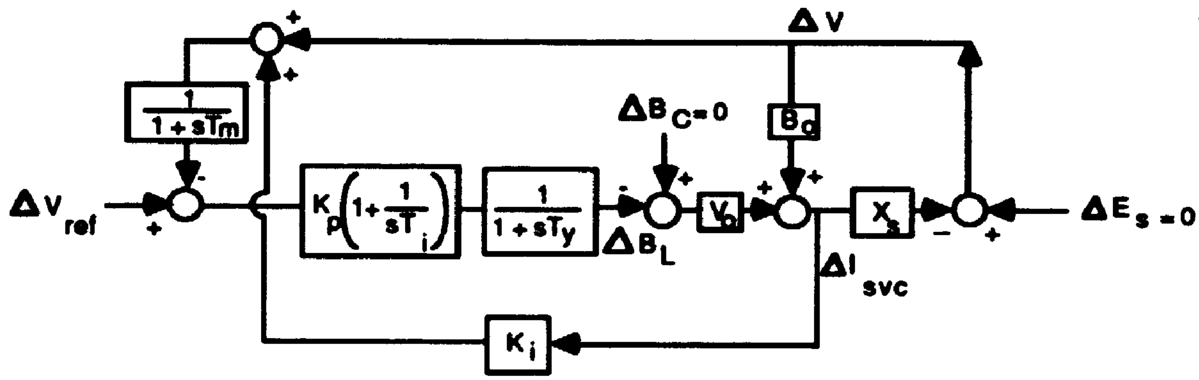

Fig. 3.9 : Proportional-Integral controller for SVC.

Proper values of the proportional gain K_p and the integral time T_i have to be determined in order to achieve the well damped voltage response.

If T_i is chosen to be approximately equal to T_y, the derivation of the appropriate gain value K_p can be simplified. The Appendix C gives the value of K_p to be

$$K_p = \frac{1}{2} \cdot \frac{1+X_s B_o}{V_o (X_s - K_i)} \cdot \frac{T_y}{T_m} \tag{3.21}$$

3.6 Effects of system dynamics

The dynamics of the system should be considered when the SVC is located in the neighbourhood of generators or other active devices. The approximate Thévenin equivalence is no longer appropriate if accurate results are required. In a simple system, the dynamics of the generator and exciter can be included in forms of transfer block diagram interacting with the SVC. The optimal controller parameters can be found through transfer function reduction or eigenvalue analysis. In a general complex system, the transfer function approach is very tedious and inconvenient. The state-variable approach is the best technique for such a system and the optimal controlled parameters can be determined based on eigenvalue analysis.

Non-linear optimization method can be employed in conjunction with the eigenvalue analysis for the determination of the optimal set of controller parameters. However, this technique can not be applied to a complex system as the computation involved is excessive and the improvement gained may not be significant.

3.7 Supplementary control

Static var compensator can enhance the dynamic performance of the system following unexpected small or large disturbances provided that an appropriate damping signal is selected and its supplementary control is effectively designed.

3.7.1 The choices of damping signal

Auxiliary signals for damping improvement can be one or a combination of the following signals ;

a) bus frequency deviation,

b) line power flow,

c) generator speed variation and

d) line current magnitude.

Local signals are preferable as they are available and can be easily measured. The selected signal should not be sensitive to noise and the SVC output to avoid high-frequency oscillation and possible control instability. In general, the damping of the local and inter-area mode oscillations is needed.

Therefore the location of the SVC can be selected in such a manner that the SVC will contribute to the damping enhancement of many poorly damped modes simultaneously. In this case, the damping signal should contain the information of the required modes. Thus the choice of the damping signal and the SVC's location must be carefully considered. The use of line current or line power flow seem to be the best solution as the machines closely connected to the selected line can be predicted to be influenced by the SVC damping control. Participations of the desired damping modes on the damping signal can be investigated by the eigenvalue analysis or the frequency response technique (which generally gives a clear indication of the contributing modes on the damping signal).

3.7.2 Damping control

The ability of a SVC to enhance system damping not only depends on the right choice of damping signal but it also relies on the design of the supplementary control. In general, a supplementary control consists of gain and phase compensation circuits which may either be phase lead or phase lag or both. The key question is - how to arrive at the proper values of the gain and the compensated phase, typically in terms of time constants of the compensation circuit.

Linear control theory is applicable for these purposes but it may be quite difficult when the system becomes very complex. Modal control [36-38] and frequency response techniques will be discussed in the next subsections for the determination of the supplementary control.

3.7.2.1 Modal control

Modal control theory can be well adapted for the design of the auxiliary control in a general linear system. The state equations of an inter-connected power system can be written in the vector-matrix differential equation form of

$$\begin{aligned} \dot{x}(t) &= Ax(t) + Bu(t) \\ y(t) &= Cx(t) \end{aligned} \qquad (3.22)$$

where x is the state vector, u the control vector comprising the output of the supplementary control and y the system output. The Laplace transform of Eqn.(3.22) gives the state equations in frequency domain

$$\begin{aligned} sX(s) &= AX(s) + BU(s) \\ Y(s) &= CX(s). \end{aligned} \qquad (3.23)$$

Since local signals are preferable, the control vector U(s) can be expressed in the form

$$U(s) = [\ u_1(s)\ u_2(s). . .u_n(s)\ ]^T$$

where $u_i(s) = H_i(s)y_i(s)$

$$y_i(s) = \text{local signal} \qquad (3.24)$$

$H_i(s)$ = damping control transfer function of

i^{th} damping signal of the SVC.

Combination of Eqns.(3.23) and (3.24) results in the closed-loop system equation

$$\begin{aligned} sX(s) &= AX(s) + BH(s)Y(s) \\ &= AX(s) + BH(s)CX(s) \qquad (3.25) \\ sX(s) &= [A + BH(s)C]X(s) \end{aligned}$$

The eigenvalues of the system can be solved from the characteristic equation

$$\det\,(sI-[A+BH(s)C]) = 0 \qquad (3.26)$$

and if $(sI-A)^{-1}$ exists it can be rearranged as

$$\det\,(I-(sI-A)^{-1}BH(s)C) = 0. \qquad (3.27)$$

If λ is the assigned eigenvalue for the least damped mode, the transfer function $H(\lambda)$ can be determined from Eqn.(3.27) as

$$\det\,(I-(\lambda I-A)^{-1}BH(\lambda)C) = 0.$$

Using the determinant identity [38]

$$\det\,(I-E.F) = \det\,(I-F.E)$$

Eqn.(3.27) can be written as

$$1 - C(\lambda I-A)^{-1}BH(\lambda) = 0$$

or

$$H(\lambda) = \frac{1}{C(\lambda I-A)^{-1}B}. \qquad (3.28)$$

Since the matrices A,B,C are known and λ is the assigned eigenvalue, the transfer function $H(\lambda)$ can be solved from the magnitude and phase of

Eqn.(3.28). Therefore only two unknowns are allowed for each transfer function. The commonly used transfer function for the supplementary control is [18]

$$H(s) = K_c \left[\frac{sT}{1+sT} \right] \cdot \left[\frac{1+sT_1}{1+sT_2} \right]^2 . \qquad (3.29)$$

A reset filter of a long reset time T is used to eliminate the effect of low frequency signal corresponding to the steady-state condition. The double lead/lag unit enables the compensator for a broad range of phase compensation. The values of T and of either T_1 or T_2 must be first selected and the values of K_c and T_2 or T_1 are solved from Eqn.(3.29).

3.7.2.2 Frequency response technique

The damping signal taken from bus quantities should contain the information of the desired damping modes. But in reality, it may comprise the influence of other modes as well. In such cases, modal control technique may not work. If the frequency response of the system is achievable by any means, the design can be based on frequency response technique even though it may not be the optimal solution. From the plots of magnitude and phase responses, the resonance frequencies and the corresponding magnitudes and phases can be identified. These frequencies correspond to the oscillation modes in the system. At these frequencies, the phase roll-off is normally sharp and phase lead compensations are normally needed. The transfer function of the local damping signal to the input V_{ref} of the SVC can be considered as a linear function G. Therefore with the application of the supplementary control, of transfer function H, the system forms a positive feedback loop conceptually illustrated in Fig. 3.10.

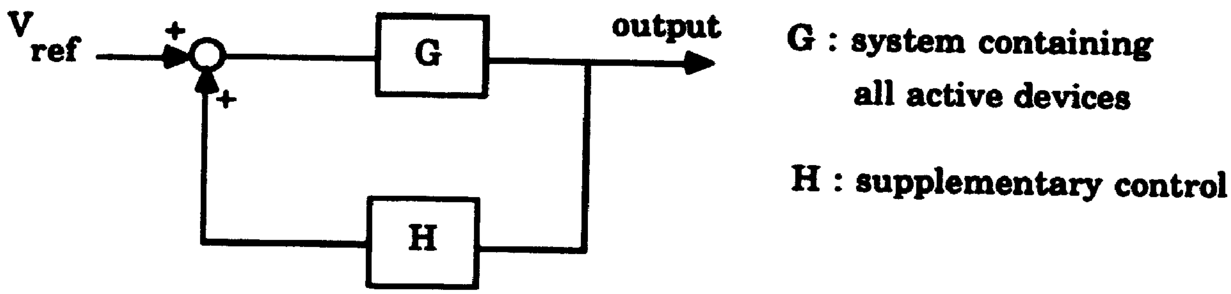

Fig. 3.10 : Conceptual control system.

As the reference voltage is kept constant the system can be considered as a unity feedback loop with zero input having a cascaded transfer function HG as shown in Fig. 3.11.

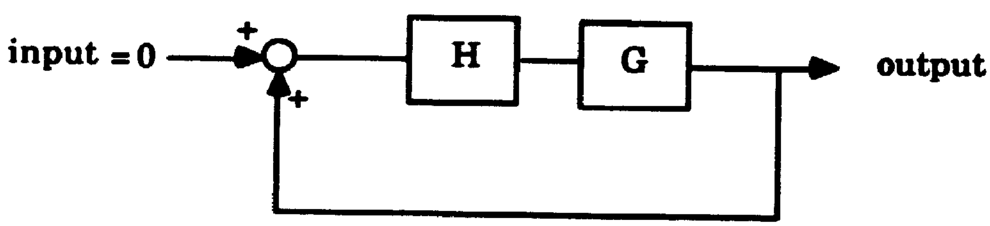

Fig. 3.11 : Conceptual unity feedback system.

Thus the concepts of series compensation can be applied even though it appears as a shunt compensation from Fig. 3.10. The magnitude and phase of H, at the frequencies of interest, are calculated from the characteristic equation of the system

$$1 - GH = 0$$

which implies $|GH| = 1$ and $\angle H = -\angle G$.

If the frequency response is performed on real frequencies, the values of the feedback gain K_e will be the extreme ones. On the other hand, if the frequency response is performed on complex frequencies at some desired damping ratio ζ, the values of K_e can be precisely known at those frequencies.

Therefore the appropriate value of K_e must be properly selected. In the case that the frequency response is performed on real frequencies, the value of K_e must be less than the minimum values calculated at different frequencies. Even if complex frequency response is available, the values of K_e at different frequencies are not the same. The appropriate value of K_e may have to be chosen. This technique requires cut and try methods as many modes of oscillation may be required to be damped simultaneously.

Eigenvalue analysis and time domain simulation of the system can be utilized to evaluate the effectiveness of the designed supplementary control. Examples of the design using modal control theory for a simple system and complex frequency response technique in a multi-machine system of EGAT are demonstrated in Chapters 4 and 5 respectively.

CHAPTER IV

APPLICATION OF SVC IN A SMIB SYSTEM

Applications of static var compensators reported in recent publications [3-6,8,10,11,41-46] are generally confined to simple power systems. The well-known single machine infinite bus (SMIB) system is widely considered because of its simplicity and because analytical solutions can be achieved for it. In this chapter a detailed analysis of a SMIB system with the application of a SVC for the purposes of increasing power transfer capability, controlling the voltage and improving system damping is done.

4.1 System configuration

The SMIB system consists of a synchronous generator connected to a very large power system, treated to be an infinite bus. The generator is connected to the infinite bus through a long transmission line. A static var compensator is located at an intermediate bus for controlling the intermediate bus voltage and for also increasing the power transfer capability of the line. Local loads of constant impedance type are assumed to exist at the generator and at the intermediate bus. Each section of the line is represented by an equivalent π-section with lumped impedances where the line-charging capacitances are integrated in the local loads. A single line diagram of the system is illustrated in Fig. 4.1 .

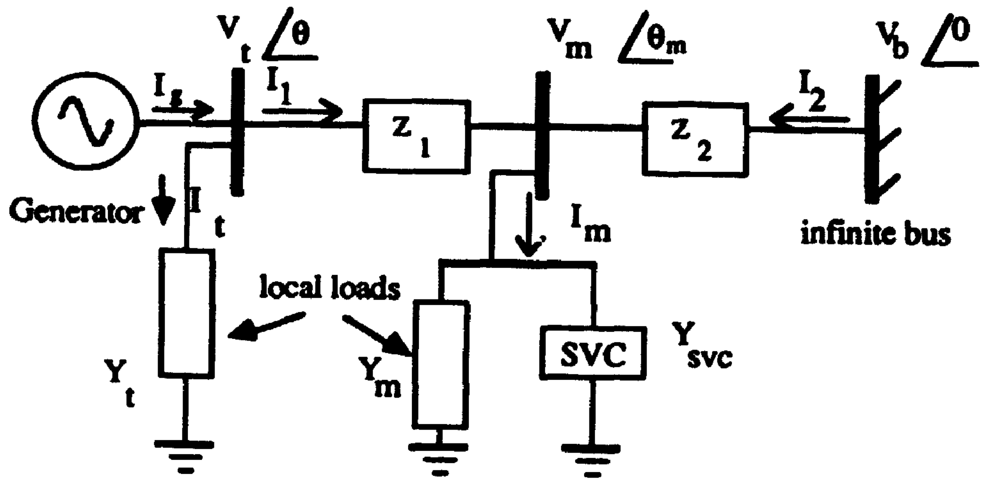

Fig. 4.1 : Single machine infinite bus system with SVC compensated line.

The SVC is considered to be a thyristor controlled reactor and fixed capacitor type although it may be replaced by a TCR+TSC type with relative ease. The initial value of the SVC's susceptance B_{svc} can either be capacitive or inductive. The initial value of B_{svc} depends on the reference voltage of the SVC, magnitude of the local loads, the line impedance and the line loading. The location of the SVC can be theoretically adjusted by selecting the relative values of Z_1 and Z_2, the line parameters. In the analysis, it is assumed that the SVC is placed in the middle of the line. The infinite bus is represented as an ideal voltage source and is treated as the reference phasor in the analysis.

4.2 Small signal dynamic model

In order to develop a better feel of the action of a static var compensator in a system, a block diagram approach similar to Ref[16] but extended to include a SVC has been undertaken. Researchers advocating the use of auxiliary signals in a SVC control to provide extra damping to a network have been unclear about the action of the SVC under various control modes. The system shown in Fig. 4.1 has all the essential components and is yet not so difficult to analyze analytically. Accordingly to extend the work of Heffron and Phillips [15] and deMello [16], techniques described by Yu [18] have been used to arrive in Fig. 4.2. The new model has addition K constants (K_1 to K_{12}).

In order to arrive at the model of Fig. 4.2, performance equations of all system subcomponents are written in p.u. values (machine base). These equations are linearized and rearranged to show interactions.

4.2.1 Small signal equations

All admittance and impedance elements of the network are represented in complex, p.u. quantities.

i.e.

$$y = g+jb \quad , \quad z = r+jx$$

All parameters, where applicable are represented in the d-q quantities e.g.

$$i = i_d+ji_q \quad , \quad v = v_d+jv_q$$

In a matrix form, the network equation are written as

$$\begin{bmatrix} i_d \\ i_q \end{bmatrix} = \begin{bmatrix} g & -b \\ b & g \end{bmatrix} \begin{bmatrix} v_d \\ v_q \end{bmatrix} , \quad \begin{bmatrix} v_d \\ v_q \end{bmatrix} = \begin{bmatrix} r & -x \\ x & r \end{bmatrix} \begin{bmatrix} i_d \\ i_q \end{bmatrix} \tag{4.1}$$

or $\quad I = YV \quad$ and $V = ZI$.

For the network shown in Fig. 4.1, the currents in the network are given as

$$I_1 = Y_1 (V_t - V_m) \tag{4.2}$$

$$I_2 = Y_2 (V_b - V_m) \tag{4.3}$$

$$I_m = V_m (Y_m + Y_{svc}) \tag{4.4}$$

The above quantities are shown in Fig. 4.1. Loads at the machine and SVC buses are represented by constant admittances Y_l and Y_m respectively.

Since $\quad I_m = I_1 + I_2 \quad$ (4.5)

eliminating the current variable from the above equations we obtain

$$Y_1V_t + Y_2V_b - (Y_1+Y_2+Y_m+Y_{svc})V_m = 0. \tag{4.6}$$

For small perturbation studies Eqn.(4.6) can be linearized as given in Eqn.(4.7) where the subscript "o" implies the operating point quantity.

$$Y_1\Delta V_t + Y_2\Delta V_b -(Y_1+Y_2+Y_m+Y_{svco})\Delta V_m -\Delta Y_{svc}V_{mo} = 0 \tag{4.7}$$

The d-q axis components of Eqn.(4.7) are;

$$\begin{bmatrix} g_1 & -b_1 \\ b_1 & g_1 \end{bmatrix} \begin{bmatrix} \Delta v_{td} \\ \Delta v_{tq} \end{bmatrix} + \begin{bmatrix} g_2 & -b_2 \\ b_2 & g_2 \end{bmatrix} \begin{bmatrix} \Delta v_{bd} \\ \Delta v_{bq} \end{bmatrix} - \begin{bmatrix} g_1+g_2+g_m & -(b_1+b_2+b_m+B_{svco}) \\ b_1+b_2+b_m+B_{svco} & g_1+g_2+g_m \end{bmatrix} \begin{bmatrix} \Delta v_{md} \\ \Delta v_{mq} \end{bmatrix}$$
$$- \begin{bmatrix} 0 & -\Delta B \\ \Delta B & 0 \end{bmatrix} \begin{bmatrix} v_{mdo} \\ v_{mqo} \end{bmatrix} = 0. \tag{4.8}$$

The Eqn.(4.8) assumes that the SVC contributes only to the changes in its susceptance ΔB_{svc} . In order to simplify the analysis, let

$$Z_o = \begin{bmatrix} g_1+g_2+g_m & -(b_1+b_2+b_{mo}) \\ b_1+b_2+b_{mo} & g_1+g_2+g_{mo} \end{bmatrix}^{-1}$$
$$= [\, Y_1 + Y_2 + Y_m + Y_{svco} \,]^{-1} \tag{4.9}$$

then the mid-point voltage phasor ΔV_m can be determined from Eqns.(4.7), (4.8) and (4.9) to be

$$\Delta V_m = Z_o[Y_1\Delta V_t + Y_2\Delta V_b] - Z_o\begin{bmatrix}-V_{mqo}\\ V_{mdo}\end{bmatrix}\Delta B. \tag{4.10}$$

The linearized form of Eqn.(4.2) is

$$\Delta I_1 = [Y_1\Delta V_t - Y_1\Delta V_m] \tag{4.11}$$

Back substitution of Eqn.(4.10) into Eqn.(4.1 yields

$$\Delta I_1 = [Y_1 - Y_1Z_oY_1]\Delta V_t - Y_1Z_oY_2\Delta V_b + Y_1Z_o\begin{bmatrix}-V_{mqo}\\ V_{mdo}\end{bmatrix}\Delta B. \tag{4.12}$$

The change in the generator current is obtained by applying Kirchoff's law at the generator bus.

$$\Delta I_g = \Delta I_1 + \Delta I_t$$
$$= \Delta I_1 + Y_t\Delta V_t. \tag{4.13}$$

Substitution of Eqn.(4.12) in Eqn.(4.13) gives

$$\Delta I_g = [Y_1 - Y_1Z_oY_1 + Y_t]\Delta V_t - Y_1Z_oY_2\Delta V_b + Y_1Z_o\begin{bmatrix}-V_{mqo}\\ V_{mdo}\end{bmatrix}\Delta B \tag{4.14}$$

which can be simplified to give

$$\Delta I_g = A_1\Delta V_t - A_2\Delta V_b + A_3\begin{bmatrix}-V_{mqo}\\ V_{mdo}\end{bmatrix}\Delta B \tag{4.15}$$

where $A_1, A_2, ..$, are 2 x 2 matrices and ;

$$A_1 = Y_1[I - Z_oY_1] + Y_t$$
$$A_2 = Y_1Z_oY_2 \tag{4.16}$$

and $$A_3 = Y_1Z_o.$$

Since the voltage components v_d and v_q of the synchronous machine, ignoring armature resistance and saturation, can be expressed by [17,18]

$$v_d = x_q\, i_q \quad \text{and} \quad v_q = e_q' - x_d'\, i_d$$

or in the matrix form

$$\begin{bmatrix} v_d \\ v_q \end{bmatrix} = \begin{bmatrix} 0 \\ 1 \end{bmatrix} e_g' - \begin{bmatrix} 0 & -x_q \\ x_d' & 0 \end{bmatrix} \begin{bmatrix} i_d \\ i_q \end{bmatrix}$$

then

$$\Delta V_t = \begin{bmatrix} 0 \\ 1 \end{bmatrix} \Delta e_q' - A_4 \Delta I_g \tag{4.17}$$

where

$$A_4 = \begin{bmatrix} 0 & -x_q \\ x_d' & 0 \end{bmatrix}.$$

Substitution of Eqn.(4.17) into Eqn.(4.15) results in

$$(I + A_1 A_4)\Delta I_g = A_1 \begin{bmatrix} 0 \\ 1 \end{bmatrix} \Delta e_q' - A_2 \Delta V_b + A_3 \begin{bmatrix} -v_{mqo} \\ v_{mdo} \end{bmatrix} \Delta B. \tag{4.18}$$

The change of the infinite bus phasor V_b can be resolved into torque angle variation $\Delta\delta$ as shown below.

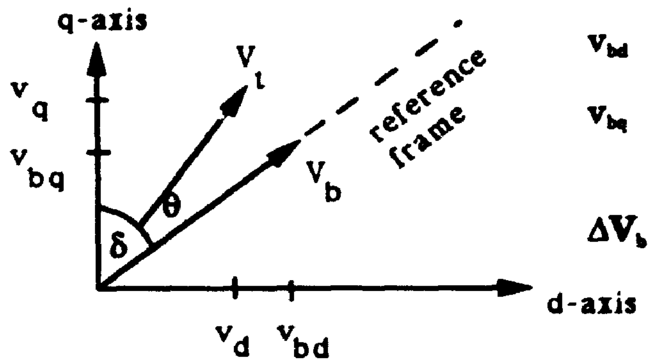

$$v_{bd} = v_b \sin\delta$$

$$v_{bq} = v_b \cos\delta$$

$$\Delta V_b = \begin{bmatrix} \Delta v_{bd} \\ \Delta v_{bq} \end{bmatrix} = v_{bo} \begin{bmatrix} \cos\delta_o \\ -\sin\delta_o \end{bmatrix} \Delta\delta. \tag{4.19}$$

To further simplify the expression in Eqn.(4.18), let

$$E_o = [I + A_1 A_4]^{-1} A_1 \begin{bmatrix} 0 \\ 1 \end{bmatrix}$$

$$F_o = [I + A_1 A_4]^{-1} A_2 \begin{bmatrix} -\cos\delta_o \\ \sin\delta_o \end{bmatrix} v_{bo} \tag{4.20}$$

and

$$G_o = [I + A_1 A_4]^{-1} A_3 \begin{bmatrix} -v_{mqo} \\ v_{mdo} \end{bmatrix}$$

then the generator current variation can be written in a compact form

$$\Delta I_g = E_o \Delta e_q' + F_o \Delta\delta + G_o \Delta B \tag{4.21}$$

or

$$\begin{bmatrix}\Delta I_{gd}\\ \Delta I_{gq}\end{bmatrix} = \begin{bmatrix}E_o^{(1)}\\ E_o^{(2)}\end{bmatrix}\Delta e_g' + \begin{bmatrix}F_o^{(1)}\\ F_o^{(2)}\end{bmatrix}\Delta\delta + \begin{bmatrix}G_o^{(1)}\\ G_o^{(2)}\end{bmatrix}\Delta B. \tag{4.22}$$

Since $\quad V_m = V_t - Z_1 I_1$

$$= V_t - Z_1(I_g - I_t)$$

$$= V_t + Z_1 Y_t V_t - Z_1 I_g$$

then $\quad \Delta V_m = [I + Z_1 Y_t]\Delta V_t - Z_1 \Delta I_g.$

Substituting ΔV_t from Eqn.(4.17) yields

$$\Delta V_m = [I + Z_1 Y_l]\begin{bmatrix}0\\ 1\end{bmatrix}\Delta e_g' - ([I + Z_1 Y_l]A_4 + Z_1)\Delta I_g.$$

Let

$$A_5 = \begin{bmatrix} r_1 & -x_1\\ x_1 & r_1\end{bmatrix} = Y_1^{-1} = \begin{bmatrix} g_1 & -b_1\\ b_1 & g_1\end{bmatrix}^{-1}$$

and $\quad A_6 = [I + Z_1 Y_l]A_4 + Z_1 = [I + A_5 Y_l]A_4 + A_5,$

then $\quad \Delta V_m = [I + Z_1 Y_l]\begin{bmatrix}0\\ 1\end{bmatrix}\Delta e_g' - A_6[E_o \Delta e_q' + F_o \Delta\delta + G_o \Delta B]$

or in a more compact form

$$\Delta V_m = E_q \Delta e_q' + F_1 \Delta\delta + G_1 \Delta B \tag{4.23}$$

or

$$\begin{bmatrix}\Delta v_{md}\\ \Delta v_{mq}\end{bmatrix} = \begin{bmatrix}E_1^{(1)}\\ E_1^{(2)}\end{bmatrix}\Delta e_g' + \begin{bmatrix}F_1^{(1)}\\ F_1^{(2)}\end{bmatrix}\Delta\delta + \begin{bmatrix}G_1^{(1)}\\ G_1^{(2)}\end{bmatrix}\Delta B \tag{4.24}$$

where

$$E_1 = [I + Z_1 Y_l]\begin{bmatrix}0\\ 1\end{bmatrix} - A_6 E_o$$

$$F_1 = - A_6 F_o \tag{4.25}$$

and $G_1 = -A_e G_e$.

4.2.2 Small signal quantities

The changes of the scalar quantities associated with the system subjected to small disturbances can be derived from the small signal equations obtained in the previous subsection. The interesting quantities are electrical torque, terminal voltage and field voltage of the generator and the mid-point voltage of the system.

4.2.2.1 Electrical torque

If the rated angular speed of the generator is selected to be 1 p.u. and the speed variation is assumed to be very small, the electrical torque (T_e) developed in the generator is proportional to the electrical output power (P_e). For convenience, the subscript "g" for generator is dropped at this point in all expressions.

Hence, $$T_e = P_e = i_d v_d + i_q v_q$$
$$= i_q e_q' + (x_q - x_d') i_d i_q$$

and $$\Delta T_e = i_{qo}\Delta e_q' + e_{qo}'\Delta i_q + (x_q - x_d') i_{do}\Delta i_q + (x_q - x_d') i_{qo}\Delta i_d$$
$$= i_{qo}\Delta e_q' + \begin{bmatrix} (x_q - x_d') i_{qo} & e_{qo}' + (x_q - x_d') i_{do} \end{bmatrix} \begin{bmatrix} \Delta i_d \\ \Delta i_q \end{bmatrix} \qquad (4.26)$$

Substitution for Eqn.(4.22) into Eqn.(4.26) yields

$$\Delta T_e = i_{qo}\Delta e_q' + \begin{bmatrix} (x_q - x_d') i_{qo} & e_{qo}' + (x_q - x_d') i_{do} \end{bmatrix} \left[\begin{bmatrix} E_e^{(1)} \\ E_e^{(2)} \end{bmatrix} \Delta e_q' + \begin{bmatrix} F_e^{(1)} \\ F_e^{(2)} \end{bmatrix} \Delta\delta + \begin{bmatrix} G_e^{(1)} \\ G_e^{(2)} \end{bmatrix} \Delta B \right]$$
$$= K_1\Delta\delta + K_2\Delta e_q' + K_9\Delta B \qquad (4.27)$$

$$\text{where}\quad \begin{bmatrix} K_1 \\ K_2 \\ K_9 \end{bmatrix} = \begin{bmatrix} 0 \\ i_{qo} \\ 0 \end{bmatrix} + \begin{bmatrix} F_o^{(1)} & F_o^{(2)} \\ E_o^{(1)} & E_o^{(2)} \\ G_o^{(1)} & G_o^{(2)} \end{bmatrix} \begin{bmatrix} (x_q - x_d')i_{qo} \\ e_{qo}' + (x_q - x_d')i_{do} \end{bmatrix} . \tag{4.28}$$

4.2.2.2 Terminal voltage

Since $V_t^2 = v_{td}^2 + v_{tq}^2$

then $\Delta V_t = \dfrac{v_{tdo}}{v_{to}} \Delta v_{td} + \dfrac{v_{tqo}}{v_{to}} \Delta v_{tq}$

$$\text{or}\quad \Delta V_t = \begin{bmatrix} \dfrac{v_{tdo}}{v_{to}} & \dfrac{v_{tqo}}{v_{to}} \end{bmatrix} \begin{bmatrix} \Delta v_{td} \\ \Delta v_{tq} \end{bmatrix} \tag{4.29}$$

From Eqns.(4.17) and (4.21), one can write

$$\begin{bmatrix} \Delta v_{td} \\ \Delta v_{tq} \end{bmatrix} = \begin{bmatrix} 0 \\ 1 \end{bmatrix} \Delta e_q' - A_4[E_o\Delta e_q' + F_o\Delta\delta + G_o\Delta B]$$

which can be simplified by defining

$$E_2 = \begin{bmatrix} 0 \\ 1 \end{bmatrix} - A_4E_o \ , \quad F_2 = -A_4F_o \quad \text{and} \quad G_2 = -A_4G_o.$$

Therefore

$$\Delta V_t = \begin{bmatrix} \Delta v_{td} \\ \Delta v_{tq} \end{bmatrix} = E_2\Delta e_q' + F_2\Delta\delta + G_2\Delta B \tag{4.30}$$

and

$$\Delta V_t = \begin{bmatrix} \dfrac{v_{tdo}}{v_{to}} & \dfrac{v_{tqo}}{v_{to}} \end{bmatrix} [\, E_2\Delta e_q' + F_2\Delta\delta + G_2\Delta B]$$

$$= K_5\Delta\delta + K_6\Delta e_q' + K_{11}\Delta B \tag{4.31}$$

$$\text{where}\quad \begin{bmatrix} K_5 \\ K_6 \\ K_{11} \end{bmatrix} = \begin{bmatrix} F_2^{(1)} & F_2^{(2)} \\ E_2^{(1)} & E_2^{(2)} \\ G_2^{(1)} & G_2^{(2)} \end{bmatrix} \begin{bmatrix} \dfrac{v_{tdo}}{v_{to}} \\ \dfrac{v_{tqo}}{v_{to}} \end{bmatrix} . \tag{4.32}$$

4.2.2.3 Field voltage

The linearized field voltage can be expressed in the form [17,18]

$$(1+sT_{do}')\Delta e_q' = \Delta E_{FD} - (x_d-x_d')\Delta i_d$$

where T_{do}' is the open-circuit field time constant of the generator. Substitution for Δi_d from Eqn.(4.22) yields

$$(1+sT_{do}'+(x_d-x_d')E_o^{(1)})\Delta e_q' = \Delta E_{FD} - (x_d-x_d')F_o^{(1)}\Delta\delta - (x_d-x_d')G_o^{(1)}\Delta B$$

let

$$K_3 = (1+(x_d-x_d')E_o^{(1)})^{-1}$$
$$K_4 = (x_d-x_d')F_o^{(1)} \qquad (4.33)$$
$$K_{10} = (x_d-x_d')G_o^{(1)}$$

then

$$(1+sT_{do}'K_3)\Delta e_q' = K_3(\Delta E_{FD} - K_4\Delta\delta - K_{10}\Delta B) \qquad (4.34)$$

4.2.2.4 Mid-point voltage

Since $V_m^2 = v_{md}^2 + v_{mq}^2$

then $$\Delta V_m = \frac{v_{mdo}}{V_{mo}}\Delta v_{md} + \frac{v_{mqo}}{V_{mo}}\Delta v_{mq}$$

or $$\Delta V_m = \begin{bmatrix} \frac{v_{mdo}}{V_{mo}} & \frac{v_{mqo}}{V_{mo}} \end{bmatrix} \begin{bmatrix} \Delta v_{md} \\ \Delta v_{mq} \end{bmatrix} \qquad (4.35)$$

Substitution from Eqn.(4.24) in Eqn.(4.29) yields

$$\Delta V_m = \begin{bmatrix} \frac{v_{mdo}}{V_{mo}} & \frac{v_{mqo}}{V_{mo}} \end{bmatrix} \left[\begin{bmatrix} E_1^{(1)} \\ E_1^{(2)} \end{bmatrix} \Delta e_q' + \begin{bmatrix} F_1^{(1)} \\ F_1^{(2)} \end{bmatrix} \Delta\delta + \begin{bmatrix} G_1^{(1)} \\ G_1^{(2)} \end{bmatrix} \Delta B \right]$$

$$= K_7\Delta\delta + K_8\Delta e_q' + K_{12}\Delta B \qquad (4.36)$$

where $$\begin{bmatrix} K_7 \\ K_8 \\ K_{12} \end{bmatrix} = \begin{bmatrix} F_1^{(1)} & F_1^{(2)} \\ E_1^{(1)} & E_1^{(2)} \\ G_1^{(1)} & G_1^{(2)} \end{bmatrix} \begin{bmatrix} \frac{v_{mdo}}{V_{mo}} \\ \frac{v_{mqo}}{V_{mo}} \end{bmatrix}. \qquad (4.37)$$

From Eqn.(4.36) it is seen that the mid-point voltage variation is related to the variations of the generator load angle, its internal voltage and indeed to the variation of SVC susceptance. When operating in voltage control mode, the SVC essentially regulates Δ B. In damping control mode, ΔV_m is made to vary for which the SVC regulates ΔB. This variation in ΔV_m produces power modulation which adds damping to the system. The behavior of stabilizing control in SVC is akin to a PSS in a generator.

4.2.2.5 Small signal model-block diagram

Relationships given by equations (4.27), (4.31), (4.34) and (4.36) are represented by the block diagram in Fig. 4.2

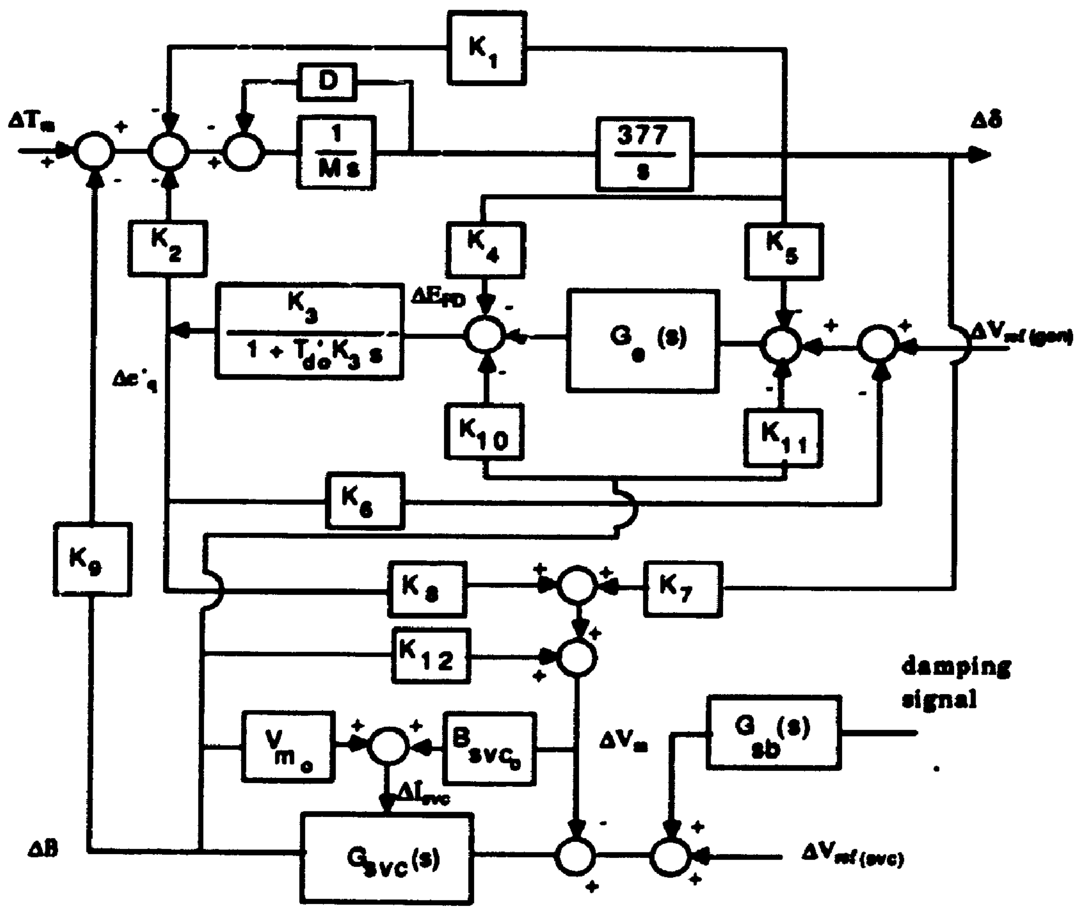

Fig. 4.2 : Small signal dynamic model of a SMIB system with a SVC

4.2.3 Damping signals for the SVC

As the purpose of this study is to seek the effectiveness of damping controls on the SVC, three damping signals are examined. These are line current, real power and reactive power flows on the transmission line. In the following subsections the model constants related to the block diagram of Fig. 4.2 are derived.

4.2.3.1 Line current

The change in line current ΔI_1 derived from Eqn.(4.2) is

$$\Delta I_1 = Y_1(\Delta V_t - \Delta V_m) \qquad (1.11)$$

and by substituting ΔV_t and ΔV_m from Eqns.(4.33) and (4.24) it becomes

$$\begin{bmatrix}\Delta i_d\\ \Delta i_q\end{bmatrix} = \begin{bmatrix}g_1 & -b_1\\ b_1 & g_1\end{bmatrix}\left[\begin{bmatrix}\Delta v_{td}\\ \Delta v_{tq}\end{bmatrix} - \begin{bmatrix}\Delta v_{md}\\ \Delta v_{mq}\end{bmatrix}\right]$$

$$= \begin{bmatrix}g_1 & -b_1\\ b_1 & g_1\end{bmatrix}\left[\begin{bmatrix}E_2^{(1)}-E_1^{(1)}\\ E_2^{(2)}-E_1^{(2)}\end{bmatrix} \begin{bmatrix}F_2^{(1)}-F_1^{(1)}\\ F_2^{(2)}-F_1^{(2)}\end{bmatrix} \begin{bmatrix}G_2^{(1)}-G_1^{(1)}\\ G_2^{(2)}-G_1^{(2)}\end{bmatrix}\right]\begin{bmatrix}\Delta e_q'\\ \Delta\delta\\ \Delta B\end{bmatrix}$$

Let $E_3 = Y_1(E_2-E_1)$, $F_3 = Y_1(F_2-F_1)$ and $G_3 = Y_1(G_2-G_1)$

then
$$\begin{bmatrix}\Delta i_{1d}\\ \Delta i_{1q}\end{bmatrix} = \begin{bmatrix}E_3^{(1)}\\ E_3^{(2)}\end{bmatrix}\Delta e_q' + \begin{bmatrix}F_3^{(1)}\\ F_3^{(2)}\end{bmatrix}\Delta\delta + \begin{bmatrix}G_3^{(1)}\\ G_3^{(2)}\end{bmatrix}\Delta B \qquad (4.38)$$

since
$$I_1^2 = i_{1d}^2 + i_{1q}^2$$

then
$$\Delta I_1 = \frac{i_{1do}}{i_{1o}}\Delta i_{1d} + \frac{i_{1qo}}{i_{1o}}\Delta i_{1q}$$

or
$$\Delta I_t = \begin{bmatrix}\frac{i_{1do}}{i_{1o}} & \frac{i_{1qo}}{i_{1o}}\end{bmatrix}\begin{bmatrix}\Delta i_{1d}\\ \Delta i_{1q}\end{bmatrix}$$

Therefore
$$\Delta I_1 = K_{13}\Delta\delta + K_{14}\Delta e_q' + K_{15}\Delta B \qquad (4.39)$$

$$\text{where} \quad \begin{bmatrix} K_{13} \\ K_{14} \\ K_{15} \end{bmatrix} = \begin{bmatrix} F_3^{(1)} & F_3^{(2)} \\ E_3^{(1)} & E_3^{(2)} \\ G_3^{(1)} & G_3^{(2)} \end{bmatrix} \begin{bmatrix} \frac{i_{1do}}{I_{1o}} \\ \frac{i_{1qo}}{I_{1o}} \end{bmatrix}. \tag{4.40}$$

4.2.3.2 Line active-power

The power flow on the line measured at the SVC can be expressed as

$$P_{line} = P_e - V_t^2 g_t - I_1^2 r_1$$

or

$$\Delta P_{line} = \Delta P_e - 2V_{to} g_t \Delta V_t - 2I_{1o} r_1 \Delta I_1.$$

From Eqns.(4.27),(4.34) and (4.39) the changes of line power becomes

$$\begin{aligned} \Delta P_{line} = & (K_1 - 2V_{to} g_t K_5 - 2I_{1o} r_1 K_{13}) \Delta\delta \\ & + (K_2 - 2V_{to} g_t K_6 - 2I_{1o} r_1 K_{14}) \Delta e_q' \\ & + (K_9 - 2V_{to} g_t K_{11} - 2I_{1o} r_1 K_{15}) \Delta B \end{aligned}$$

thus

$$\Delta P_{line} = K_{16} \Delta\delta + K_{17} \Delta e_q' + K_{18} \Delta B \tag{4.41}$$

4.2.3.3 Line reactive-power

The reactive power flow on the line taken at the SVC location is

$$Q_{line} = Q_e + V_t^2 b_t - I_1^2 x_1$$

or

$$\Delta Q_{line} = \Delta Q_e + 2V_{to} b_t \Delta V_t - 2I_{1o} x_1 \Delta I_1.$$

since

$$\begin{aligned} Q_e &= v_q i_d - v_d i_q \\ &= (e_q' - x_d' i_d) i_d - x_q i_q^2 \\ &= e_q' i_d - x_d' i_d^2 - x_q i_q^2 \end{aligned}$$

then

$$\begin{aligned} \Delta Q_e &= i_{do} \Delta e_q' - (e_{qo}' - 2x_d' i_{do}) \Delta i_d - 2x_q i_{qo} \Delta i_q \\ &= i_{do} \Delta e_q' - [e_{qo}' - 2x_d' i_{do} \;\; -2x_q i_{qo}] \begin{bmatrix} \Delta i_d \\ \Delta i_q \end{bmatrix} \end{aligned}$$

Substituting Eqn.(4.22) for the generator current yields

$$\Delta Q_e = i_{do}\Delta e_q' + [e_{qo}' - 2x_d' i_{do} \quad -2x_q i_{qo}] \left[\begin{bmatrix} E_0^{(1)} \\ E_0^{(2)} \end{bmatrix} \Delta e_q' + \begin{bmatrix} F_0^{(1)} \\ F_0^{(2)} \end{bmatrix} \Delta\delta + \begin{bmatrix} G_0^{(1)} \\ G_0^{(2)} \end{bmatrix} \Delta B \right]$$

$$= K_{19}\Delta\delta + K_{20}\Delta e_q' + K_{21}\Delta B \tag{4.42}$$

where
$$\begin{bmatrix} K_{19} \\ K_{20} \\ K_{21} \end{bmatrix} = \begin{bmatrix} 0 \\ i_{do} \\ 0 \end{bmatrix} + \begin{bmatrix} F_o^{(1)} & F_o^{(2)} \\ E_o^{(1)} & E_o^{(2)} \\ G_o^{(1)} & G_o^{(2)} \end{bmatrix} \begin{bmatrix} e_{qo}' - 2x_d' i_{do} \\ -2x_q i_{qo} \end{bmatrix} . \tag{4.43}$$

Hence
$$\Delta Q_{line} = (K_{19} + 2V_{to}b_t K_5 - 2I_{1o}x_1 K_{13})\Delta\delta$$
$$+ (K_{20} + 2V_{to}b_t K_6 - 2I_{1o}x_1 K_{14})\Delta e_q'$$
$$+ (K_{21} + 2V_{to}b_t K_{11} - 2I_{1o}x_1 K_{15})\Delta B$$
$$= K_{22}\Delta\delta + K_{23}\Delta e_q' + K_{24}\Delta B \tag{4.44}$$

4.2.4 Summary of small signal quantities

$$\Delta T_e = K_1\Delta\delta + K_2\Delta e_q' + K_9\Delta B \tag{4.27}$$

$$\Delta V_t = K_5\Delta\delta + K_6\Delta e_q' + K_{11}\Delta B \tag{4.31}$$

$$\Delta V_m = K_7\Delta\delta + K_8\Delta e_q' + K_{12}\Delta B \tag{4.35}$$

$$(1+sT_{do}'K_3)\Delta e_q' = K_3(\Delta E_{FD} - K_4\Delta\delta - K_{10}\Delta B) \tag{4.34}$$

$$\Delta I_1 = K_{13}\Delta\delta + K_{14}\Delta e_q' + K_{15}\Delta B \tag{4.39}$$

$$\Delta P_{line} = K_{16}\Delta\delta + K_{17}\Delta e_q' + K_{18}\Delta B \tag{4.41}$$

and
$$\Delta Q_{line} = K_{22}\Delta\delta + K_{23}\Delta e_q' + K_{24}\Delta B \tag{4.44}$$

4.3 Model parameters

The constants K's derived in the previous section are system dependent. The following typical system parameters, in per unit values, are chosen to illustrate the numerical values of the constants K's and their variations with the generated power.

$r_1 = r_2 = 0.01$, $x_1 = x_2 = 0.4$

$Y_t = Y_m = 0.1 - j0.05$, $V_b = 1.0$ and $P_e = 0.2$ to 1.0

A computer program is written to calculate the values of these constants (K's) for any condition. The calculated values of K_1 to K_{24} at discrete point in the entire range of generated power and as functions of B_{svc} are shown in Figs. 4.3(a) to 4.3(x) respectively.

It can be seen that most of the constants vary with the generated power and the SVC susceptance. The variations of K_1 to K_6 are similar to those reported in [19] where they are plotted as a function of real and reactive power of the generator. The other constants K_7 to K_{24} are newly introduced. As can be seen from the results in Fig.(4.3) the constant K_3 which is a function of only the network and SVC admittances is independent of the power flow on the line whereas K_2, K_4, $K_{9\text{-}12}$, $K_{17\text{-}24}$ increase in value as the power increase, constants $K_{5\text{-}8}$, and K_{13} reduce with increasing power and constants K_1, $K_{15\text{-}16}$ initially increase and then decrease with increa·ī· ᵛ power.

Examination oɩ ɾigs.4.3(a) and 4.3(p) shows that the values of K_1 and K_{16} are approximately equal and that the value of B_{svc} has significant infl·ence on the on the values of K_1 and K_{16} as it modifies the line impedance and therefore the P,δ relationship.

Figs. 4.3(k) and 4.3(l) show the sensitivity of the terminal and midpoint line voltages to the variation in the SVC susceptance. Although the values of K_{11} and K_{12} do not change much with the power flow on the

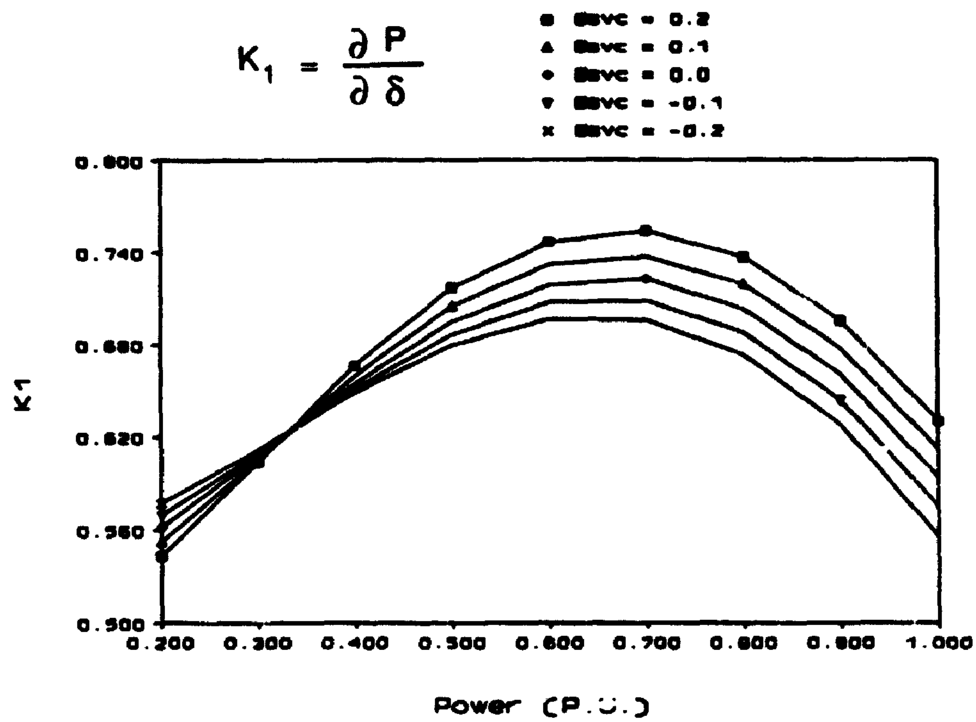

Fig. 4.3(a) : Constant K_1

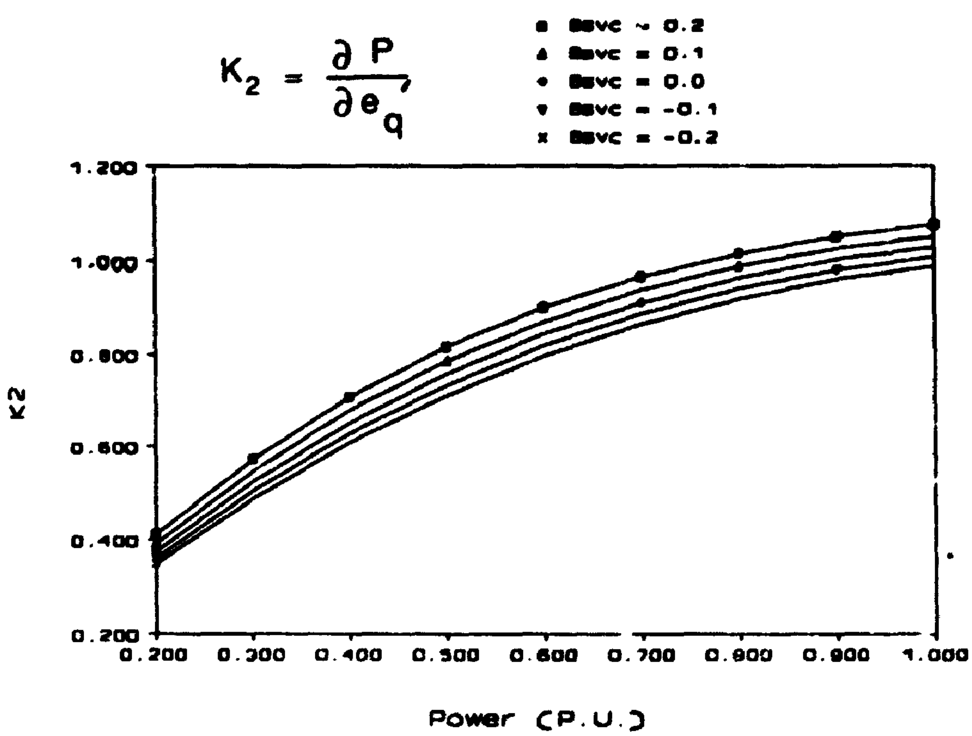

Fig. 4.3(b) : Constant K_2

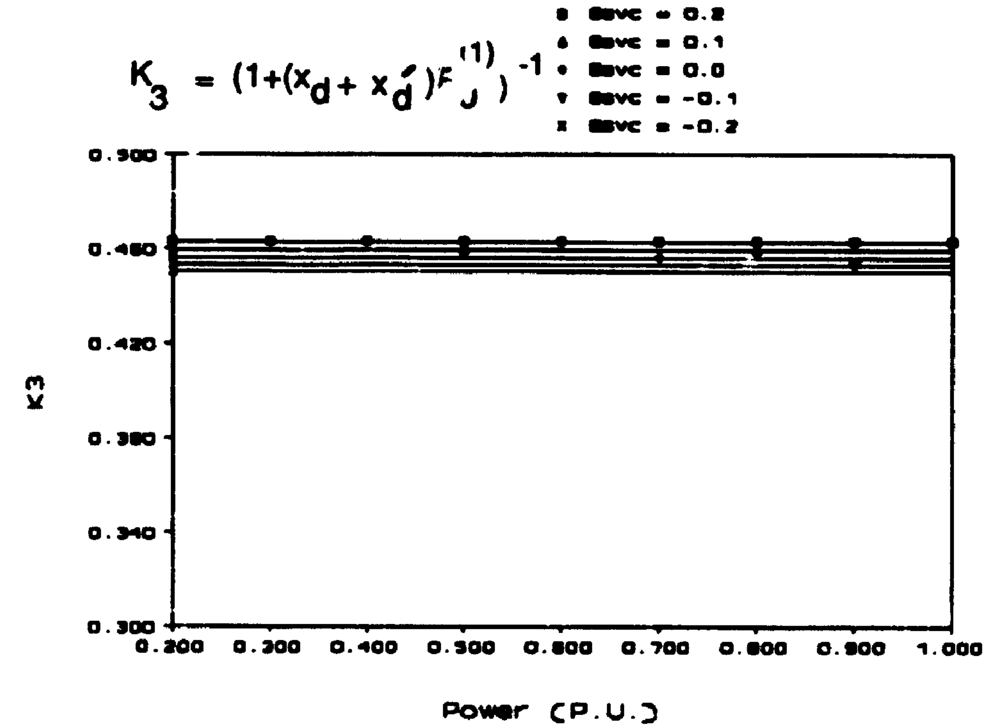

Fig. 4.3(c) : Constant K_3

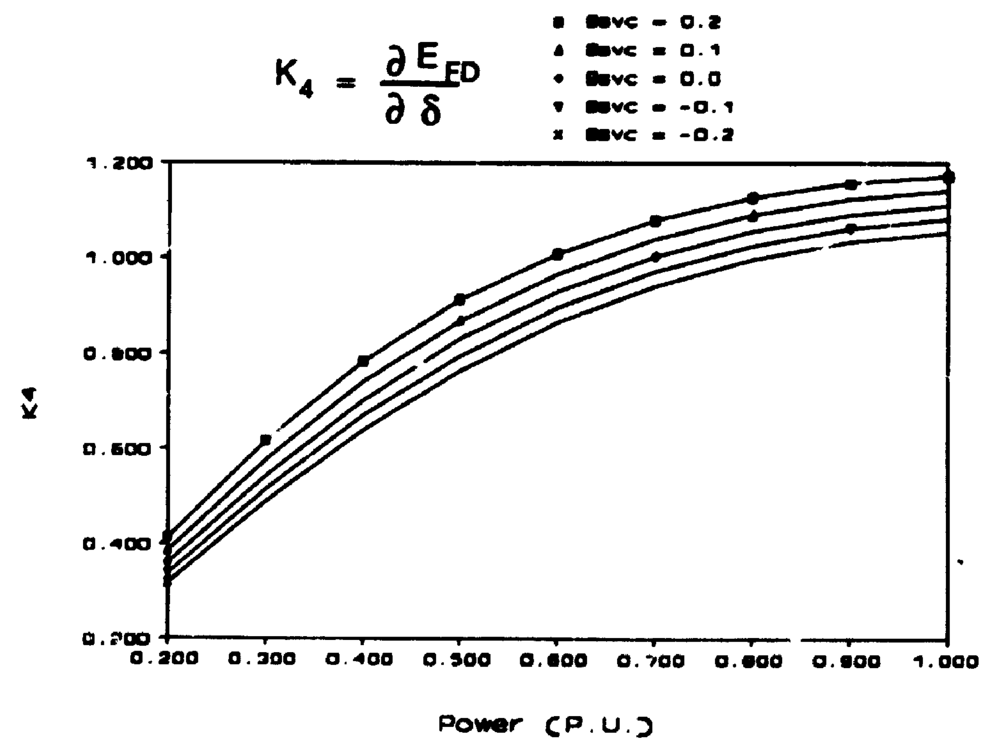

Fig. 4.3(d) : Constant K_4

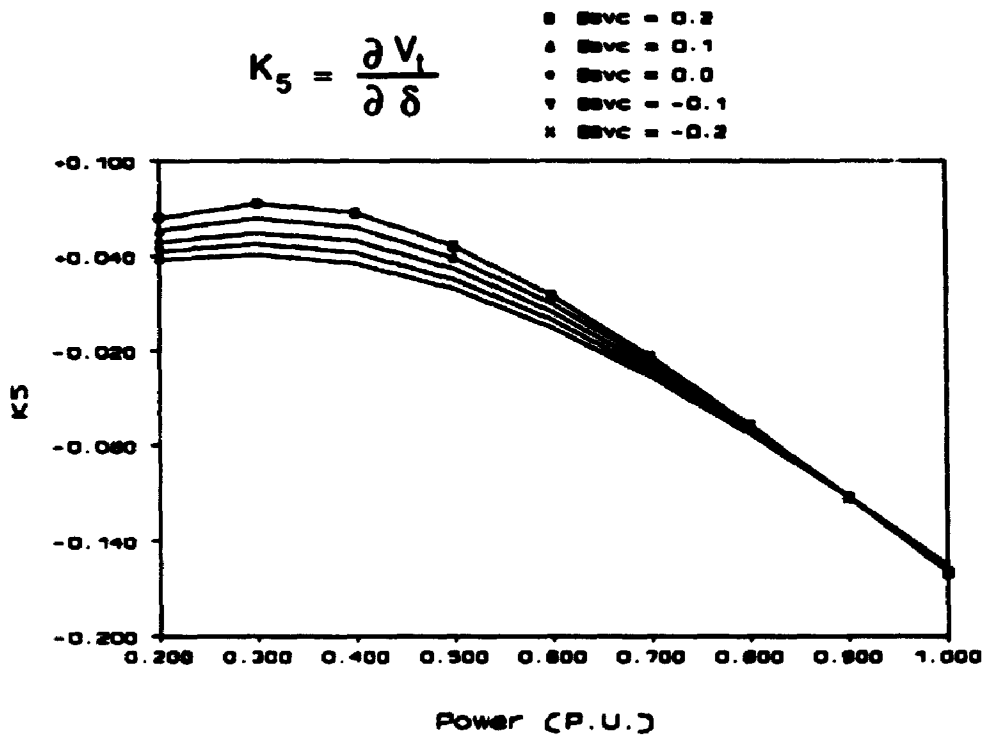

Fig. 4.3(e) : Constant K_5

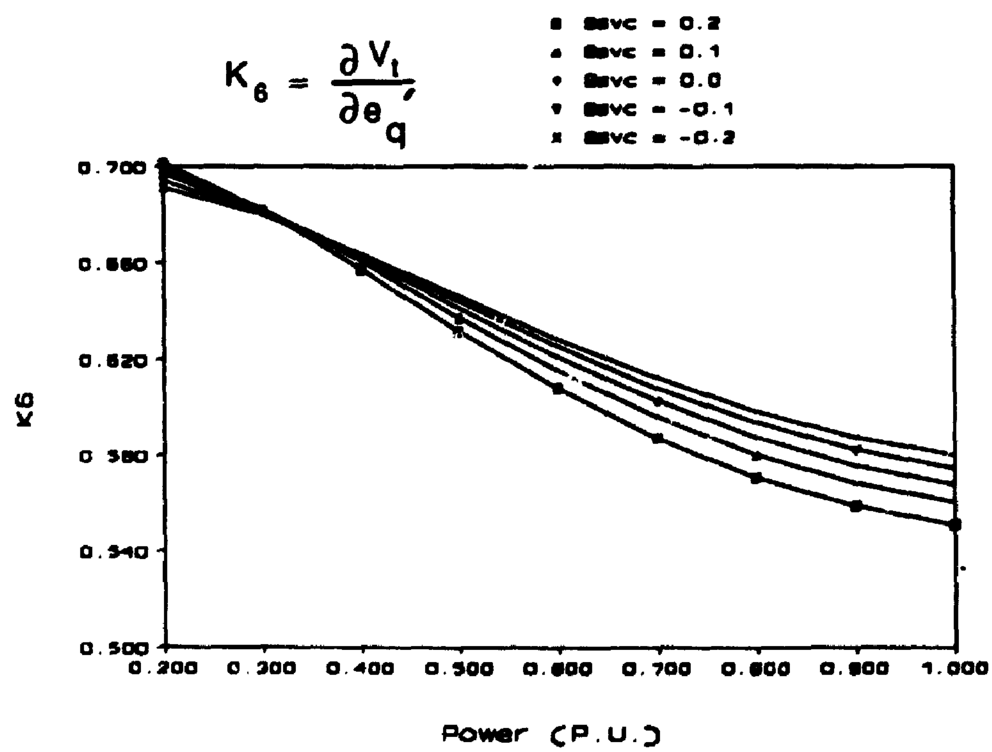

Fig. 4.3(f) : Constant K_6

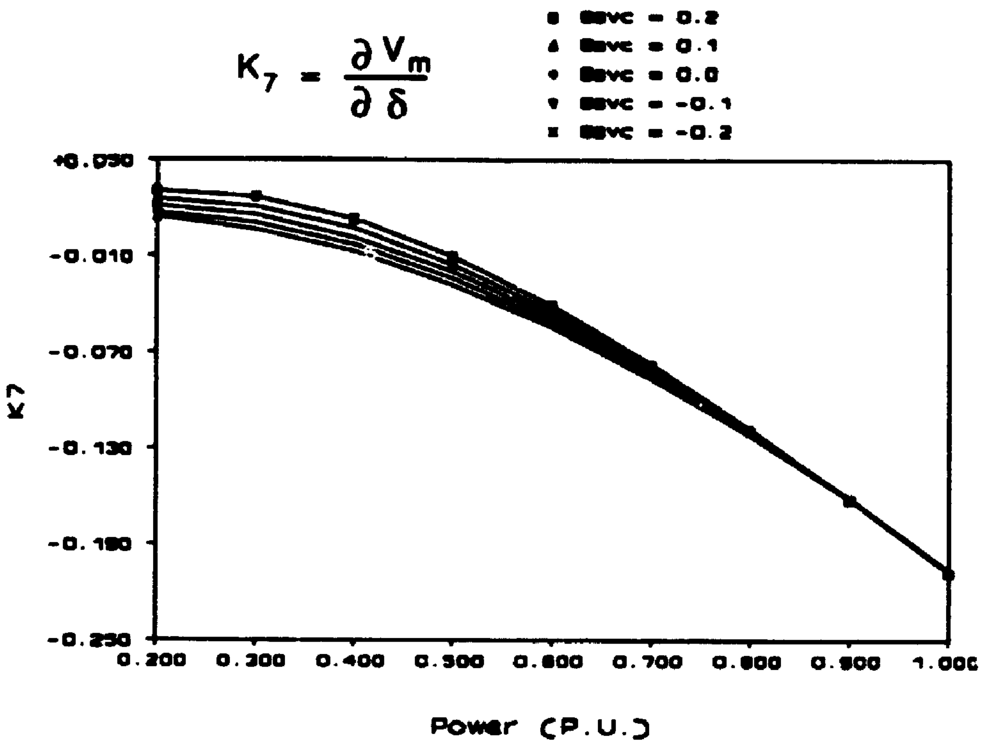

Fig. 4.3(g) : Constant K_7

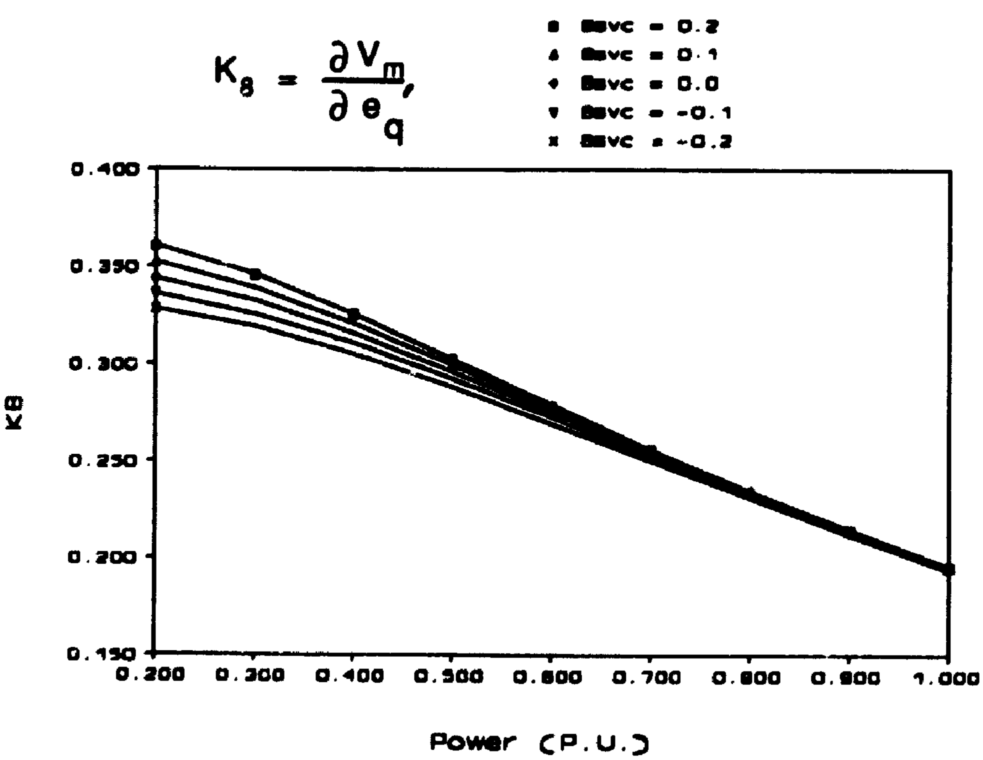

Fig. 4.3(h) : Constant K_8

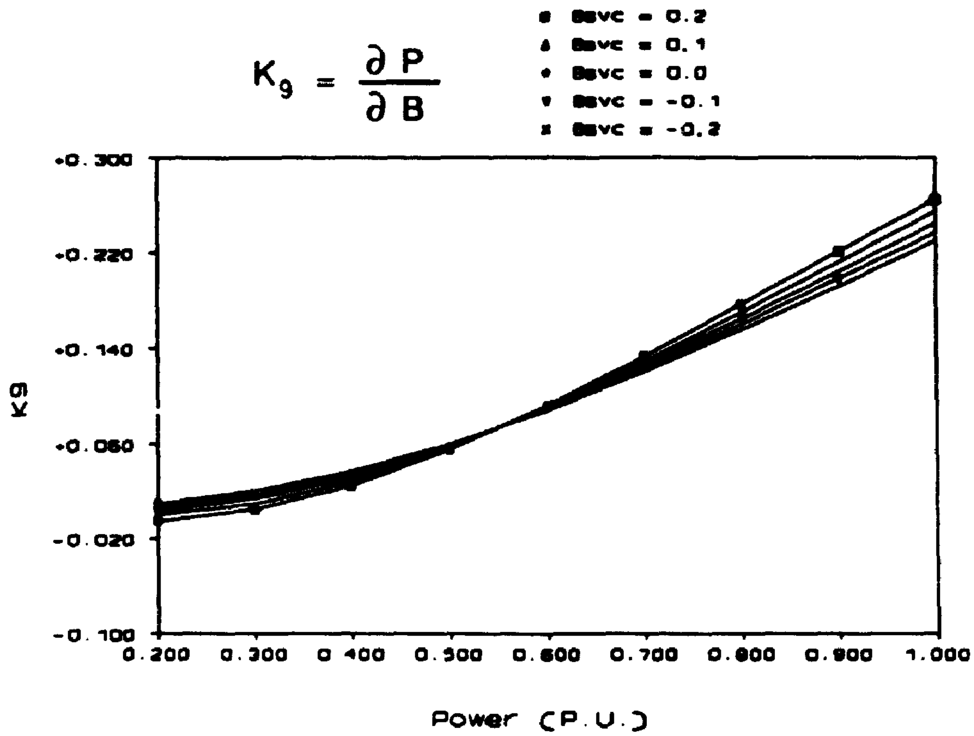

Fig. 4.3(i) : Constant K_9

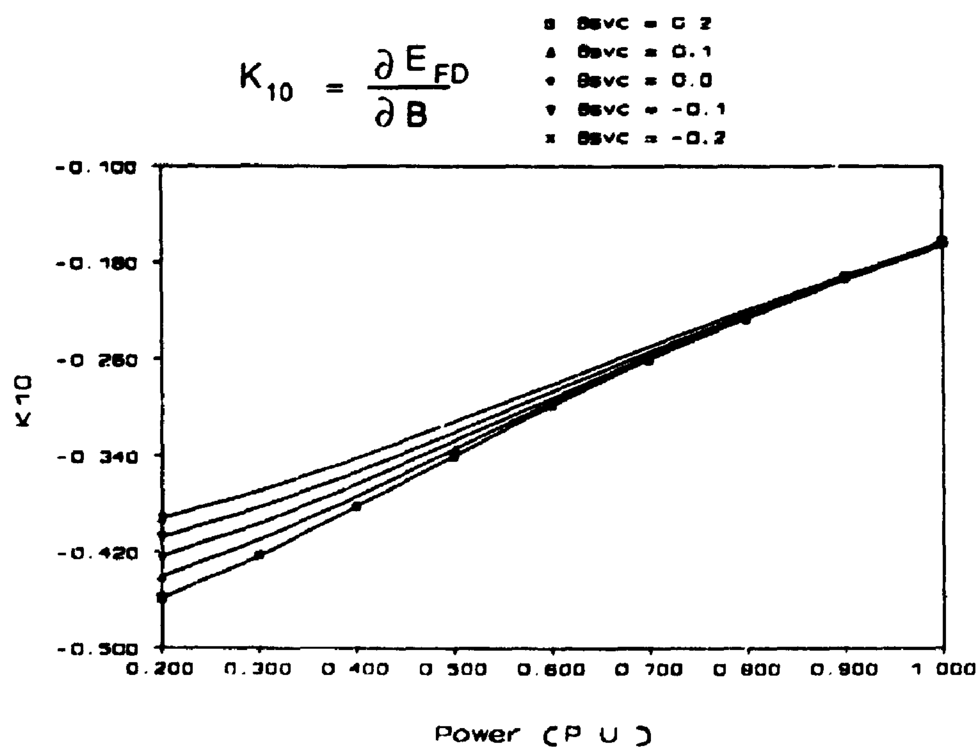

Fig. 4.3(j) : Constant K_{10}

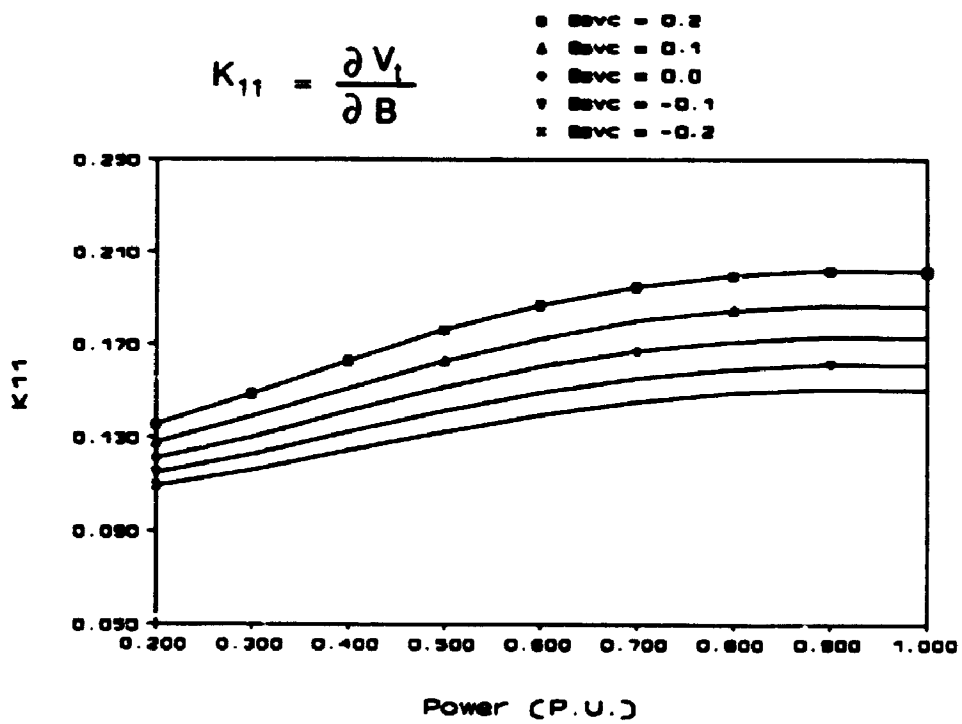

Fig. 4.3(k) : Consatnt K_{11}

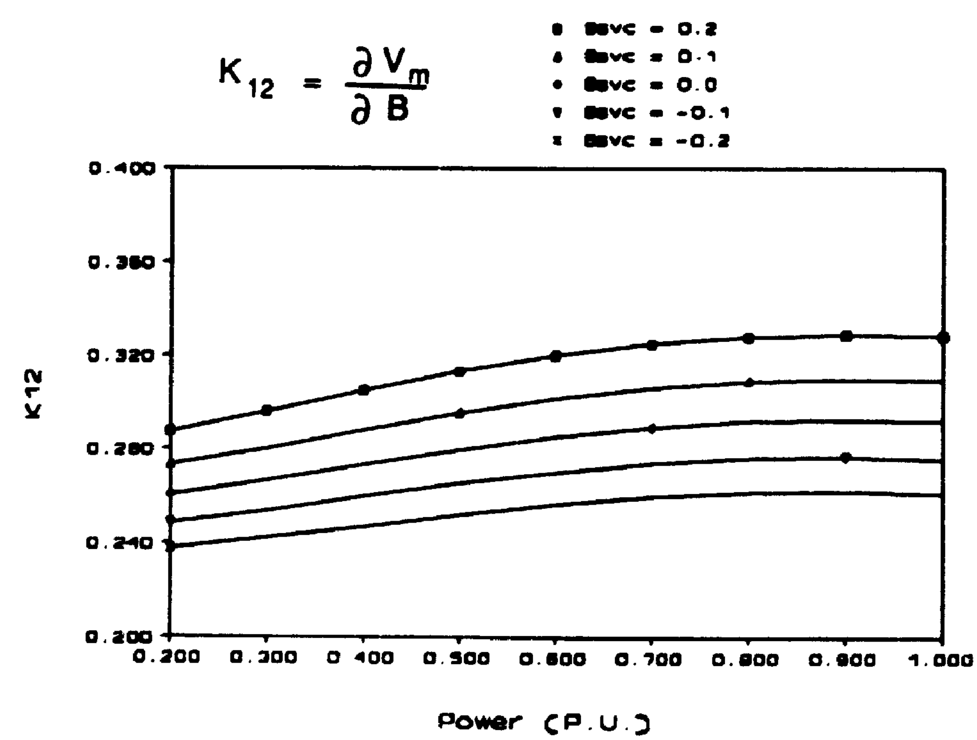

Fig. 4.3(l) : Constant K_{12}

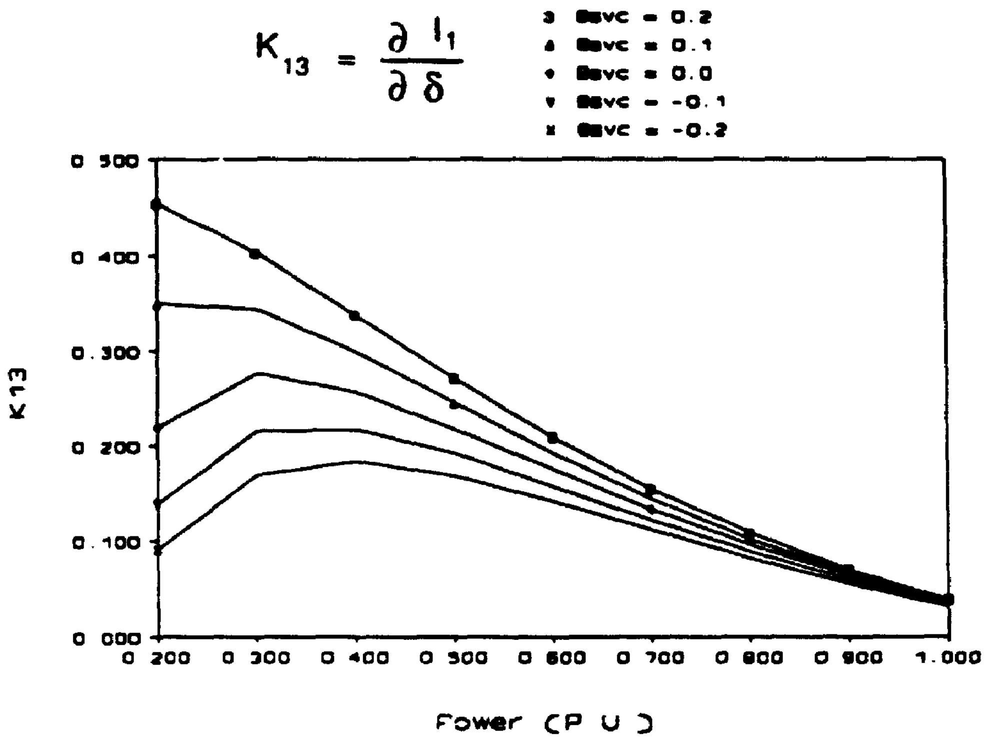

Fig. 4.3(m) : Constant K_{13}

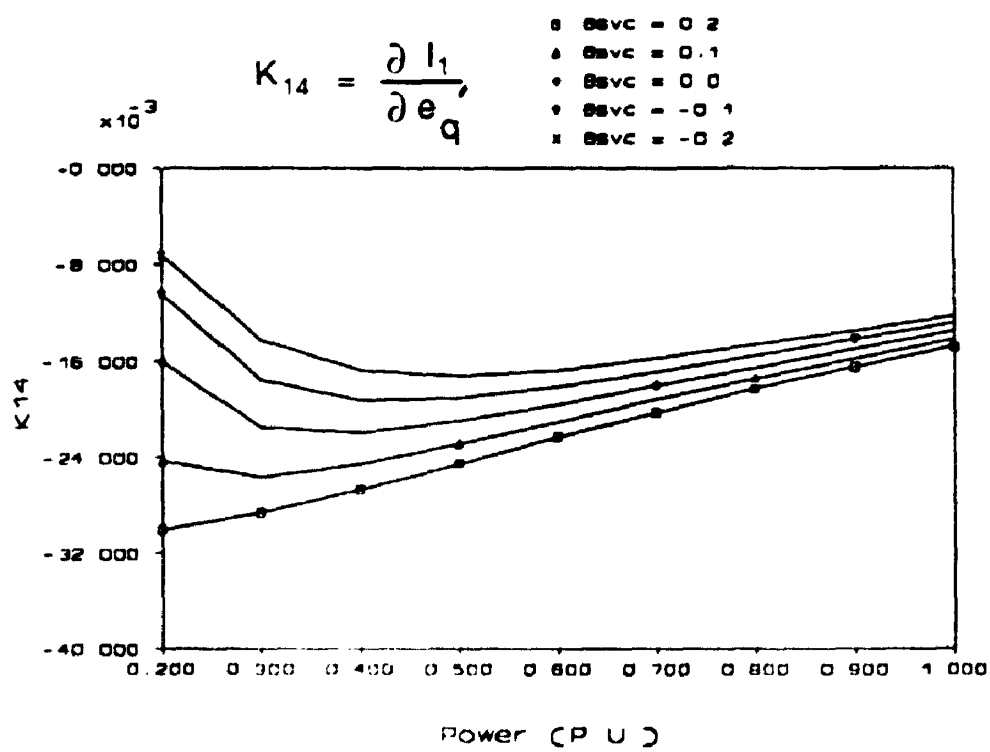

Fig. 4.3(n) : Constant K_{14}

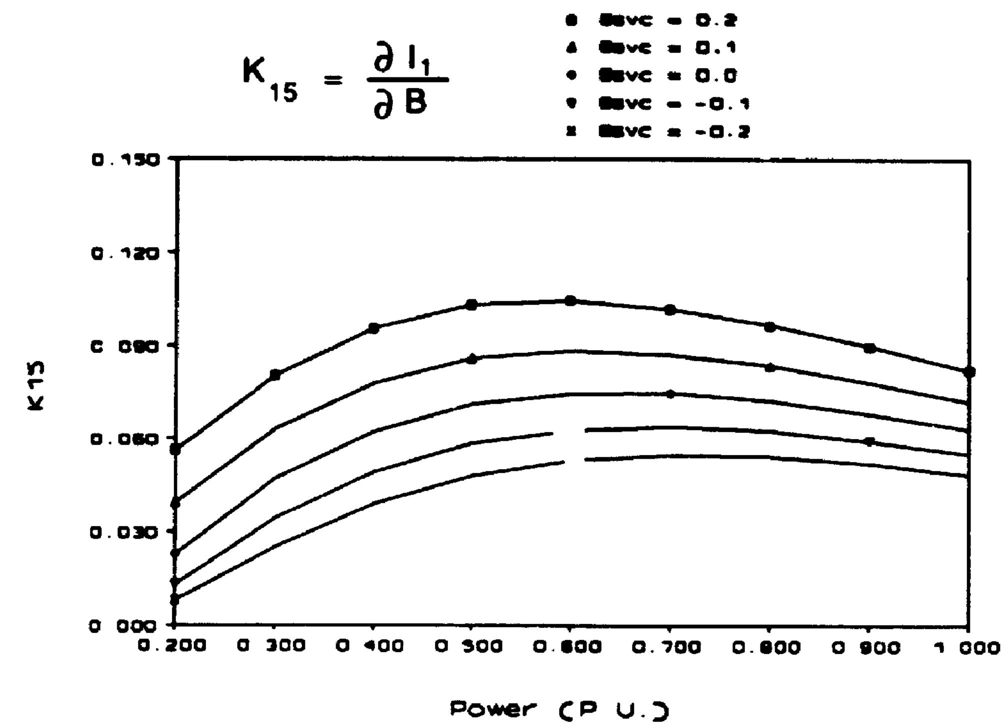

Fig. 4.3(o) : Constant K_{15}

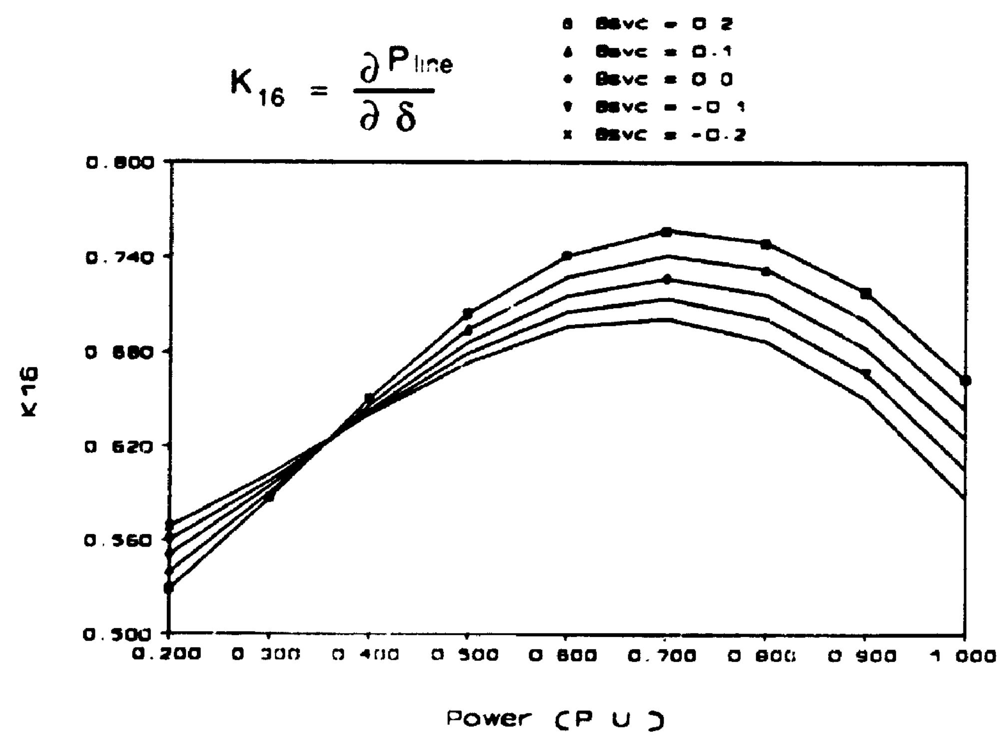

Fig. 4.3(p) : Constant K_{16}

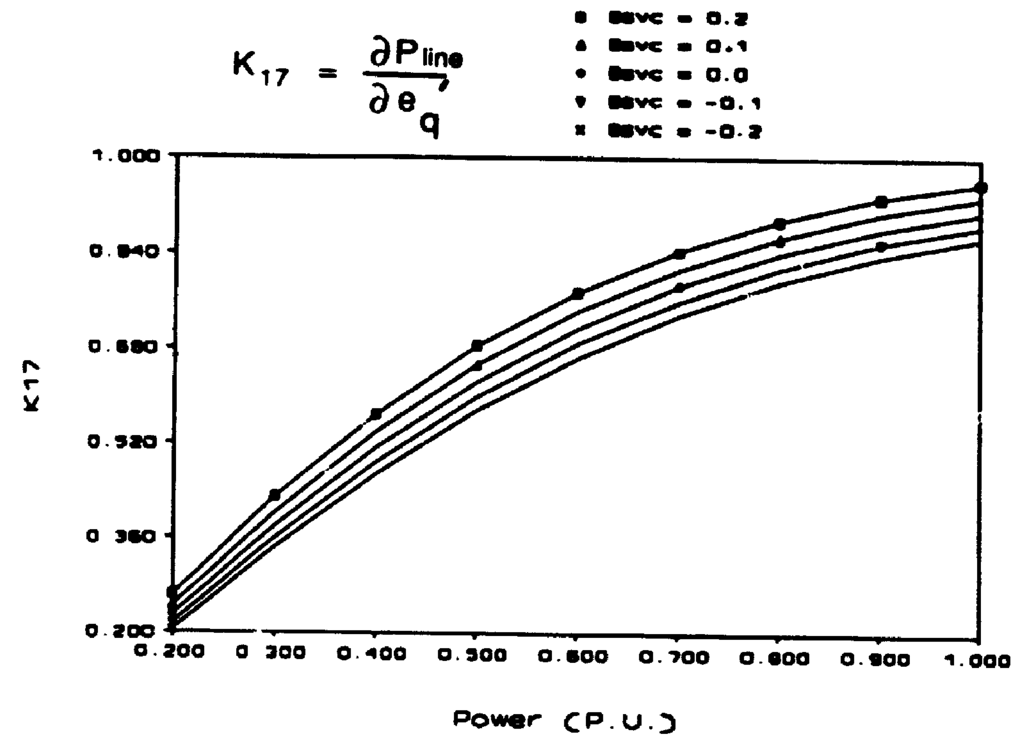

Fig. 4.3(q) : Constant K_{17}

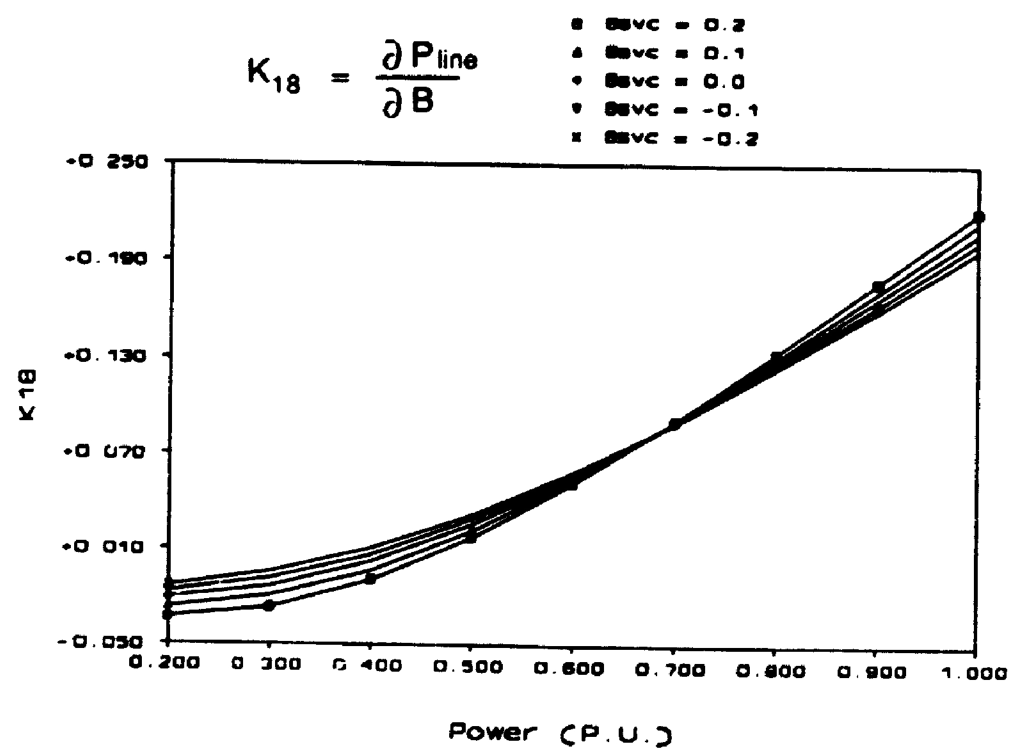

Fig. 4.3(r) : Connstant K_{18}

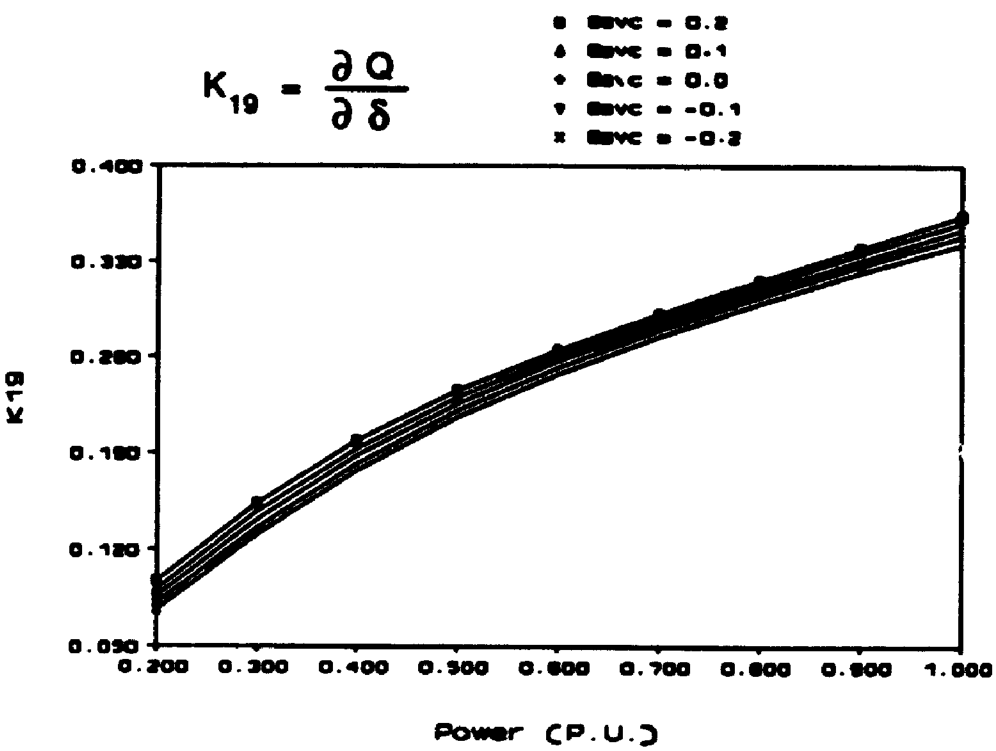

Fig. 4.3(s) : Constant K_{19}

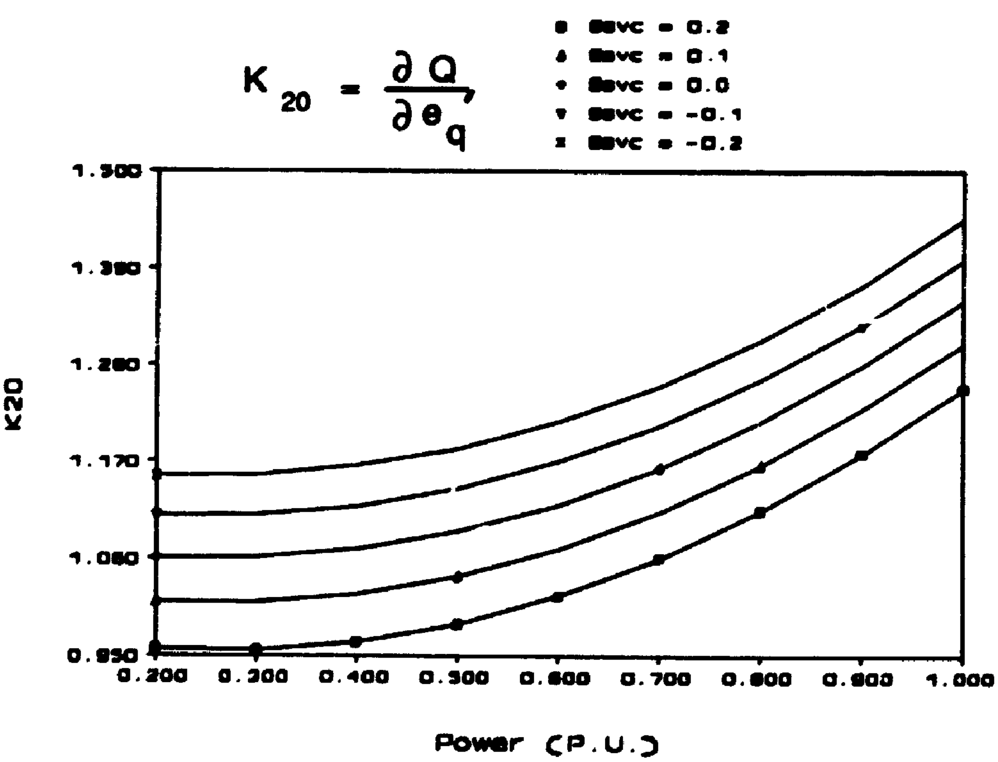

Fig. 4.3(t) : Constant K_{20}

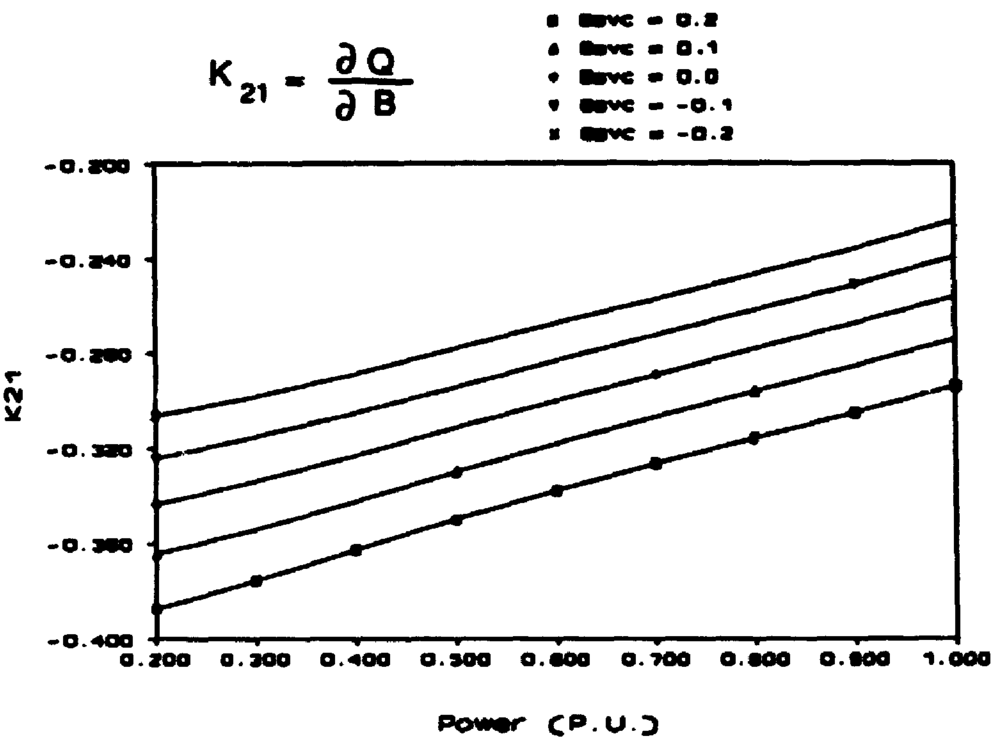

Fig. 4.3(u) : Constant K_{21}

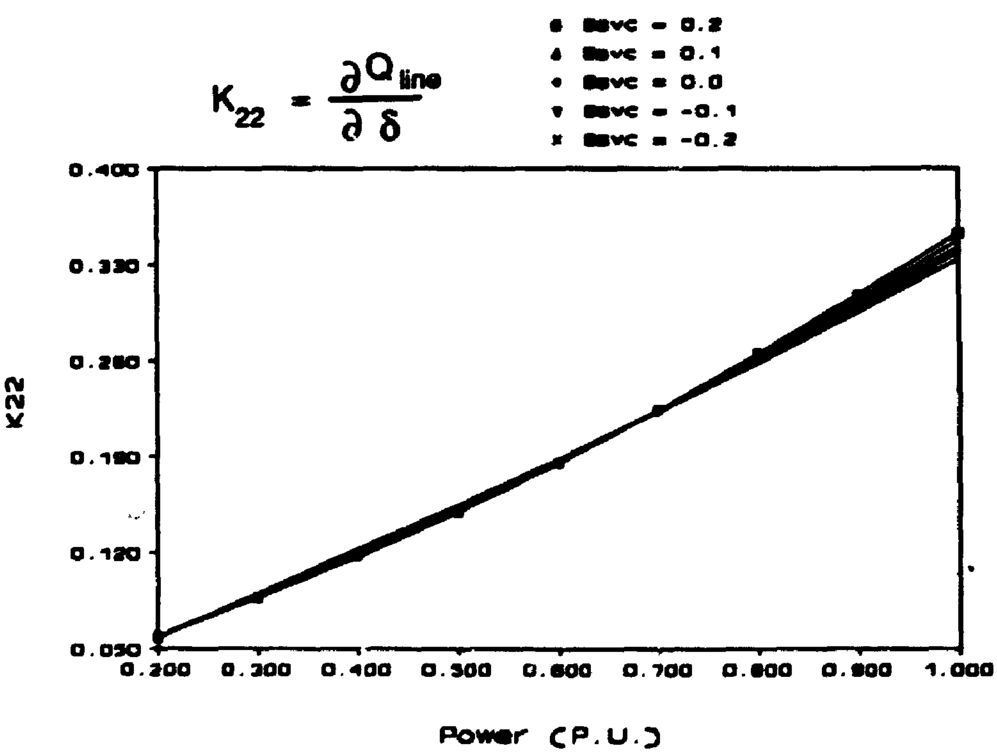

Fig. 4.3(v) : Constant K_{22}

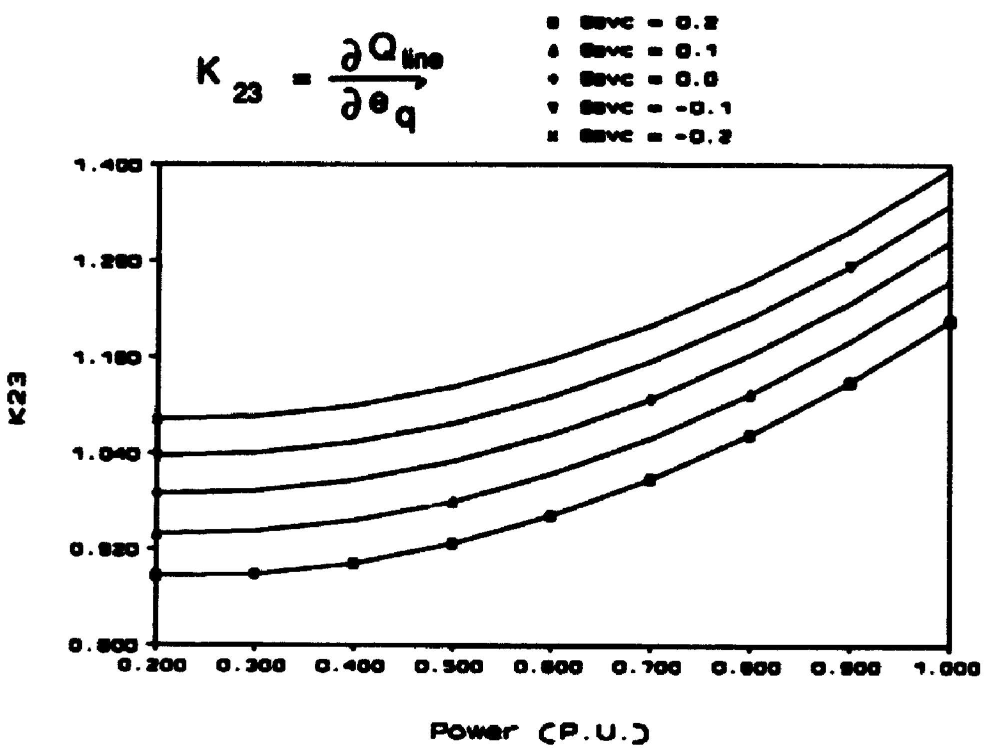

Fig. 4.3(w) : Constant K_{23}

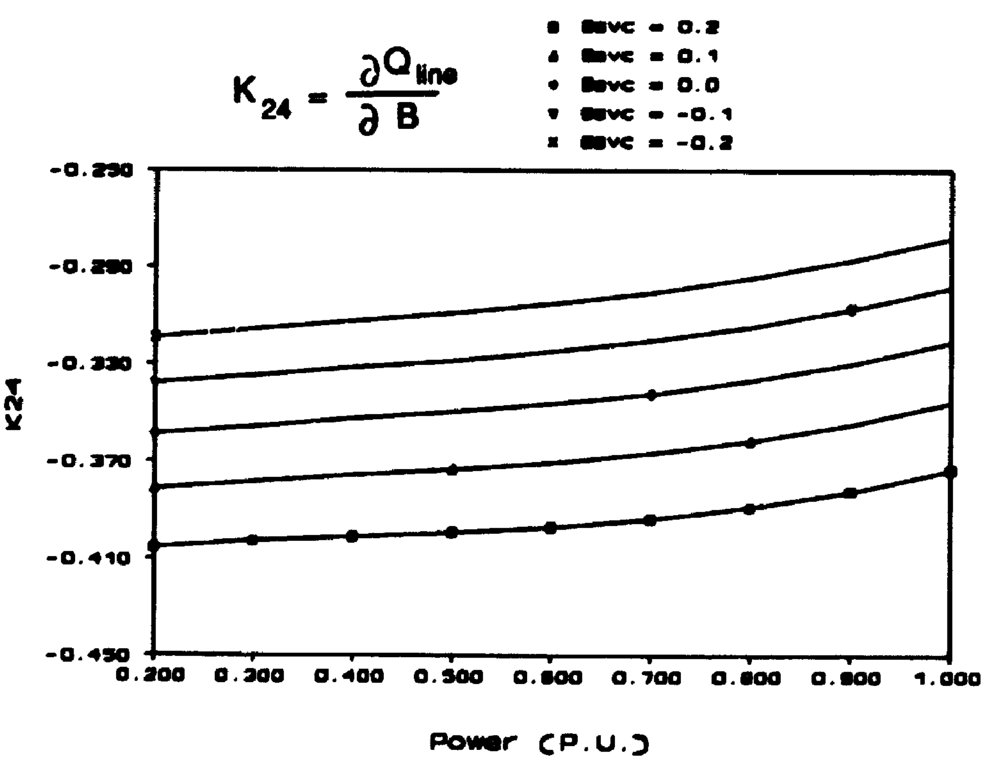

Fig. 4.3(x) : Constant K_{24}

line however, as expected their values depend significantly on the value of B_{svc}. Also the values of K_{11} and K_{12} are highest when the SVC operates in the capacitive range.

Values of K_{20-21}, K_{23-24} in Figs.4.3(t),(u),(w) and (x) are expected to change significantly with the value of B_{svc} as all of these constants are related to the changes in the reactive power of the line. It is also to be expected that the values of these constants will be highest when the SVC operates in the inductive range. Figs. 4.3(s) and 4.3(v) which depict K_{19} and K_{22} (variation of Q with respect to variation δ) are shown not to change appreciably with B_{svc} as the reactive power flow on a line has a weak coupling with the load angle δ.

4.4 System dynamics

The model developed in the preceding section is valid for any type of controller for the exciter and the SVC. However, the dynamics of the system being described in the following subsections is based on the IEEE type 1 rotating exciter and a PI controller for the SVC. The models of the exciter and that of the SVC are illustrated in Fig. 4.4.

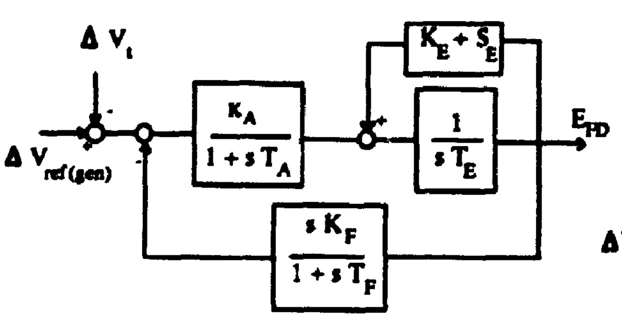

a) IEEE type 1 exciter

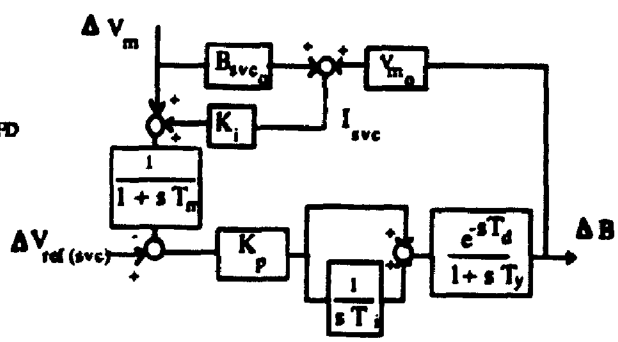

b) SVC model with PI controller

Fig. 4.4 : Dynamic models of the exciter and the SVC

4.4.1 Optimal control parameters

The dynamic behaviour of the system depends strongly on the chosen values of the controlled parameters. Thus these parameters must be optimally determined. State-space equations of the system can be written from the models of Figs. 4.2 and 4.4 and are of the general forms

$$\dot{x} = Ax + Bu$$

$$y = Cx.$$

The elements of the system matrix A are implicit functions of the constants K, system parameters, gain values and time constants of the controllers. Eigenvalue analysis and non-linear optimization technique are applied to determine the optimal set of the controlled parameters.

The objective function is to minimize the real part of the dominant eigenvalue subjected to the constraints that the real part of all eigenvalues are negative and the damping ratio of other complex eigenvalues are within 0.3-0.7.

4.4.1.1 Exciter control parameters

The optimal control parameters of the exciter are obtained for the system without the application of the SVC to realize a practical situation that these parameters should not unnecessarily be adjusted with the application of the SVC. The machine parameters taken from [16] and are given below in p.u. values

$x_d = 1.6$ $x_d' = 0.32$ $x_q = 1.55$ $T_{do}' = 5.9$ s

$M = 2H = 4.74$ $D = 0.0$ $\omega_b = 377.0$.

Typical values of the exciter are [18]

$K_A = 45$ $T_A = 0.05$ s $S_E = 0.074$

$K_E = -.05$ $T_E = 0.5$ s $V_{ref(gen)} = 1.05$ p.u.

The optimal values of K_F and T_F are determined by a multi-variable Pattern search optimization method. The optimized values of K_F and T_F for the entire operating range of the generated power obtained from the analysis are illustrated in Figs. 4.5(a) and 4.5(b) respectively. The average values of K_F and T_F over the operating range are chosen and found to be

$K_{F(opt)} = 0.045$ and $T_{F(opt)} = 2$ s.

4.4.1.2 SVC control parameters

The current droop K_i, reference voltage in p.u. and times constants associated with the SVC are chosen to be

$K_i = .02$, $T_m = 0.016$, $T_d = 1$ ms, $T_y = 5$ ms and $V_{ref(svc)} = 1.02$.

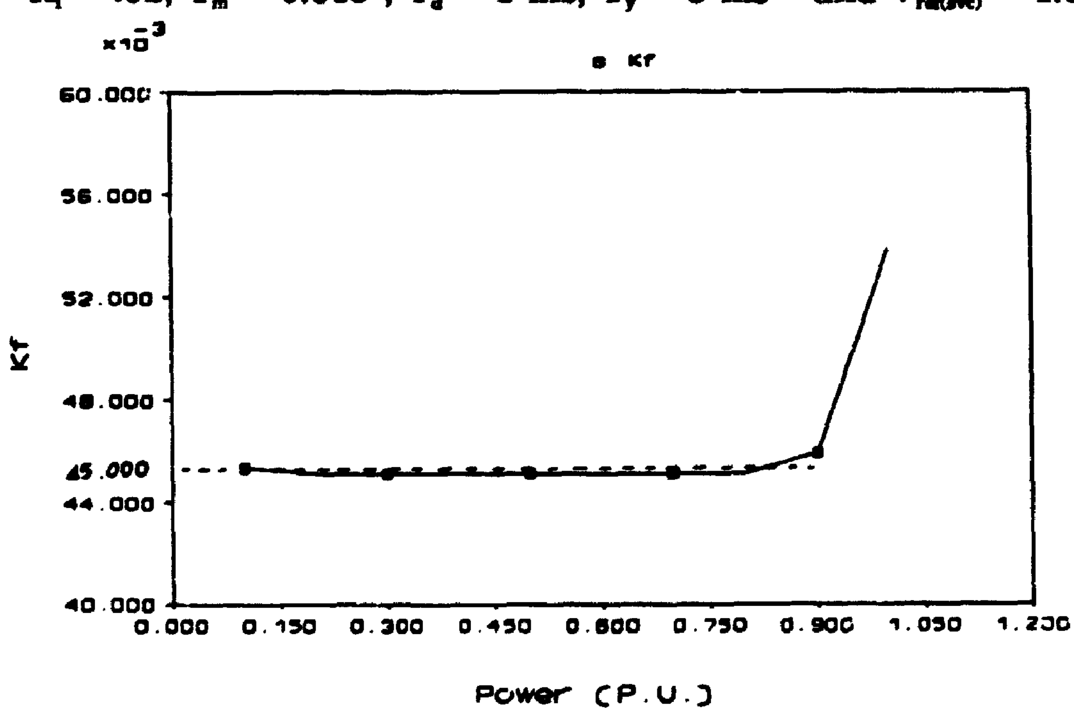

Fig. 4.5(a) : Optimal value K_F of the exciter

2 of/de 2

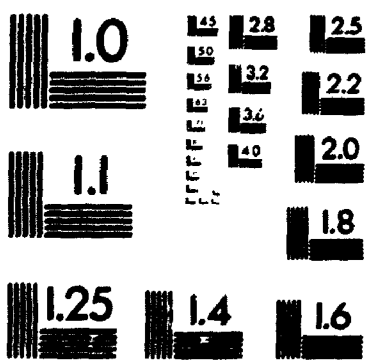

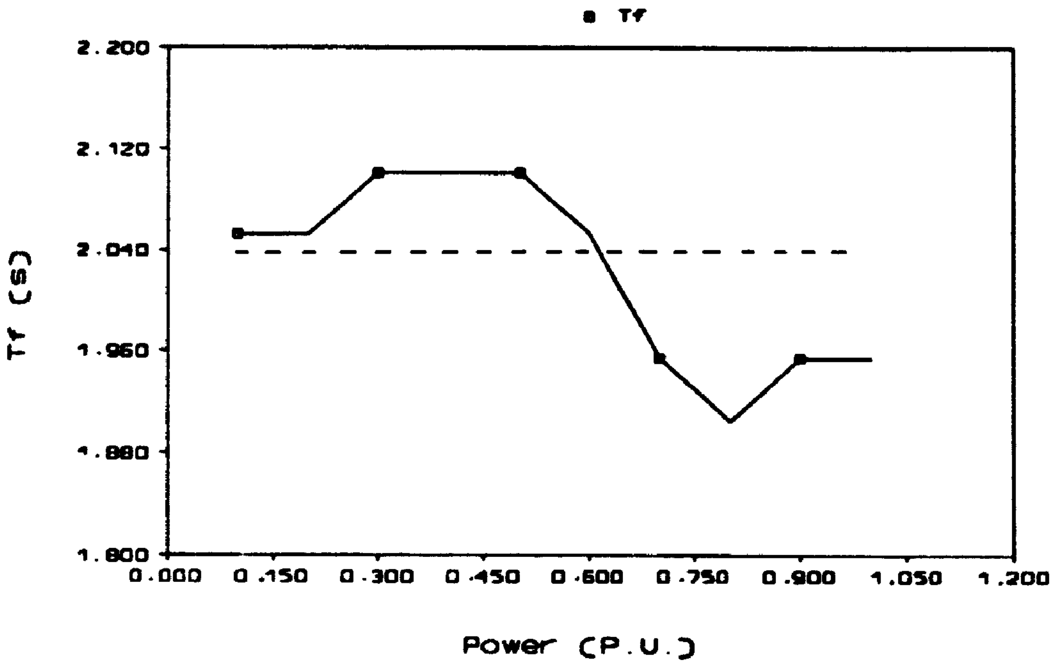

Fig. 4.5(b) : Optimal value T_F of the exciter

The optimal values of the proportional gain K_p and the integral time constant T_i are obtained from the same optimization technique. These optimal values are shown in Figs. 4.6(a) and 4.6(b). Both K_p and T_i depend on the level of the generated power and can be divided into two regions which are low loading ($\approx$ < .45 pu) and high loading conditions (> .45 pu). The reason for the substantial changes in these parameters at about 0.4-0.5 p.u. power level is that the constants K_6 and K_9 change their signs in this region. In this case the average values should not be used. Therefore the optimal values of K_p and T_i for high loading condition, which is more realistic in practice, are chosen and found to be

$$K_p = 20 \quad \text{and} \quad T_i = 0.014 \text{ s.}$$

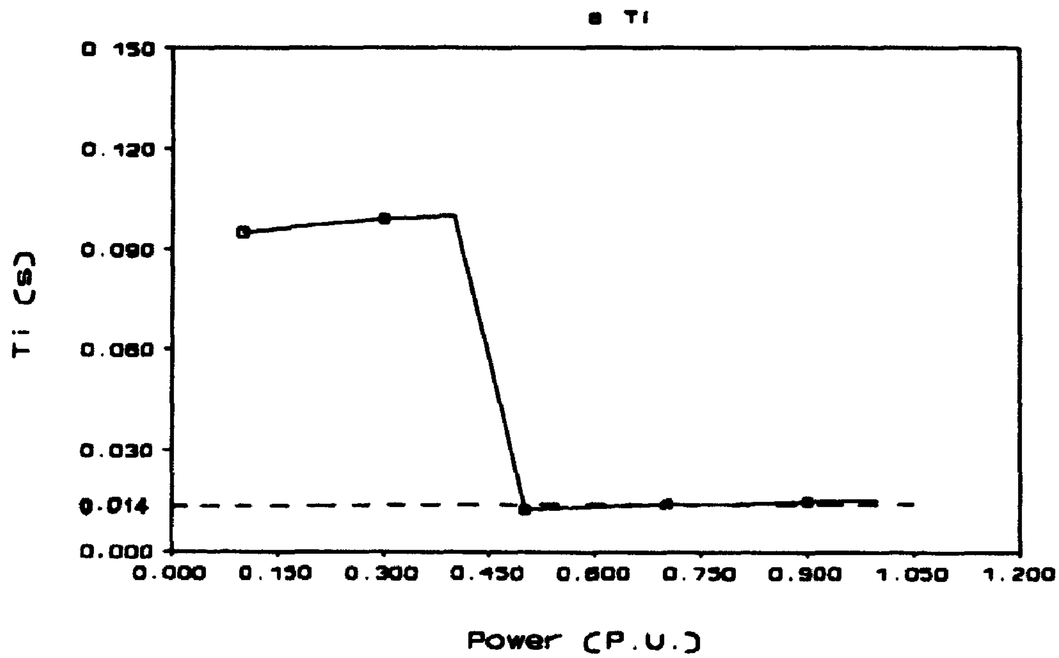

Fig. 4.6(a) : Optimal value of T_i for the SVC

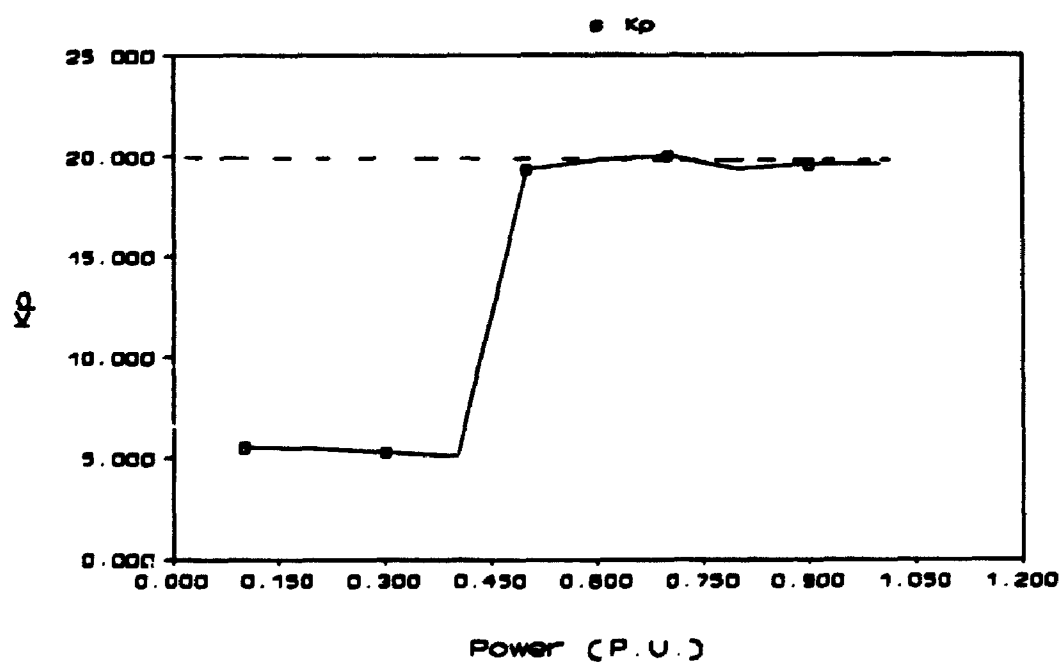

Fig. 4.6(b) : Optimal value K_p for the SVC

4.4.2 Step responses

The step responses of the system to a 5% step change in the mechanical input power to the generator operating at 1.0 p.u. with the application of

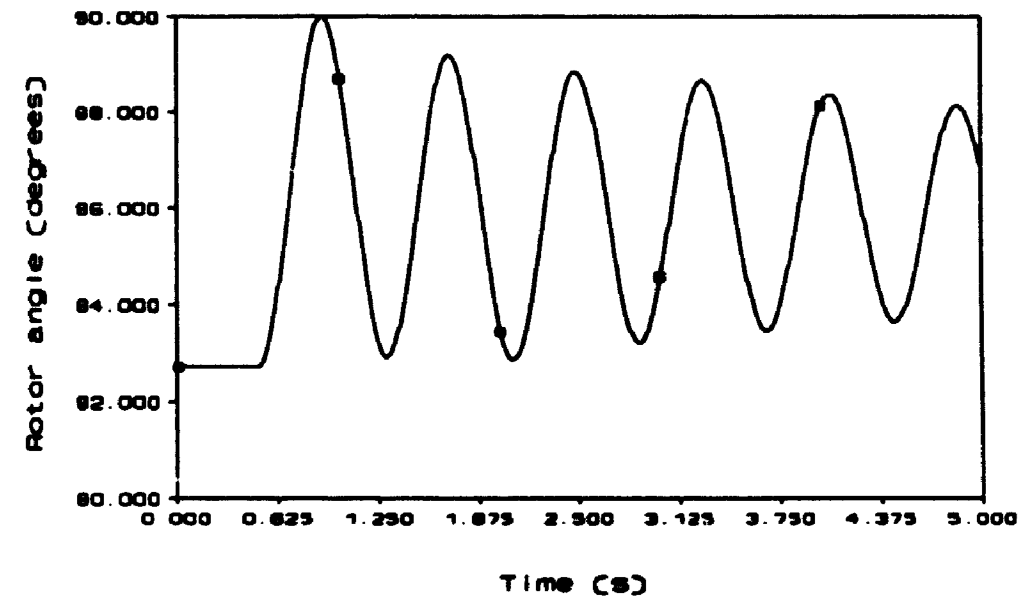

Fig. 4.7(a) : Rotor angle response to a 5% step change in the mechanical power of the SMIB system with SVC

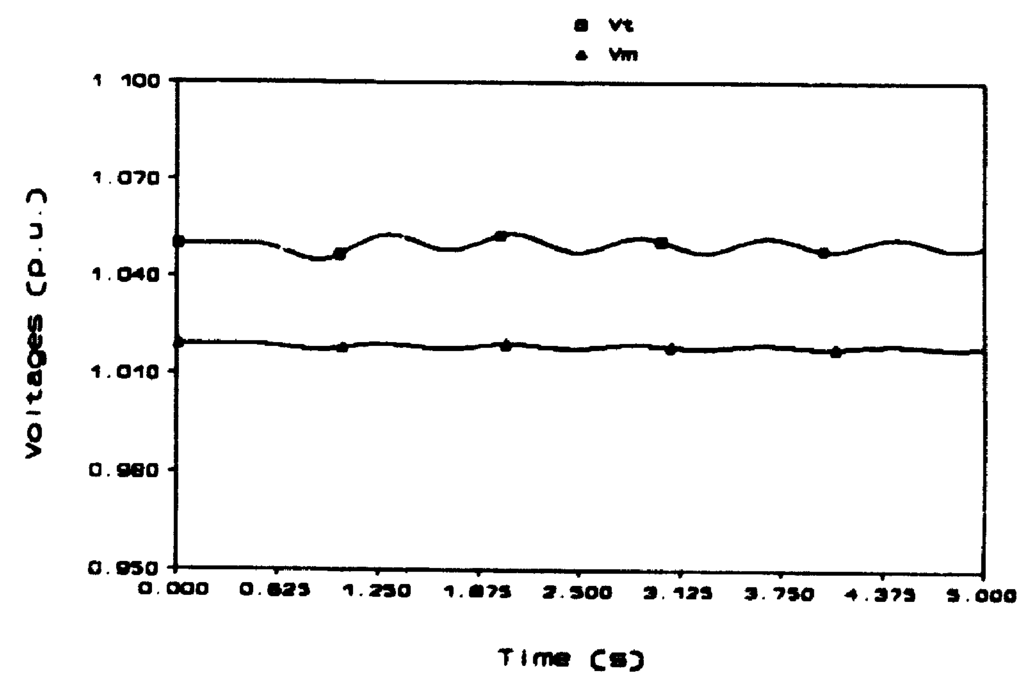

Fig. 4.7(b) : Voltage responses to a 5% step changes in the mechanical power of the SMIB system with SVC

SVC for mid-point voltage control are shown if Figs. 4.7(a) and 4.7(b). It is to be observed from the result of Fig. 4.7(a) that the damping of the inertial mode is ery poor whereas the mid-point voltage in Fig. 4.7(b) is well regulated by the SVC. The damping of the inertial mode can be improved through the addition of a supplementary control on the SVC. This improvement is described in the following sections.

4.5 System damping improvement

The transfer function of the supplementary control of the SVC is described in Chapter 3. It takes the form

$$H(s) = K_c \cdot \left[\frac{sT}{1+sT}\right] \cdot \left[\frac{1+sT_1}{1+sT_2}\right]^2 \qquad (3.29)$$

To illustrate the damping improvement, the line current measured at the SVC location is selected as the damping signal. The reset time T and lead time constant T_1 are chosen to be 10 s and 1 s respectively. The gain K_c and the lag time constant T_2 are calculated using modal control theory as described earlier to satisfy the desired damping of about 0.4. The calculated values of the gain K_c and the lag time constant T_2 at different levels of the generated power are tabulated in Table 4.1. The average values of K_c and T_2 are adopted as the optimal parameters over the entire range and found to be 0.02 and 0.09 s respectively. With the application of damping control using line current as a damping signal and the designed parameters, the damping of the inertial mode is significantly improved as illustrated in Fig. 4.8 .

Table 4.1 : Calculated gain K_e and T_2 of the supplementary control at the SVC of the SMIB system

P	K_e	T_2
0.2	.02258	.06541
0.3	.02711	.06666
0.4	.02733	.07103
0.5	.02556	.07684
0.6	.02293	.08339
0.7	.02032	.08946
0.8	.01794	.09474
0.9	.01586	.09923
1.0	.01404	.10303
1.1	.01249	.10628
1.2	.01112	.10912

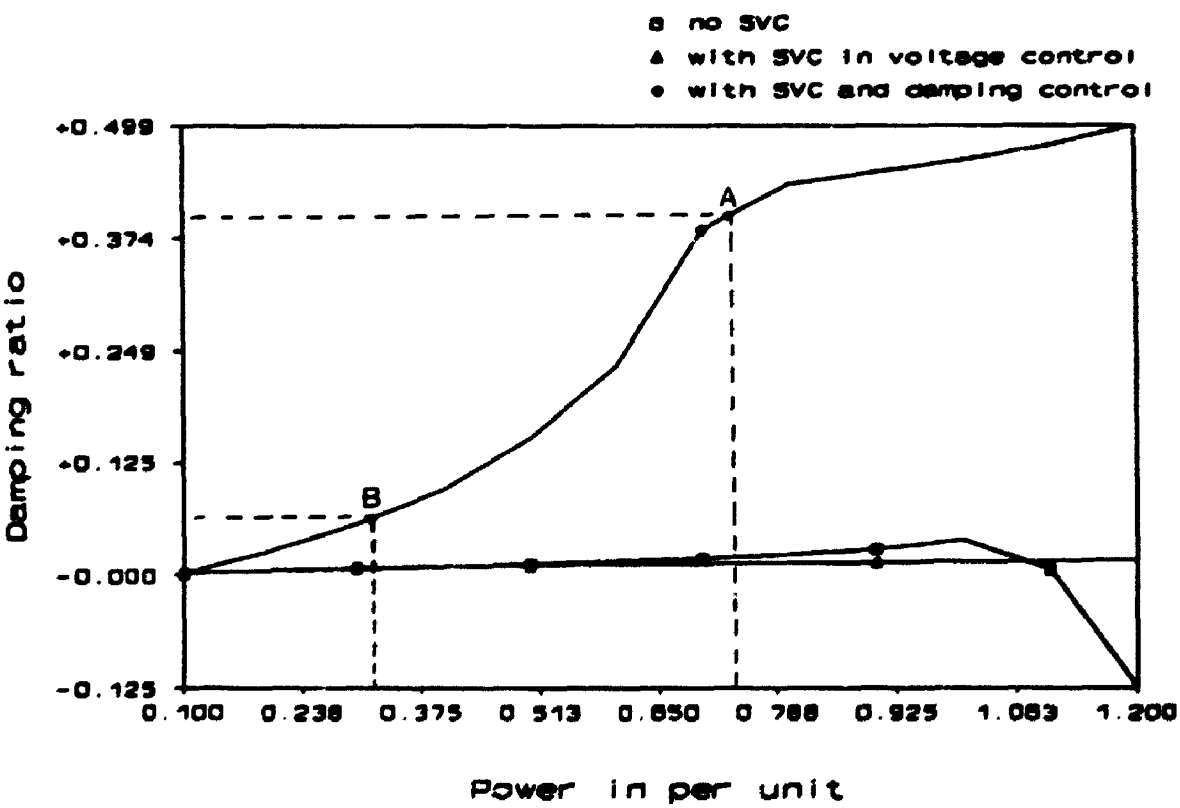

Fig. 4.8 : Inertial mode damping improvement of the SMIB system through the supplementary control of the SVC

It will be observed from Fig. 4.8 that at o.1 pu power the damping is very low (0.014). It is so because the damper circuit of the synchronous machine are not modelled. With the application of supplementary control a significant improvement at high power level is observed because the stabilizer parameters are fixed for the high loading values.

The effectiveness of the supplementary control is evaluated over a wide range of generated power. Figures 4.9(a) and 4.9(b) depict the responses of the system to a 5% increase in the mechanical input power at different loading levels. It is very clear from Fig. 4.9(a) that the inertial mode damping of the system is greatly increased with a little sacrifice on the mid-point voltage as seen from Fig. 4.9(b). If one remembers that the selection of the fixed values of K_c and T_2 were chosen corresponding to a value of P = 0.7 pu. For this selection, the values of damping ratio are shown in Fig. 4.8. Given that, it is easy to see that the damping ratio drops appreciably below P = 0.7 at point A and at P = 0.3 at point B it is reduced from about 0.4 to about 0.06. Low level of damping at P = 0.3 is clearly observed in Figs. 4.9(a) and (b). In order to add system damping, voltage regulation at the SVC bus is considered as a secondary importance. A transient stability program [48] is used to investigate the system performance and the effectiveness of the supplementary control under severe disturbances. The rating of the SVC is chosen to be +0.5 pu

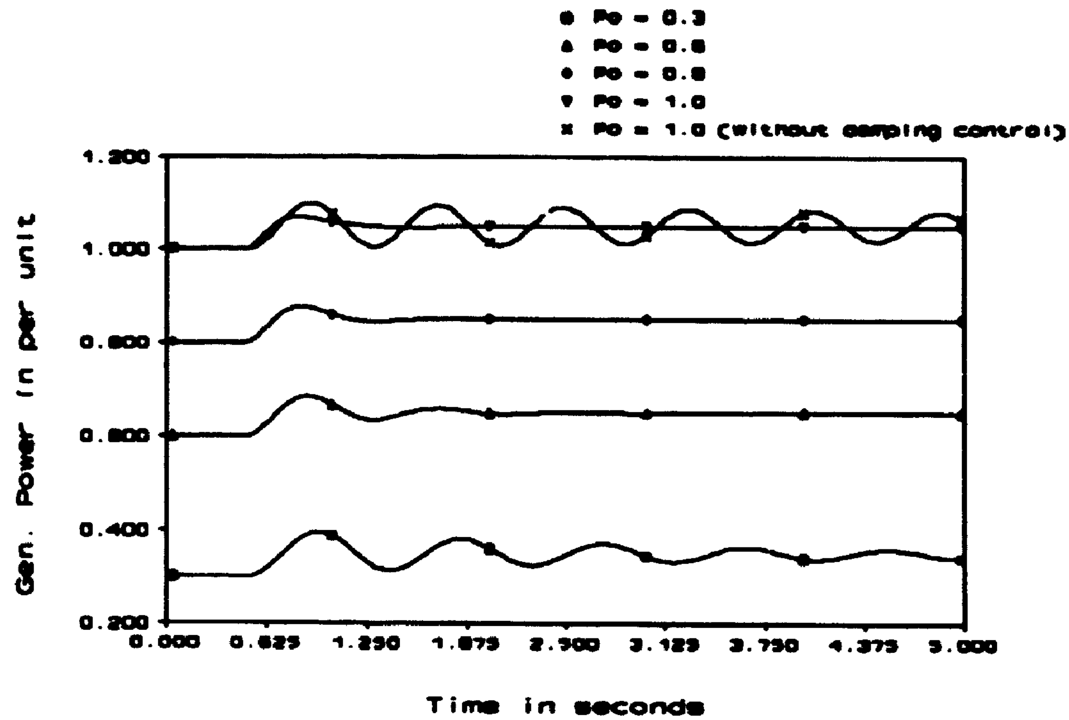

Fig. 4.9(a) : Generator's power responses to a 5% increase in the mechanical power of the SMIB system with damping control at the SVC

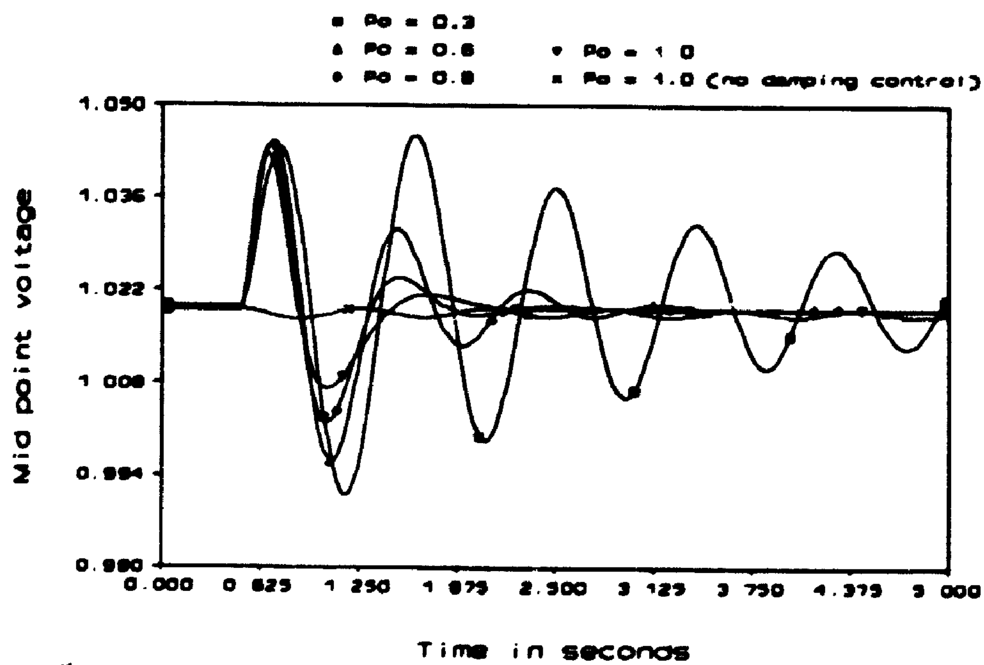

Fig. 4.9(b) : Mid-point voltage responses to a 5% increase in the mechanical power of the SMIB system with damping control at the SVC

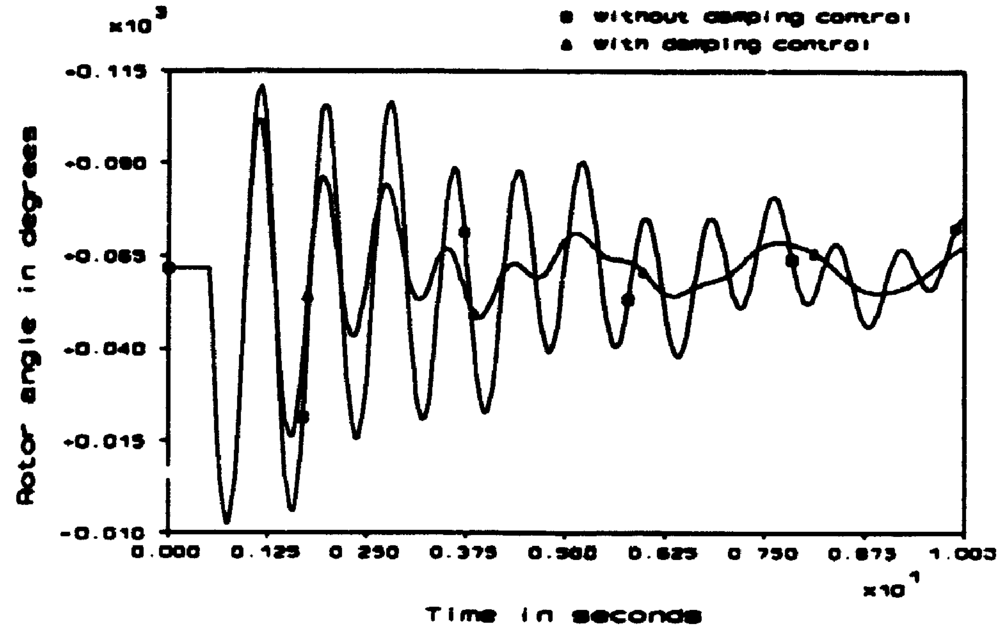

Fig. 4.10(a) : Rotor angle response of the SMIB system to a temporary ircrease in local load (0.2 pu resistance) for P=0.7 pu.

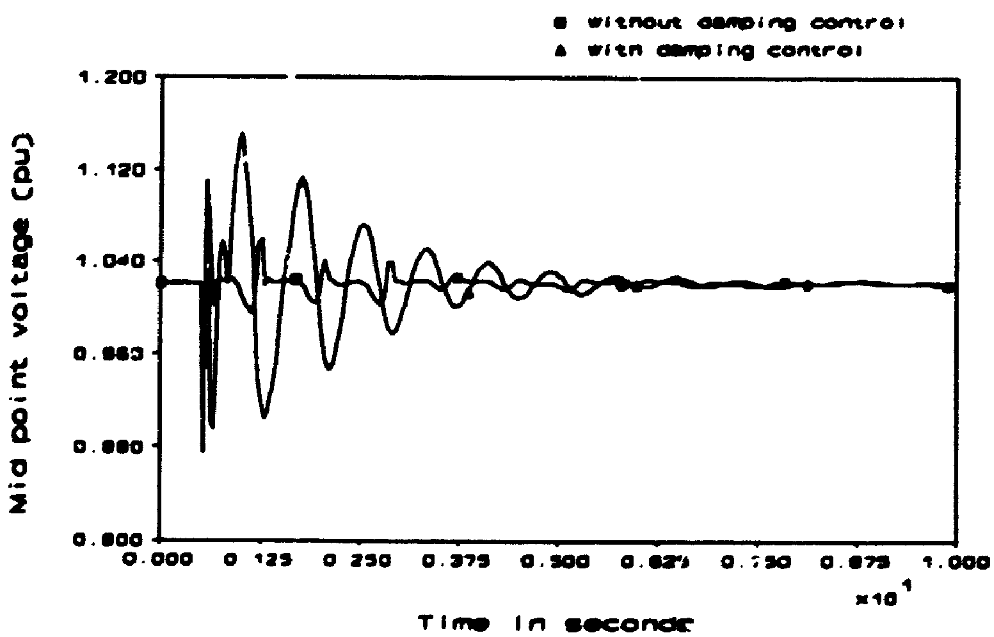

Fig. 4.10(b) : Mid-point voltage response of the SMIB system to a temporary increase in local load (0.2 pu resistance) for P=0.7 pu.

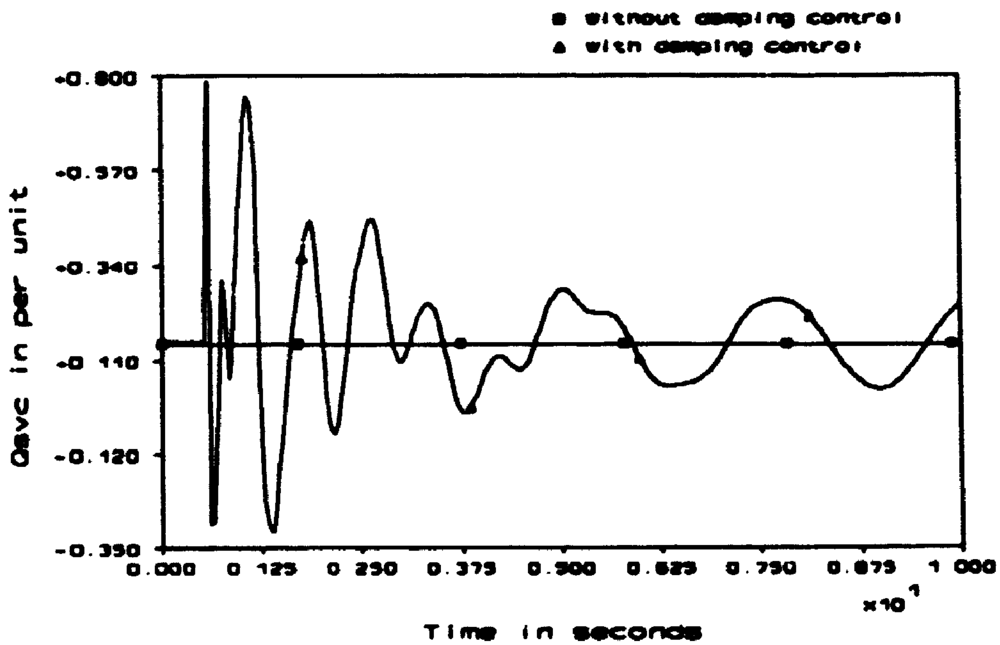

Fig. 4.10(c) : Response of Q_{svc} of the SMIB system to a temporary increase in local load (0.2 pu resistance) for P=0.7 pu.

capacitive and -0.5 pu inductive. A major disturbance was created by an increase in local load (0.2 pu resistance) at the generator for 3 cycles and the responses of the system with damping control are presented in Figs. 4.10(a) to 4.10(c). These results shows the robustness of the designed stabilizer.

Therefore it can be concluded that the supplementary control of the SVC in the single machine infinite bus system is very effective in improving the system damping under small as well as large disturbances over a wide range of operating conditions. Even though the SMIB system is rather simple it can be applied to a practical radial system where remote generators are connected to a load centre through a long transmission line. The application of SVCs for improving system damping in a multi-machine system is demonstrated in Chapter 5 by using the simplified system of the Electricity Generating Authority of Thailand.

CHAPTER V

APPLICATION OF SVCs IN A COMPLEX SYSTEM

In the previous Chapter design of controllers and the effectiveness of the application of a SVC at the midpoint of a long transmission line has been demonstrated. A relatively simple SMIB system was used to test the enhancement of the system damping with the application of supplementary damping signals in a SVC. The system although simple is very useful because for most long line situations with appropriate selection of parameters, very useful results are obtained. However in a complex interconnected system, identification of suitable SVC locations and the design of SVCs' controls become more difficult than the simple SMIB system. To demonstrate the effectiveness of the application of SVCs in a multi-machine system, the system of the Electricity Generating Authority of Thailand (EGAT) is chosen.

5.1 The EGAT system

The EGAT is a state enterprise which is responsible for the generation and transmission of electricity for the whole country of Thailand. It consists of four operating regions subdividing the entire country as illustrated in Fig. 5.1. The Region 1, comprising the most populated area,

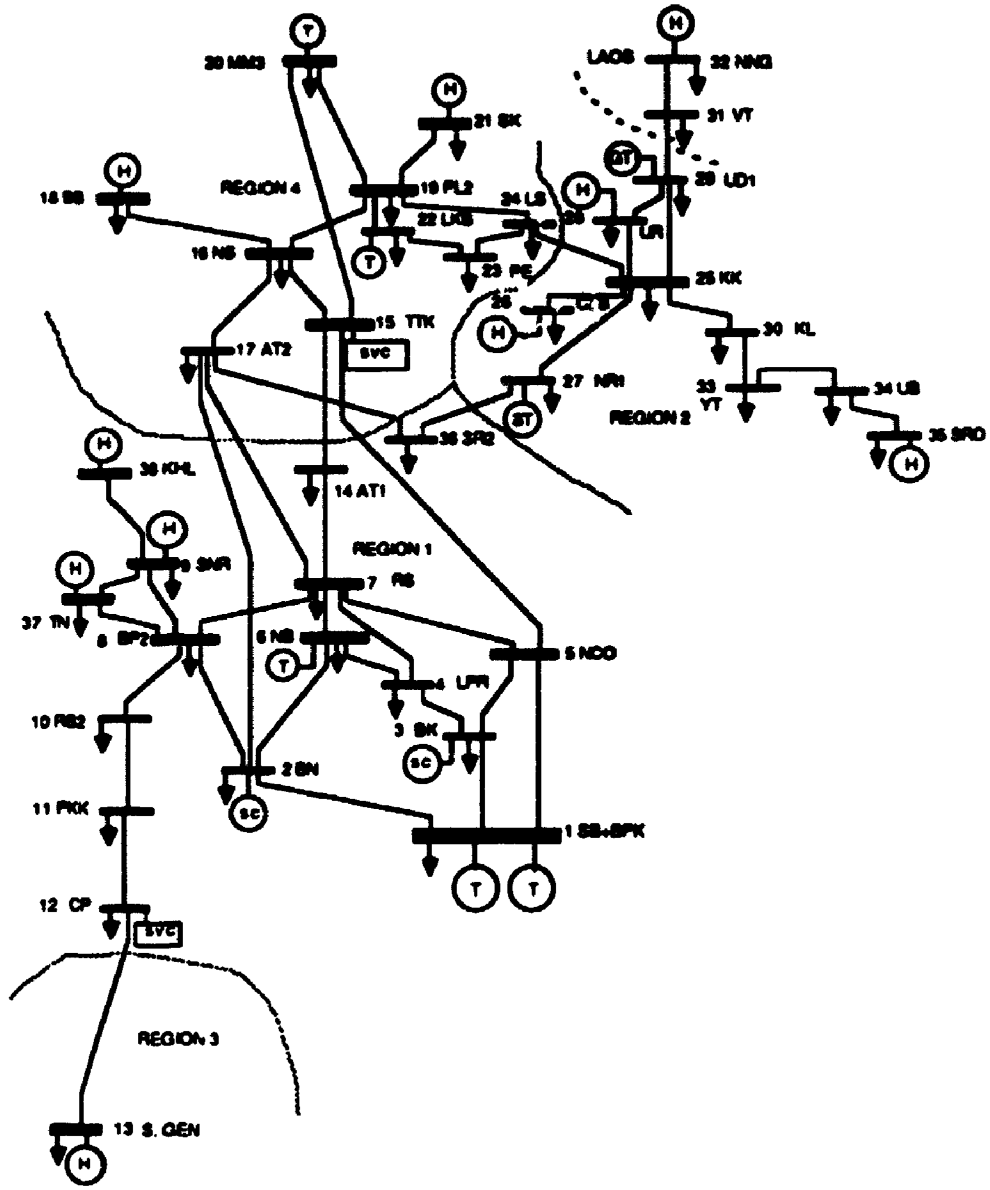

Fig. 5.1 : Simplified EGAT system.

possesses three large thermal plants, large hydro power stations in the West and large industrial and residential loads. It has strong links to the Region 4 in the North which has large thermal and hydro power plants. To cope with the increasing load growth of nearly 10% annually, new generating units are installed at the thermal plant in the North where natural resources are abundant. 500 kV lines are constructed to strengthen the transmission of power between Region 1 and Region 4.

A static var compensator of rating 300 Mvar capacitive and ·100 Mvar inductive is installed at bus TTK to regulate the voltage and to increase the transient and dynamic stabilities of the system. The Region 2 covers the north-eastern part of the country where power generation is inadequate. Seasonal unavailability of water in this region puts an immense constraint on the operation of the EGAT system. Therefore, Region 2 relies heavily on the import of power from the Region 4 through the vital tie-lines LS-KK and SR2-NR1 as shown in Fig. 5.1. For economic reasons, Region 2 imports electric power from the neighbouring country Laos as well. The system of Region 2 is radial and weak, thus a great attention is focused on this area for the application of SVCs to improve the dynamic performance of the system.

The southern part of the country forms Region 3 where many small thermal and hydro stations are sited. This region is geographically linked with the Region 1 through a very long transmission line carrying imported power into the region. A small SVC of rating ± 50 Mvar is located at CP, at about the midspan of the line, to control the voltage at CP and also to increase the transmission capacity of the line. The total installed capacity of the entire EGAT system is about 6000 MW, most of which resides in the Region 1 and the Region 4.

5.2 Objectives of the studies

The purpose of conducting system studies for the EGAT system is to investigate the possibility of using the existing SVCs to enhance the performance of the system through the controls of the SVCs. Additional SVCs will also be considered to further improve the system behaviour. Proposal to add new SVCs requires the identification of suitable SVC locations and the design of their controls. Development of a methodology for the EGAT system is regarded to make a general design contribution. EGAT system is used to further ensure that the outcome of the results of the work in this thesis may be of value to the EGAT and not wasted. To achieve these objectives the following systematic studies are carried out;

a) load flow study,

b) determination of appropriate control parameters for the existing SVCs,

c) eigenvalue analysis, to identify the poorly damped oscillation modes in the system,

d) evaluation of the system performance under large disturbance using a transient stability program,

e) exploitation of the existing SVCs to add to the system damping

f) determination of additional SVC locations and design of their controls to further improve the performance of the system.

5.3 System representation

System studies are conducted based on the information provided by the EGAT. In the network only lines rated at 500 kV, 230 kV and 115 kV are represented. Also the system is assumed to operate at the peak load thereby implying that all generators and lines are in service. Some approximations are made to reduce the complexity of the system (e.g. some buses are eliminated and their loads are transferred to the adjacent buses). All loads are assumed to be voltage and frequency independent. For the dynamic stability study, all synchronous machines are represented by detailed machine models. The IEEE type 1 rotating exciters are assumed to be employed on all generators as no better information was available.

On the basis of the nature of the system the objective of the study is to concentrate on the dynamic behaviour of the machines in the Region 2. For this reason, the dynamics of the Region 3 which is very remote from other regions is ignored by representing the entire region as an equivalent load. The large thermal plants in the southern part of the Region 1 are lumped together and treated as an infinite bus in the analysis.

5.4 Load flow study

The bus and the line data of the simplified EGAT system are listed in the Appendix D. The purpose of conducting load flow study is to determine

Table 5.1 : LOAD FLOW RESULTS

BUS	NAME	VOLT	ANGLE	P_L	Q_L	P_G	Q_G
1	SB + BPK	1.000*	0.0	1005.2	622.1	2424.7	1167.7
2	NO 2 BN	0.973	-2.2	414.2	310.4	0.0	0.0
3	NO 3 BK	0.976	-3.0	537.0	214.2	0.0	0.0
4	NO 4 LPR	0.971	-3.4	334.9	183.8	0.0	0.0
5	NO 5 NCO	0.988	-1.6	0.0	0.0	0.0	0.0
6	NO 6 NB	0.970*	-3.2	237.6	216.2	160.0	68.8
7	NO 7 RS	0.975	-3.1	298.0	161.0	0.0	0.0
8	NO 8 BP2	1.003	1.7	182.0	64.9	0.0	0.0
9	NO 9 SNR	1.038*	8.6	0.0	0.0	400.0	75.5
10	NO10 RB2	1.005	-0.3	96.1	27.5	0.0	0.0
11	NO11 PKK	1.024	-5.4	12.4	23.0	0.0	0.0
12	NO12 CP	1.050*	-21.8	24.1	14.4	0.0	34.0
13	NO13 Sgen	1.050	-31.3	70.6	-25.0	0.0	0.0
14	NO14 AT1	0.989	-3.0	155.0	68.0	0.0	0.0
15	NO15 TTK	1.050*	1.6	0.0	0.0	0.0	114.7
16	NO16 NS	1.042	2.1	65.2	28.6	0.0	0.0
17	NO17 AT2	0.991	-3.9	95.3	52.6	0.0	0.0
18	NO18 BB	1.070*	10.4	58.2	36.5	350.0	16.6
19	NO19 PL2	1.059	5.8	0.0	0.0	0.0	0.0
20	NO20 MM3	1.050*	15.4	361.7	228.2	825.0	134.5
21	NO21 SK	1.086*	9.2	2.2	2.8	160.0	21.4
22	NO22 LKB	1.046*	7.5	53.6	26.3	100.0	5.4
23	NO23 PE	1.035	-0.4	16.6	9.7	0.0	0.0
24	NO24 LS	1.043	-2.0	7.2	5.7	0.0	0.0
25	NO25 KK	1.033	-14.3	104.7	2.9	0.0	0.0
26	NO26 CLB	1.063*	-8.9	14.8	11.8	40.0	9.4
27	NO27 NR1	1.004*	-23.3	176.7	11.4	12.0	5.3
28	NO28 UR	1.040*	-15.7	0.6	1.5	16.0	1.5
29	NO29 UD1	1.002*	-21.8	141.8	41.1	12.0	2.0
30	NO30 KL	1.000	-20.9	17.5	12.5	0.0	0.0
31	NO31 VT	1.018	-20.6	27.3	9.2	0.0	0.0
32	NO32 NNG	1.040*	-18.4	0.0	0.0	60.0	9.4
33	NO33 YT	0.991	-27.9	61.1	31.4	0.0	0.0
34	NO34 UB	1.031	-33.8	44.7	25.9	0.0	0.0
35	NO35 SRD	1.063*	-32.7	3.4	2.0	36.0	9.4
36	NO36 SR2	0.980	-8.4	130.7	64.3	0.0	0.0
37	NO37 TN	1.040*	8.3	0.0	0.0	40.0	1.8
38	NO38 KHL	1.050*	12.4	0.0	0.0	240.0	3.6

* PV BUS (Voltage : per unit , Power : MW, Mvar)

the initial operating condition of the system including parameters such as voltage magnitudes and angles, rotor angles of all machines etc. The load flow module in the transient stability program [48] is used for performing the load flow study. The results of this study are shown in Table 5.1. The load flow results indicate that the voltages at all buses are well kept within the nominal range and the SVCs at CP and TTK supply reactive powers of 34 Mvar and 115 Mvar respectively to support the system under peak load.

5.5 SVC control parameters

The optimal control parameters for the existing SVCs at CP and TTK can be calculated by assuming that these SVCs are primarily designed for voltage regulation. The control of the SVCs is assumed to be a proportional controller with phase lead/lag compensation in order to be compatible with the simulation program [48]. Eqn.(3.19) can be used to determine the optimal values of the time constants T_1 and T_2 once the gain K_p and other quantities are known.

$$T_1 = \frac{[2(B_o+S_c)(B_o+S_c+K_pV_o)\,T_2T_y^*]^{1/2} - (B_o+S_c)(T_2+T_y^*)}{K_p\,V_o} \qquad (3.19)$$

The short-circuit capacity S_c at each bus can be approximately obtained from the Jacobian matrix of the load flow study.

Since
$$\begin{bmatrix} \Delta P \\ \Delta Q \end{bmatrix} = \begin{bmatrix} J_1 & J_2 \\ J_3 & J_4 \end{bmatrix} \begin{bmatrix} \Delta\delta \\ \Delta V/V \end{bmatrix}$$

Using the decoupled load flow approximations, we have

$$\Delta Q = J_4 \, \Delta V/V$$

$$S_c = \Delta Q\big|_{\Delta V/V = 1} = J_4$$

The short-circuit capacity of the EGAT system at TTK and CP buses and other quantities obtained from load flow study are tabulated in Table 5.2.

Table 5.2 : SVCs' bus quantities (p.u.)

Bus No.	Name	V_o	Q	B_o	S_c	Remarks
12	CP	1.05	.34	.31	6.9	Base MVA =100
15	TTK	1.05	1.147	1.04	53.5	

Assuming that the required SVC characteristics and the time constants of the measuring circuit and the thyristors are ;

current droop = 0.5% or K_p = 200,

thyristor's time constant T_y = 0.05 s and

filter time constant T_m = 0.01 s.

The optimal lead and lag time constants T_1 and T_2 can be calculated from Eqn.(3.19) and are of the quadratic forms from which any combination of T_1 and T_2 can be selected.

TTK SVC		CP SVC	
$T_1 = 0.19814\sqrt{T_2} - 0.2597(T_2+0.06)$		$T_1 = 0.06527\sqrt{T_2} -.0343(T_2+.06)$	
T_2	T_1	T_2	T_1
0.4	0.006	0.5	.027 *
0.3	.015	0.4	.0255
0.2	.021 *	0.3	.0234
0.1	.020	0.2	.0203

* selected values

5.6 Eigenvalue analysis

Eigenvalue analysis is a useful technique and is widely used in linear control systems. Since power systems are highly non-linear, linearized models are derived from the dynamic equations governing the behaviour of the system. Reference [47] gives the details of the system modelling for a very large power system. However basic concepts of the system modelling are briefly reviewed in the following subsections.

5.6.1 System modelling

A multi-machine model consists of many modules representing each active device which can be either synchronous generator, hvdc converter or static var compensator in the system. Each controlled device is modelled as a voltage-controlled current injection into the system at the connected bus. It is represented in the state-variable form as :

$$\dot{x}_d = A_d x_d + B_d u$$

and

$$i_d = C_d x_d - Y_d V \qquad (5.1)$$

where x_d = state vector of each device,

u = device control vector,

i_d = device current vector,

V = bus voltage vector,

Y_d = device admittance matrix,

and A_d, B_d, C_d = device matrices with appropriate dimensions.

The interactions of all devices with the system are described by the relation

$$i_d = Y_n V \tag{5.2}$$

where Y_n is the admittance matrix of the network. The entire system can be modelled by stacking all device models together with the network interactions in a proper fashion. It can be represented in the combined form

$$\begin{bmatrix} \dot{x} \\ 0 \end{bmatrix} = \begin{bmatrix} A_s & B_s \\ C_s & -(Y_n+Y_d) \end{bmatrix} \begin{bmatrix} x \\ V \end{bmatrix} \tag{5.3}$$

where A_s, B_s and C_s are the modified matrices and x is the entire state vector of the system. The model of Eqn.(5.3) can be reduced into a common form

$$\dot{x} = A x$$

where $$A = [A_s + B_s (Y_n + Y_d)^{-1} C_s] \tag{5.4}$$

by matrix manipulations.

5.6.2 Eigenvalue analysis

The machine parameters of the EGAT system required for eigenvalue analysis are listed in the Appendix E and a small signal stability (S^3) program developed by a co-researcher Mr. M.S. Moorty is applied to the EGAT system to investigate

a) all eigenvalues,

b) each inertial mode oscillation,

c) participation of all devices to each inertial mode and

d) the validity of the designed SVCs control parameters.

For the system to be stable, the real part of all eigenvalues must be negative. The damping of each mode can be evaluated from its eigenvalue. The participation of all states to any particular mode is a new concept used in many references [37-39] to determine the optimum locations of power system stabilizers (PSSs) to improve the performance of the system through excitation control of some generators. A concept of voltage participation is similar to that of state participation but it describes the sensitivity of eigenvalues to changes in bus admittances or line reactances. As a high value of voltage participation factor implies high sensitivity of eigenvalues to the shunt admittance at a bus, that bus is regarded to be the best candidate for applying a SVC. This aspect is fully researched by Mr. M.S. Moorty [52]. This concept can therefore be applied to identify the best locations of the SVCs for damping purposes. The implementation of this technique will be discussed in detail later.

5.6.3 System eigenvalues

All eigenvalues of the simplified EGAT system with all SVCs operating in a voltage control mode are shown in Table 5.3. The system is proven to be stable since the real part of all eigenvalues are negative. Identification of each oscillation mode is achievable through the investigation of the participation factors of all states. Since the inertial mode oscillation of each machine is the primary concern in the study, the participation to other modes are not considered. From the results of the eigenvalue analysis, the inertial oscillation mode of each machine and the participation of all active devices are identified in Table 5.4.

Table 5.3 : System eigenvalues

No.	EIGENVALUES		|Wn|	DAMPING
1	-420.3200	+j 0.0000	420.32004	1.00000
2	-149.5414	+j 0.0000	149.54141	1.00000
3	-115.8649	+j 0.0000	115.86494	1.00000
4	-108.4701	+j 0.0000	108.47008	1.00000
5	-95.9855	+j 0.0000	95.98548	1.00000
6	-93.8544	+j 0.0000	93.85445	1.00000
7	-92.3093	+j 0.0000	92.30927	1.00000
8	-80.1786	+j 0.0000	80.17859	1.00000
9	-74.7788	+j 0.0000	74.77882	1.00000
10	-70.6195	+j 0.0000	70.61954	1.00000
11	-65.5662	+j 0.0000	65.56625	1.00000
12	-58.5196	+j 0.0000	58.51952	1.00000
13	-54.7216	+j 0.0000	54.72162	1.00000
14	-47.3854	+j 0.0000	47.38541	1.00000
15	-37.1279	-j 59.5681	70.19145	0.52895
16	-37.1279	+j 59.5681	70.19145	0.52895
17	-34.5356	+j 0.0000	34.53557	1.00000
18	-27.9135	+j 0.0000	27.91346	1.00000
19	-24.6294	+j 0.0000	24.62941	1.00000
20	-18.8714	+j 0.0000	18.87136	1.00000
21	-18.2395	+j 0.0000	18.23951	1.00000
22	-17.7662	+j 0.0000	17.76625	1.00000
23	-17.7417	+j 0.0000	17.74174	1.00000
24	-17.5385	+j 0.0000	17.53852	1.00000
25	-17.4761	+j 0.0000	17.47614	1.00000
26	-17.4035	+j 0.0000	17.40353	1.00000
27	-17.3765	+j 0.0000	17.37648	1.00000
28	-17.3286	+j 0.0000	17.32864	1.00000
29	-17.3105	+j 0.0000	17.31047	1.00000
30	-17.2981	+j 0.0000	17.29812	1.00000
31	-17.2442	+j 0.0000	17.24425	1.00000
32	-17.2293	+j 0.0000	17.22927	1.00000
33	-17.1965	+j 0.0000	17.19649	1.00000
34	-16.0381	-j 20.9872	26.41367	0.60719
35	-16.0381	+j 20.9872	26.41367	0.60719
36	-3.9759	+j 0.0000	3.97585	1.00000
37	-3.9105	+j 0.0000	3.91055	1.00000
38	-3.8795	+j 0.0000	3.87945	1.00000
39	-3.7221	+j 0.0000	3.72210	1.00000
40	-3.6548	+j 0.0000	3.65479	1.00000
41	-3.5921	+j 0.0000	3.59210	1.00000
42	-3.5676	+j 0.0000	3.56764	1.00000
43	-3.3360	+j 0.0000	3.33603	1.00000
44	-3.0355	+j 0.0000	3.03551	1.00000
45	-2.9566	-j 12.2929	12.64346	0.23384
46	-2.9566	+j 12.2929	12.64346	0.23384
47	-2.9076	+j 0.0000	2.90764	1.00000
48	-2.6001	+j 0.0000	2.60011	1.00000
49	-2.4150	+j 0.0000	2.41498	1.00000
50	-1.9213	+j 0.0000	1.92132	1.00000
51	-1.6778	+j 0.0000	1.67783	1.00000
52	-1.2774	-j 12.8886	12.95178	0.09863
53	-1.2774	+j 12.8886	12.95178	0.09863

Table 5.3 : System eigenvalues (continued)

No.	EIGENVALUES			|Wn|	DAMPING
54	-1.2245	-j	9.6602	9.73752	0.12575
55	-1.2245	+j	9.6602	9.73752	0.12575
56	-1.0770	-j	1.5913	1.92151	0.56050
57	-1.0770	+j	1.5913	1.92151	0.56050
58	-1.0059	-j	8.7940	8.85138	0.11364
59	-1.0059	+j	8.7940	8.85138	0.11364
60	-0.8953	-j	1.6011	1.83440	0.48806
61	-0.8953	+j	1.6011	1.83440	0.48806
62	-0.8941	+j	0.0000	0.89410	1.00000
63	-0.8587	+j	0.0000	0.85867	1.00000
64	-0.7759	-j	1.2243	1.44945	0.53531
65	-0.7759	+j	1.2243	1.44945	0.53531
66	-0.7750	-j	10.0157	10.04561	0.07715
67	-0.7750	+j	10.0157	10.04561	0.07715
68	-0.6734	-j	0.9294	1.14771	0.58669
69	-0.6734	+j	0.9294	1.14771	0.58669
70	-0.6695	-j	0.9506	1.16266	0.57582
71	-0.6695	+j	0.9506	1.16266	0.57582
72	-0.5675	-j	0.9409	1.09877	0.51651
73	-0.5675	+j	0.9409	1.09877	0.51651
74	-0.5600	-j	0.6332	0.84532	0.66246
75	-0.5600	+j	0.6332	0.84532	0.66246
76	-0.5327	-j	8.9488	8.96469	0.05942
77	-0.5327	+j	8.9488	8.96469	0.05942
78	-0.5159	+j	0.0000	0.51593	1.00000
79	-0.4632	-j	7.4249	7.43935	0.06226
80	-0.4632	+j	7.4249	7.43935	0.06226
81	-0.4277	-j	0.6647	0.79046	0.54111
82	-0.4277	+j	0.6647	0.79046	0.54111
83	-0.4257	-j	0.3207	0.53297	0.79875
84	-0.4257	+j	0.3207	0.53297	0.79875
85	-0.4123	-j	5.0063	5.02329	0.08207
86	-0.4123	+j	5.0063	5.02329	0.08207
87	-0.4022	-j	6.6518	6.66399	0.06036
88	-0.4022	+j	6.6518	6.66399	0.06036
89	-0.3937	-j	0.6551	0.76428	0.51518
90	-0.3937	+j	0.6551	0.76428	0.51518
91	-0.3669	-j	9.4389	9.44606	0.03884
92	-0.3669	+j	9.4389	9.44606	0.03884
93	-0.3633	-j	0.4651	0.59022	0.61556
94	-0.3633	+j	0.4651	0.59022	0.61556
95	-0.3544	+j	0.0000	0.35439	1.00000
96	-0.2767	-j	0.3751	0.46610	0.59366
97	-0.2767	+j	0.3751	0.46610	0.59366
98	-0.2234	-j	5.0963	5.10118	0.04379
99	-0.2234	+j	5.0963	5.10118	0.04379
100	-0.1744	-j	7.0369	7.03909	0.02477
101	-0.1744	+j	7.0369	7.03909	0.02477
102	-0.1497	-j	6.0506	6.05245	0.02473
103	-0.1497	+j	6.0506	6.05245	0.02473
104	-0.1375	-j	9.5086	9.50960	0.01446
105	-0.1375	+j	9.5086	9.50960	0.01446

Table 5.4 : System eigenvalues and participations of all machines.

Mode			Machine														SVC	
No	ω_n	ζ	UD1	NNG	SRD	UR	SK	BB	MM3	NR1	LKB	CLB	KHL	SNR	TN	NB	TTK	CP
1	5.0233	.0821	.0043	.0178	.0016	.0174	.0770	.0135	.0210	.8381	.0075	.0013	.0004	.0004	-	-	.0011	-
2	5.1012	.0438	.0169	.0692	.0046	.1026	.4754	.0493	.0728	.1618	.0213	.0063	.0012	.0013	-	-	-.0001	-
3	6.0525	.0247	.0196	.0908	.0025	.6227	.2428	.0039	.0050	.0020	.0006	.0016	.0002	.0001	-	-	.0001	-
4	6.6640	.0640	-	-.0004	-	-.0008	.0096	.0044	.0024	-	-	-	.5608	.4231	.0120	-	-	-
5	7.0391	.0248	.0794	.5916	.0062	.2435	.0265	.0053	.0020	.0002	.0010	.0025	.0014	.0008	-	-	-	-
6	7.4395	.0623	.0041	.0476	-.0004	-.0030	.0927	.7944	.0493	-	.0133	-	.0059	.0028	-	-	.0007	-
7	8.8514	.1136	-.0017	.0230	-.0182	.0020	.0521	.1270	.2761	-	.5152	.0021	-	-	-	-	.0001	-
8	8.9647	.0594	-	-	-	-	-	-	-.0002	-	-	-	.4335	.5696	.0024	-	-	-
9	9.4461	.0388	-.0654	.0234	1.0292	.0022	-.0016	-.0025	-.0166	-	.0037	.0138	-	-	-	-	-	-
10	9.5096	.0145	.9362	.1201	-.0531	.0006	-	-.0004	.0024	-	.0014	-.0064	-	-	-	-	-	-
11	9.7375	.1258	-.0006	.0010	-.0030	-	.0038	.0152	.5947	-	.4087	.0068	-	-	-	-	.0012	-
12	10.0456	.0772	.0025	.0084	.0140	.0006	-	-.0004	.0130	-	.0002	.9770	-	-	-	-	-	-
13	12.6435	.2338	-	-	-	-	-	-	-	-	-	-	.0030	.0126	1.0597	-.0004	-	-
14	12.9518	.0986	-	-	-	-	-	-	.0002	-	-	-	-	-	-.0004	1.0138	-	-
15	26.4137	.6072	-	-	-	-	.0029	.0072	.0068	.0006	-	-	-	.0001	-	.0003	.9824	-
16	70.1914	.5289	-	-	-	-	-	-	-	-	-	-	-	.0006	-	-	-	.9991

It can be seen from Table 5.4 that almost all of the inertial modes are poorly damped especially for the machines in the Region 2. Based on the participation of each mode coherency machines can be identified. For example, the machines in the West of the Region 1 form a coherency group and swing together against the infinite bus and other machines. The MM3 machine at bus 20 has a very strong coupling with the LKB machine at bus 22. Strong coupling is observed between NNG machine in Laos and UR machine in the Region 2. The participations of SVCs at CP and TTK to these inertial modes are very small. The eigenvalues of the SVCs are well damped and they verify the design of SVCs control parameters for voltage control. The eigenvector of each mode is also available from the S^3 program. The eigenvectors of all modes are indicated in Table 5.5. The eigenvectors are phasor quantities and the knowledge of the eigenvector for a particular mode gives a clear indication of how the participating machines swing. They may either oscillate together or even opposing each other. Inter-area modes of oscillation can be identified if many machines in one region swing against other machines in another zone. For the case of mode 5, this mode is created by NNG machine in Laos and it swings oppositely against UR and SK machines in the Region 2 and Region 4 respectively.

5.6.4 Large disturbance study

To test the robustness of the stabilizer desinged for the steady-state stability the system response for a large disturbance was studied.

Table 5.5 : System eigenvalues and eigenvectors of all inertial modes.

Mode			Machine														SVC	
No	ω_n	ζ	UD1	NNG	SRD	UR	SK	BB	MM3	NR1	LKB	CLB	KHL	SNR	TN	NB	TTK	CP
1	5.0233	.0821	.07∠-18	.07∠-18	.06∠-23	.11∠-10	.06∠-20	.03∠-28	.03∠-32	1.0∠0	.03∠-33	.04∠-31	·	·	·	·	.02∠-76	·
2	5.1012	.0438	.19∠-90	.22∠-90	.15∠-97	.33∠-102	.24∠-102	.08∠-97	.1∠-97	1.0∠0	.12∠-91	.14∠-100	.01∠96	.01∠96	·	·	.03∠-152	·
3	6.0535	.0347	.25∠-5	.31∠-6	.3∠-9	1.0∠0	.22∠-173	.03∠-168	.03∠-175	.10∠-166	.02∠180	.09∠-9	.01∠178	.01∠-177	·	·	·	·
4	6.6640	.0640	·	.05∠84	·	.10∠-162	.11∠177	.08∠7	.03∠8	·	·	·	1.0∠0	.73∠-2	.45∠-11	·	·	·
5	7.0391	.0348	.64∠2	1.0∠0	.34∠-4	.78∠175	.13∠171	.09∠-40	.04∠-24	.07∠-170	.08∠-27	.19∠-5	.08∠-169	.02∠-167	·	·	·	·
6	7.4395	.0623	.36∠146	.64∠153	.13∠58	.17∠-94	.33∠176	1.0∠0	.24∠1	·	.26∠10	·	.10∠-175	.06∠-179	·	·	·	·
7	8.8514	.1136	.19∠129	.23∠-160	.51∠82	.09∠-151	.15∠-168	.24∠-168	.37∠32	·	1.0∠0	.41∠55	·	·	·	·	·	·
8	8.9647	.0594	·	·	·	·	·	·	.02∠106	·	·	·	1.0∠0	.96∠-177	.22∠176	·	·	·
9	9.4461	.03[illegible]6	.22∠69	.08∠-158	1.0∠0	.03∠179	.01∠102	.01∠113	.03∠-110	·	.04∠-131	.17∠-27	·	·	·	·	·	·
10	9.5086	.0145	1.0∠0	.21∠176	.42∠-114	.02∠153	·	.01∠82	.01∠-156	·	.02∠-169	.1∠-86	·	·	·	·	·	·
11	9.7376	.1258	.11∠-83	.06∠-26	.28∠-104	·	.07∠-50	.11∠-40	.57∠158	·	1.0∠0	.52∠-153	·	·	·	·	.06∠-147	·
12	10.0456	.0772	.06∠140	.02∠-168	.19∠143	.01∠-179	·	.01∠60	.04∠-148	·	.02∠145	1.0∠0	·	·	·	·	·	·
13	12.[illegible]36	.2338	·	·	·	·	·	·	·	·	·	·	.02∠177	.03∠178	1.0∠0	.01∠106	·	·
14	12.9518	.0866	·	·	·	·	·	·	.01∠166	·	·	·	·	·	.04∠-81	1.0∠0	·	·
15	26.4137	.6072	·	·	·	·	.01∠102	.01∠108	·	.01∠104	·	·	·	·	·	·	.83∠-46	·
16	70.1914	.5289	·	·	·	·	·	·	·	·	·	·	·	·	·	·	·	.55∠-16

Employing transient stability program [48] a temporary large load change (increase) was created at LS bus for 3 cycles to disturb the system in the Region 2 and Region 4. The load change was simulated by temporary connecting a 0.1 p.u. resistance at the LS bus which can be deemed as a severe case since the tie-line LS-KK is the most vital line for the Region 2 and it is heavily loaded. The responses of rotor angles of all machines and voltages at some buses obtained from the program are illustrated in Figs. 5.2(a) and 5.2(b) respectively.

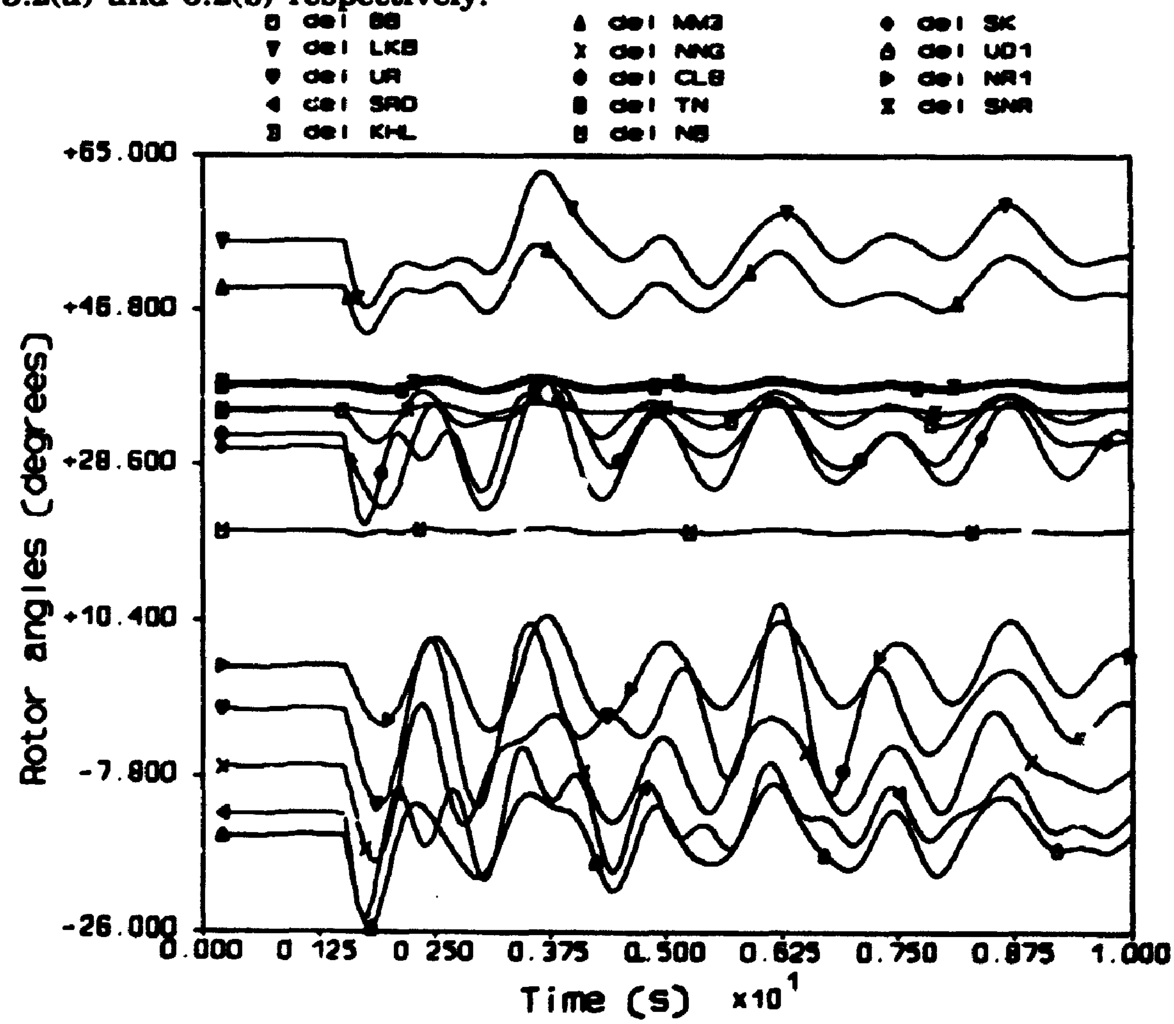

Fig. 5.2(a) : Rotor angle responses of the simplified EGAT system to a temporary increase in local load (0.1 pu rersistance) at LS without damping control.

The rotor angle responses of the system shown in Fig. 5.2(a) indicate that the system is able to survive a major disturbance. However, the dynamic performance of the system is very poor due to inadequate damping. The dynamic behaviour of the machines in the Region 2 is obviously undesirable and some countermeasures have to be taken. The strong coupling between the LKB and MM3 machines reveals a close agreement of eigenvalue analysis and the transient study. The voltage responses of the system to the disturbance as seen from Fig.5.2(b) fluctuate within

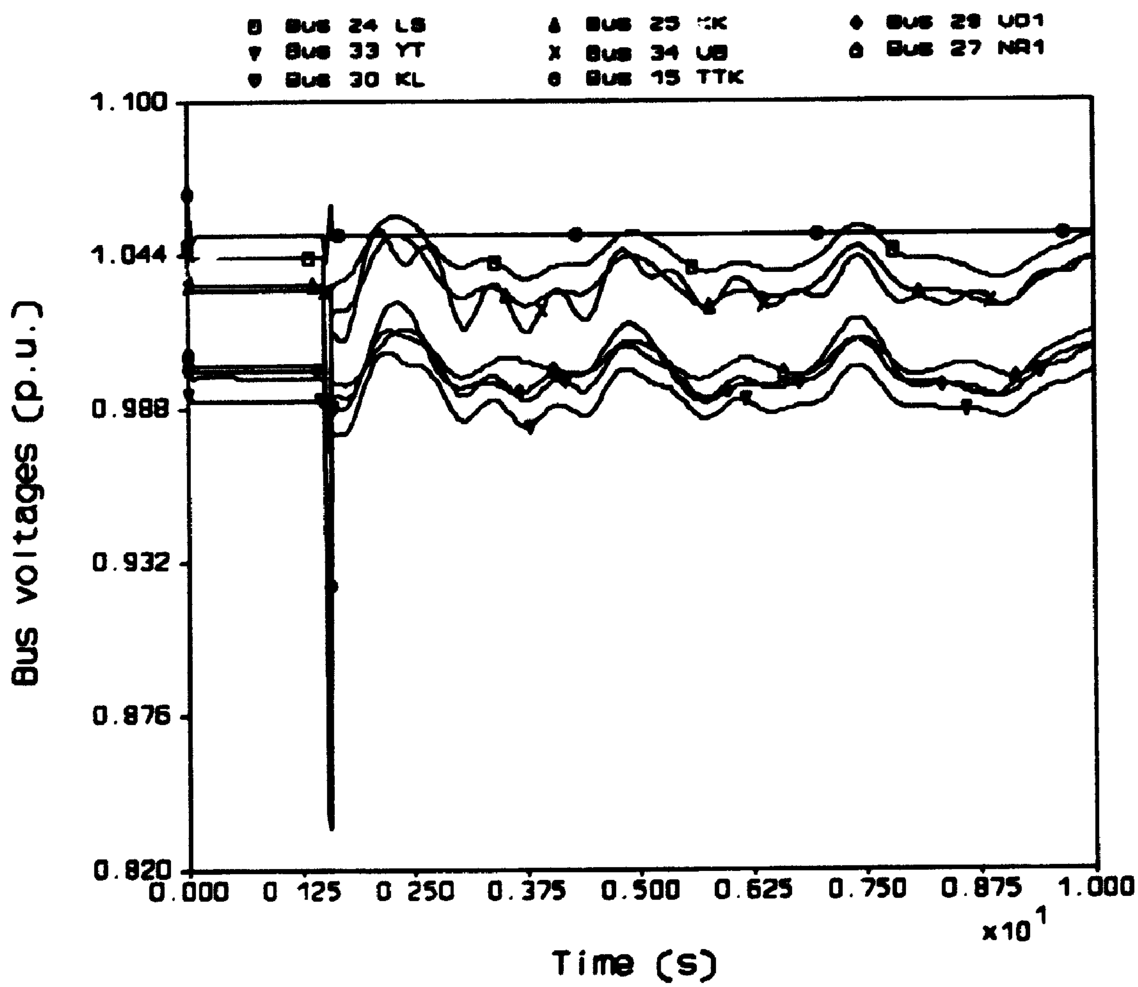

Fig. 5.2(b) : Voltage responses of the simplified EGAT system to a temporary increase in local load (0.1 pu resistance) at LS without damping control.

± 2.5% and take a very long settling time on account of poor damping. The voltage response of the TTK bus is extremely good which indicates that the control parameters of the SVC are correctly designed. Even though the voltage responses are acceptable but poor system damping imposes a restriction to further increase the generated power of some machines and line loadings of the system particulary in the Region 2.

5.7 Steady-state stability improvement using the existing SVCs

The existing SVCs at CP and TTK can be used to improve the dynamics of the system through their supplementary controls. Unfortunately, the modal control technique, successfully employed in Chapter 4, can not be directly applied in a multi-machine system for the following reasons;

a) there are many modes of oscillation in the system, the modes that are likely to be improved by the SVCs have to be determined,

b) the local signals taken from the bus quantities may contain the information of many modes, in order to increase the damping of some desired modes the supplementary control has to be judiciously designed and

c) the improvement gained for one mode may have an adverse effect on the others due to system complexities.

5.7.1 Tentatively improved oscillation modes

As the dynamics of the Region 3 has been ignored in the analysis, the supplementary control of the CP SVC will not be considered. Therefore the supplementary control of the TTK SVC will be designed to improve the system damping. From the geographical inspection, the TTK SVC should have some effects on the machines in the Region 4. This observation is also true as confirmed by the participation factors of TTK SVC as shown in Table 5.4. In Table 5.4, the oscillation modes 1, 2 and 5, correspond to NR1, SK and MM3 machines. These are only slightly influenced by the TTK SVC. The participation is very small due to the fact that the SVC is designed solely for voltage control.

5.7.2 Design of damping control

The frequency response technique described in Section 3.7.2.2 is utilized in the design of the supplementary control at TTK SVC. One of the powerful features of the S^3 program is the frequency response. Frequency responses of any bus or line quantities to a sinusoidal input at any control device in the system can be calculated. The scanning frequency can be either real or complex at any desired damping ratio ζ.

Conventionally, the frequency response of a system is evaluated using the real frequency. But for the context of this application, the system gain and phase information estimated at the desired damping ζ are needed. Since the damping of the MM3 machine is about 0.125 from Table 5.4, the desired damping is chosen to be 0.15. The line current

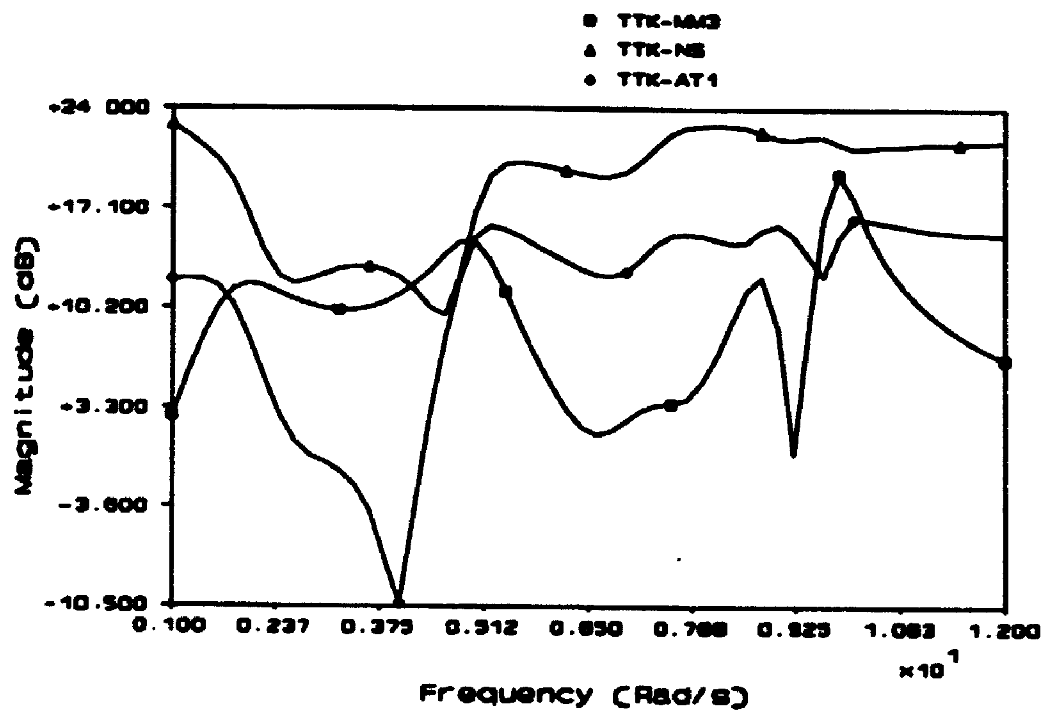

Fig. 5.3(a) : Magnitude response of line currents taken at TTK bus of the EGAT system without damping control.

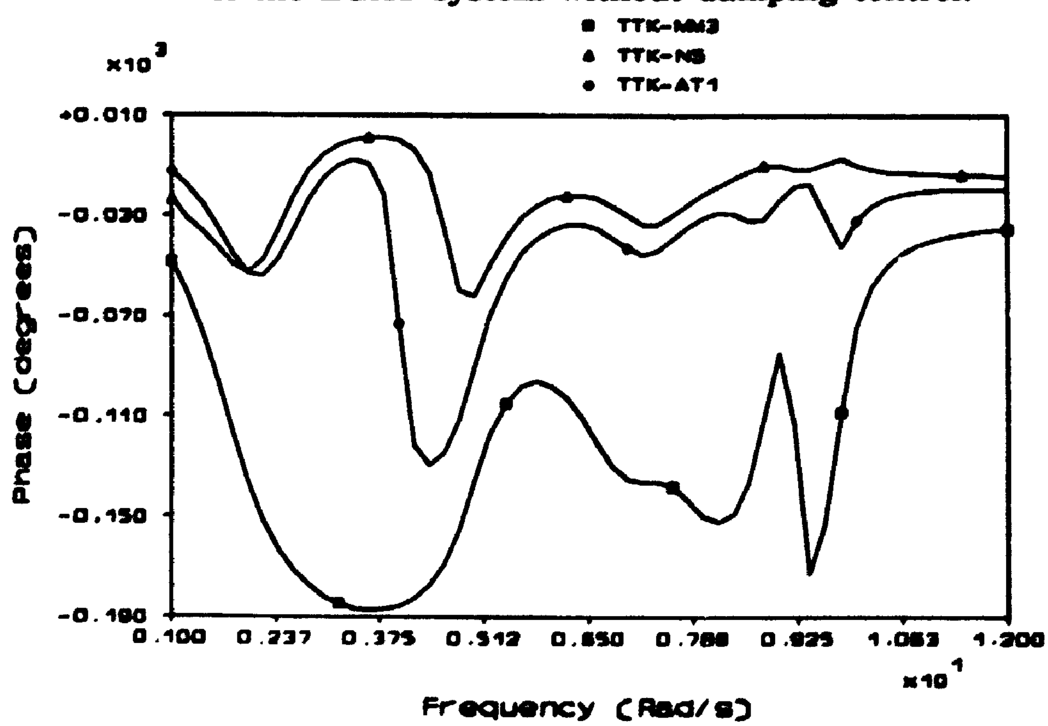

Fig. 5.3(b) : Phase response of line currents taken at TTK bus of the EGAT system without damping control.

magnitude at the TTK bus is chosen to be the damping signal. Important questions arise for the damping signal (the current) as to from which line should it be taken and whether it conveys the information of the desired modes? The frequency response of line current magnitudes at TTK bus to a sinusoidal input at the reference of the TTK SVC is illustrated in Figs. 5.3(a) and 5.3(b). The peaks of the magnitude response indicate that the scanned frequencies correspond to the eigenfrequencies of the system. It is very clear from Fig. 5.3(a) that the current signal of the line TTK-MM3 is the most sensitive signal. The magnitudes and phases at the peak frequencies are listed in Table 5.6 .

Table 5.6 : System gain and phase at TTK bus

Mode	Freq.(rad/s)	Gain(dB)	Phase(degree)
1,2	5.0	14.77	-135.6
8	8.8	12.26	-110.9
11	9.8	19.51	-108.4

The peak frequencies coincide with the oscillation modes as indicated in Table 5.4. These frequencies are slightly shifted from the original values because they are calculated at 0.15 damping.

The design of the damping control is based on the pole assignment technique [34] with a minor modification as more than one modes are considered simultaneously. To satisfy the conditions listed in Table 5.6, phase compensation and gain must be provided at the indicated frequencies. By using the well-known magnitude and phase criteria of root locus technique, the magnitudes and phases of the compensation circuits for each mode can be determined.

5.7.3 Design steps

The design techniques for the supplementary control are as follows :

a) determine the required phase lead/lag for each mode,

b) adjust the phase lead/lag requirements to be within practical limits,

c) locate poles and zeroes to contribute phase compensation for all modes,

d) calculate the magnitude of the compensation network at each mode and the corresponding gain value,

e) choose the minimum gain value and verify the design with the eigenvalue analysis,

f) repeatedly adjust the gain so that the damping of all modes is maximally achieved and

g) verify the design with transient stability simulation.

5.7.4 Illustration of the design

a-b) Compensated phase :

By employing phase criterion and the technique mentioned in Section 3.7.2.2, the required phase compensation Φ_c and its adjusted value for each mode are tabulated in Table 5.7.

Table 5.7 : Phase compensation requirements

Mode	Freq.(rad/s)	Phase(degree)	Φ_c	Φ_c(adjusted)
1,2	5.0	-135.6	135.6	45
8	8.8	-110.9	110.9	40
11	9.8	-108.4	108.4	35

The adjusted phases are based on the practical limitation that phase contribution by a single lead network should be less than 60 degrees and the number of compensation units is limited in the simulation programs. All phase lead units will contribute to the total phase requirement.

c) Poles and Zeroes allocation :

From classical control theory, a phase lead network of the form

$$H(s) = \frac{(1+\alpha Ts)}{(1+Ts)} \quad , \alpha > 1$$

contributes the maximum phase of Φ_m at the frequency ω_n where

$$\omega_n = \frac{1}{\sqrt{\alpha}T} \quad \text{and} \quad \Phi_m = \sin^{-1}\left(\frac{\alpha-1}{\alpha+1}\right) \quad \text{or} \quad \alpha = \frac{1+\sin\Phi_m}{1-\sin\Phi_m}. \tag{5.5}$$

Therefore the poles and the zeroes , in terms of α and T values for each compensator can be calculated using Eqn. (5.5). The results are shown in Table 5.8.

Table 5.8 : Calculated poles and zeroes.

Mode	Freq.(rad/s)	Φ_c	α	T	P_c	Z_c	P_s
1,2	5.0	60	5.828	.0828	-12.07	-2.07	-.75+j4.943
8	8.8	50	4.599	.0530	-18.87	-4.10	-1.32+j8.70
11	9.8	50	3.690	.0531	-18.82	-5.10	-1.47+j9.689

The net phase lead by all units is slightly in excess of the required phase lead to offset the phase lag in the current measuring unit in the simulated program [48]. The supplementary control must be activated only when the low-frequency oscillation begins to develop and it should be automatically terminated when the system oscillation ceases. In addition, it should not interfere with the normal control function of the SVC. Therefore a washout unit of time constant 10 s is added to serve this requirement. Thus the transfer function of the supplementary control takes the form

$$H(s) = K_c \left[\frac{10s}{1+10s}\right] \cdot \left[\frac{1+.4828s}{1+.0828s}\right] \cdot \left[\frac{1+.2436s}{1+.0530s}\right] \cdot \left[\frac{1+.2436s}{1+.0531s}\right] .$$

d) Gain calculation :

The location of poles and zeroes of the compensator and the desired

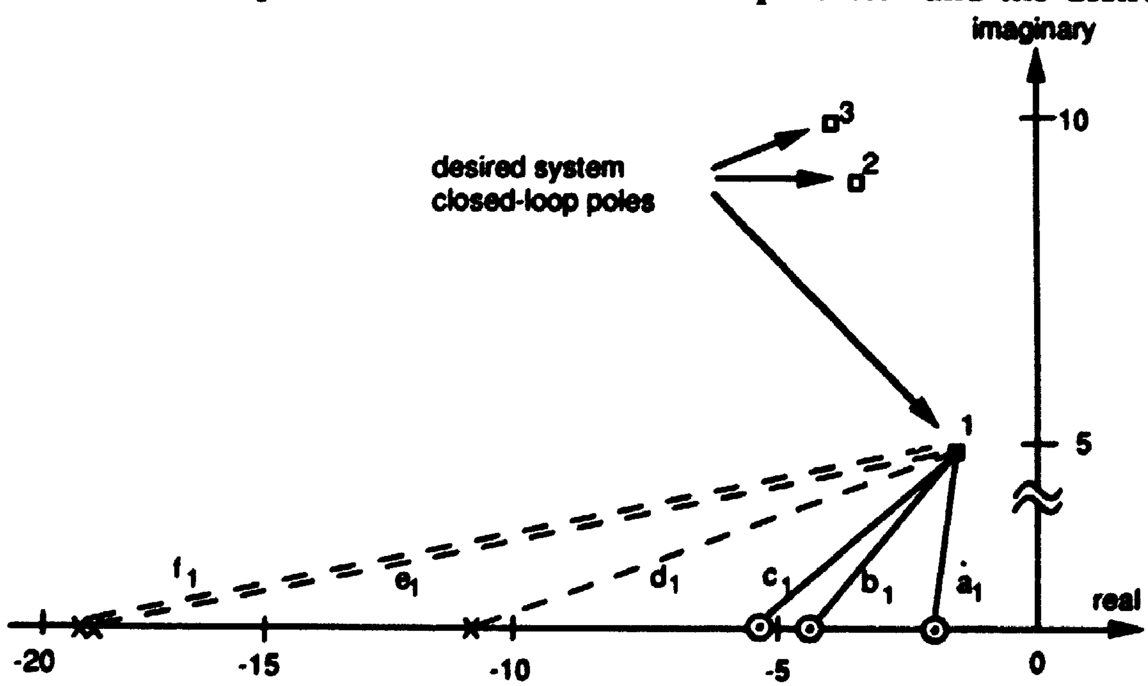

Fig. 5.4 : Poles and zeroes location

closed-loop poles of the system are illustrated in Fig. 5.4. The required closed-loop poles of the system for each mode are located at points 1, 2 and 3. The poles and zeroes of the compensating network are placed on the real axis of the S-plane. Consider the oscillation mode corresponding to 5 rad/s at point 1, the magnitude of the cascaded compensating network is calculated from the distances between point 1 and pole-zero locations and the factor α of each unit as

$$|H(s)| = K_c . \alpha_1\alpha_2\alpha_3 . \frac{a_1\ b_1\ c_1}{d_1\ e_1\ f_1} .$$

The value of K_c is computed from the system gain corresponding to this mode at point 1. Similarly, the values of K_c for other modes at points 2 and 3 can be determined. The calculated values of distances and K_c are indicated in Table 5.9.

Table 5.9 : Calculated values of TTK compensating network

	Mode 1,2	Mode 8	Mode 11
Freq.	5 rad/s	8.8 rad/s	9.8 rad/s
a	5.116	8.732	9.318
b	5.973	9.134	10.147
c	6.585	9.486	10.451
d	12.353	13.830	14.385
e	18.738	19.547	19.931
f	18.783	19.589	19.971
H(s)	4.578K_c	14.132K_c	17.988K_c
G(s)	5.476	4.102	9.451
K_c	0.0398	0.0172	0.0058

e-f) Gain adjustment :

Despite the known values of K_c for each mode, damping enhancement can not be achieved for all modes as only one value of K_s is allowable. If the gain K_s is chosen to satisfy only one particular mode, the damping of the other modes may worsen and the system may become even unstable. Therefore, repeated eigenvalue analysis must be performed to ascertain the best value of K_s. The optimal value of K_s is found to be 0.0025 from eigenvalue analysis. The damping of the designed modes is improved but it is not as great as expected primarily because the value of K_s is chosen to be a compromise value. Table 5.10 shows the improved eigenvalues of the system as well as the participation of all inertial modes including SVCs. It is evident that the TTK SVC participates in almost all modes with the supplementary control. The participation of many machines to the desired modes is decreased. The reduction of the participations of the machines that strongly influence the oscillation modes is a clear indication of damping improvement for those modes.

g) Transient stability validation :

Transient stability study is performed to verify the designed supplementary control. The type of fault and its location are the same as in the previous case in order to examine the effectiveness of the damping control. Figure 5.5(a) illustrates rotor angle responses of all machines to the fault. It can be seen that the damping of nearly all modes is increased especially for the designed modes corresponding to NR1, SK, LKB and MM3 machines. Thus the design of the supplementary control at TTK SVC is successful.

Table 5.10 : System eigenvalues and participations of all machines with damping control at TTK SVC.

Mode			Machine														SVC	
No	ω_n	ζ	UD1	NNG	SRD	UR	SK	BB	MM3	NR1	LKB	CLB	KHL	SNR	TN	NB	TTK	CP
1	5.0004	.0827	.0031	.0128	.0011	.0121	.0664	.0115	.0205	.3569*	.0067	.0016	.0003	.0003	-	-	.0138	-
2	5.0738	.0535	.0069	.0281	.0019	.0415	.2043*	.0210	.0319	.1439	.0081	.0026	.0005	.0005	-	-	.0129	-
3	6.0482	[illegible]	.0203	.0939	.0026	.6350	.2245	.0038	.0052	.0022	.0004	.0017	.0002	-	-	-	.0018	-
4	6.6645	[illegible]	-	-.0004	-	.0008	.0107	.0041	.0006	-	-	-	.5604	.4227	-	-	-	-
5	7.0388	.0253	.0794	.5934	.0062	.2449	.0530	.0029	.0027	.0004	.0017	.0049	.0016	.0010	-	-	-.0002	-
6	7.4134	.0642	.0039	.0467	-.0005	-.0042	.1145	.7419	.0703	-	.0149	-	.0063	.0030	-	-	.0091	-
7	8.7020	.1172	-.0010	.0242	-.0115	-.0018	.0585	.1915	.3406	-	.3538*	.0034	-	-	-	-	.0408	-
8	8.9648	.0594	-	-	-	-	-	-	-.0002	-	-	-	.4332	.5698	.0024	-	-	-
9	9.4460	.0379	-.0721	.0210	1.0229	.0022	-.0008	-.0016	-.0031	-	-.0005	.0176	-	-	-	-	.0004	-
10	9.5086	.0145	.9418	.1221	-.0599	.0006	-	-.0001	.0018	-	.0011	-.0066	-	-	-	-	-	-
11	9.5824	.1433	-	-	-	-	.0028	.0127	.3876*	-	.5725	.0023	-	-	-	-	.0315	-
12	10.0424	.0766	.0031	.0020	.0171	.0006	-	-	.0079	-	.0010	.9766	-	-	-	-	.0004	-
13	12.6434	.2338	-	-	-	-	-	-	-	-	-	-	.0030	.0125	1.0597	-.0004	-	-
14	12.9483	.0987	-	-	-	-	-	-	.0002	-	-	-	-	-	-.0004	1.0135	.0006	-
15	32.2527	.2598	-	-.0002	-.0001	-.0004	-.0064	.0118	-.0047	.0006	-	-	-	.0001	-	.0002	.9995	-
16	70.1703	.5288	-	-	-	-	-	-	-	-	-	-	-	.0006	-	-	-.0005	.9995

* improved mode

The corresponding voltage responses at various buses are also indicated in Fig. 5.5(b). Similar to the case of SMIB system, damping improvement of the system is achieved through voltage modulation at TTK bus. Therefore, the voltage variation of the system is greater with the application of damping control particularly after the removal of the fault. However, voltage variation, after the transient period, is confined to within ± 3%.

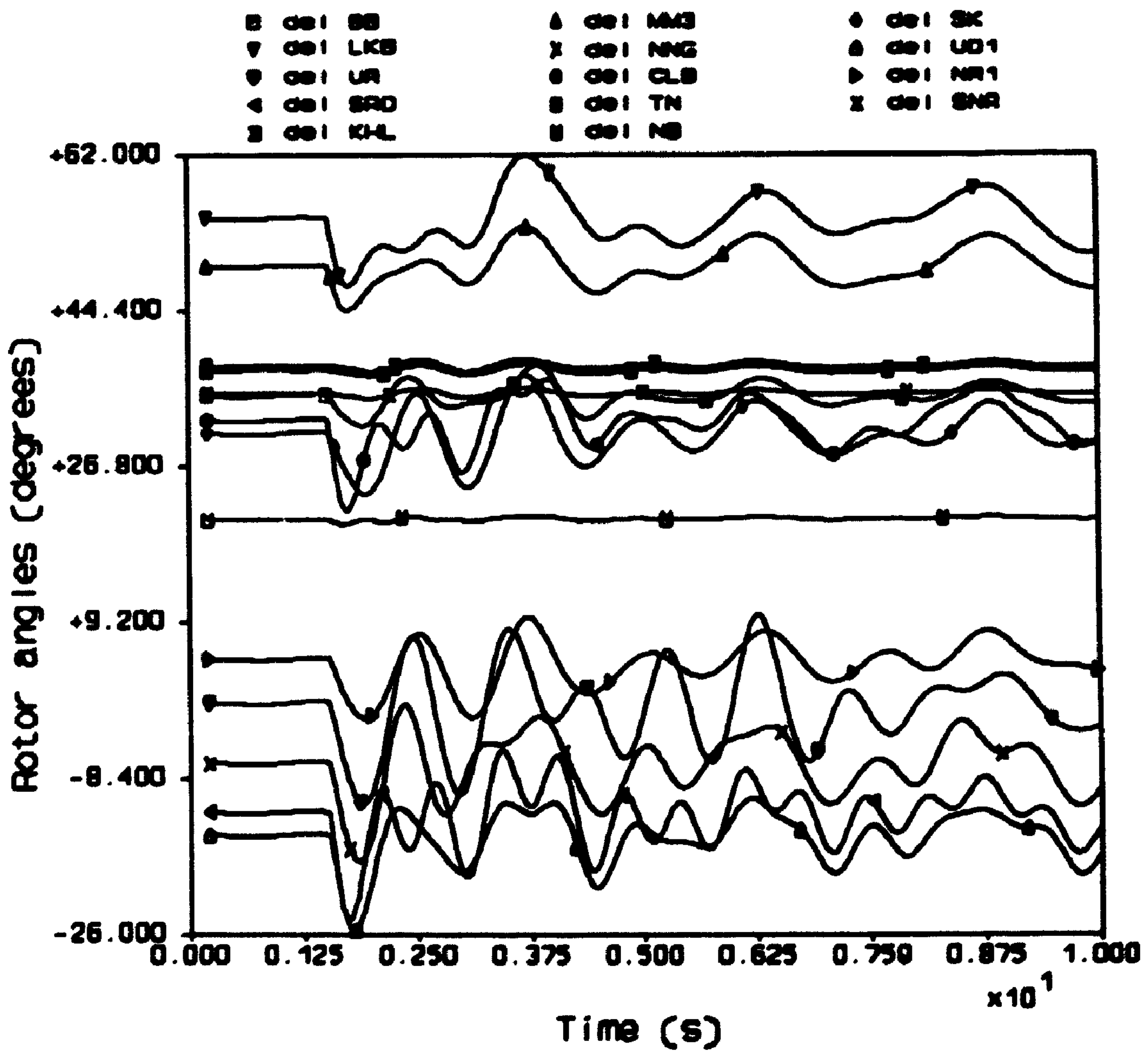

Fig. 5.5(a) : Rotor angle response of the simplified EGAT system to a temporary increase in local load (0.1 pu resistance) at LS with damping control at TTK SVC.

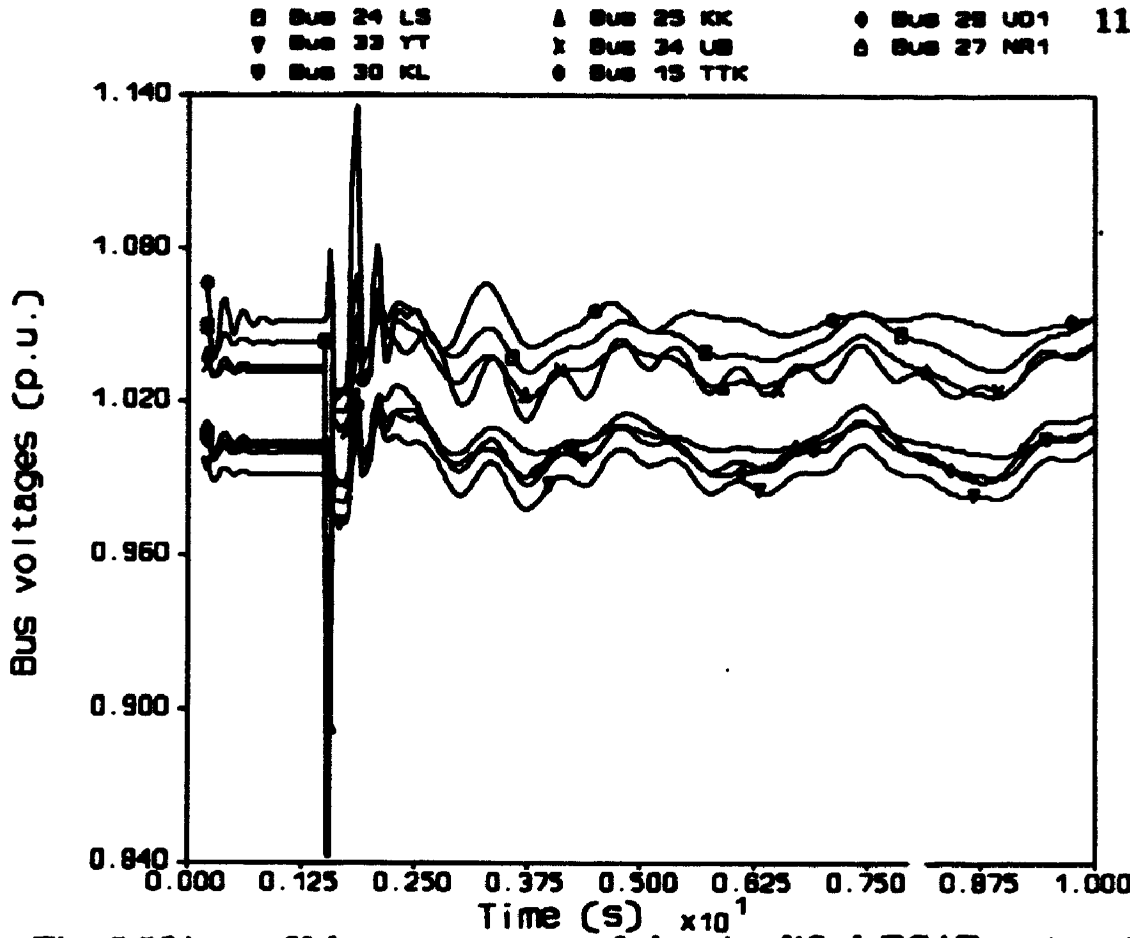

Fig. 5.5(b) : **Voltage responses of the simplified EGAT system to a temporary increase in local load (0.1 pu resistance) at LS with damping control at TTK SVC.**

5.8 Further system dynamic improvement

Even though the dynamic performance of the system as shown in Figs. 5.5(a) and 5.5(b) is satisfactory, further improvement can be made, if desired, by locating another SVC for controlling the voltage as well as for adding system damping for other modes. The criteria for the determination of SVC location and the design of a damping controller for other modes are demonstrated in the following subsections.

5.8.1 Suitable SVC location

The location of an additional SVC depends very much on the desired objectives and often requires engineering judgement. For the purpose of controlling the voltage, a good candidate location of a SVC is where :

a) the voltage variation is the greatest considering all possible realistic contingencies,

b) the short-circuit level is low (to minimize the rating of the SVC),

c) large power excursion is expected under severe contingencies,

d) it is a conjunctive location to many weak nodes in the system so that the voltage of the neighbouring buses can also be regulated,

f) the information of the desired damping modes is locally available.

Short-circuit levels of the system calculated at various strategic buses in the Region 2 using the approximation technique described in Section 5.5 are shown in Table 5.11 .

Table 5.11 : Short-circuit levels at various buses in Region 2

Bus No.	Name	S_c(p.u.)
23	PE	8.24
24	LS	45.0
25	KK	38.12
27	NR1	49.78
29	UD1	17.5

The S^3 program [52] also offers a measurable factor called the "Voltage Participation Factor" mentioned in Section 5.6.2. It indicates, for a particular mode, the influence of changes in shunt conductance or susceptance at a bus on the eigenvalue of that mode. Table 5.12 shows the Voltage Participation Factors to all inertial oscillation modes at the buses identified in Table 5.11. For these calculations the SVC at TTK bus is regarded to be in damping control. A suitable location for the new SVC, considered from the short-circuit consideration is at PE. But this location does not satisfy many other conditions since PE bus is geographically not

Table 5.12 : Voltage Participation Factors at various buses in Region 2.

Oscillation mode			Corresp.	Voltage Participation Factors				
No.	ω_n	ζ	machine	23 PE	24 LS	25 KK	27 NR1	29 UD1
1	5.004	.0827	NR1	.0325	.0322	.0257	.0277	.0353
2	5.074	.0535	SK	.0590	.0572	.0451	.0265	.0578
*3	6.048	.0251	UR	.0011	.0016	.0148	.0015	.0528
4	6.665	.0603	KHL	.0001	.0001	.0001	.0001	.0001
*5	7.039	.0253	NNG	.0049	.0055	.0162	.0028	.1078
6	7.413	.0642	BB	.0087	.0066	.0012	.0019	.0093
7	8.702	.1172	LKB	.0470	.0246	.0101	.0031	.0046
8	8.965	.0594	SNR	-	-	-	-	-
9	9.446	.0379	SRD	.0007	.0013	.0084	.0009	.0027
*10	9.5.9	.0145	UD1	.0002	.0004	.0019	.0002	.0104
11	9.582	.1433	MM3	.0099	.0058	.0034	.0014	.0014
12	10.042	.0766	CLB	.0002	.0005	.0049	.0005	.0005
13	12.643	.0987	TN	-	-	-	-	-
14	12.948	.2338	NB	-	-	-	-	-

* poorly damped machine

† calculated by using the S^3 [52].

an imposing site. SVC location at LS would be better suited if it was to increase the power transfer capability of the tie-line LS-KK as well as to damp the oscillation modes of the machines in the North. Although the short-circuit level at KK is greater than that at UD1, a new SVC should be located at KK for the reasons that KK is connected to many weak buses and it may experience a very large power excursion if there was a fault on the main tie-line LS-KK.

A consideration based on the damping contribution as determined by the Voltage Participation Factors, shown in Table 5.12 reveals that the SVC should be located at UD1 bus. Since damping improvement is gained through bus voltage modulation by the SVC and as there is a machine at UD1, there will be a conflict on controlling the voltage of UD1. Fast controllability of the SVC will force the excitation of UD1 machine to back off. Moreover, the modulation of bus voltage to damp other oscillation modes aggravates the conflict. In spite of the fact that the voltage participation to all modes at KK are not that high, KK is the best location as it participates in almost all modes and a SVC at this location can be justified for voltage control. Since many lines are connected to KK, the SVC can be designed to selectively damp any desired mode by taking a damping signal from the appropriate line. Therefore an additional SVC may be located at KK considering both the voltage and damping control capabilities as well as its geographical importance.

5.8.2 SVC rating

Typically, the rating of a SVC is obtained from transient stability studies. Possible power system contingencies have to be considered and transient stability program has to be repeatedly run while the rating of the SVC is adjusted so that the system survives the severest condition. Since under the worst condition, some machines and lines or loads must be tripped from the system so that the rest of the system is able to operate satisfactorily. Such a complete study is considered to be beyond the scope of this thesis.

The size of the SVC at KK is therefore arbitrarily selected to be ± 50 Mvar. A small rating SVC is considered under the assumption that the SVC is floating under normal condition and will respond to only changes in the system voltage and as a requirement of damping control.

Therefore a SVC is added at KK bus and its control parameters are determined by using the same technique as employed in Section 5.5. With the same current droop of 0.5%, the lead and lag time constants are found to be 0.2 s and 0.024 s respectively. The system eigenvalues and their participations with KK SVC are shown in Table 5.13.

The transient performance of the system, with the additional SVC at KK operating in voltage control, is very much improved as illustrated in Figs. 5.6(a) and 5.6(b). Not only is the voltage at the bus KK better regulated, also the rotor angles of all machines, as shown in Fig. 5.6(a) are better damped. This outcome agrees well with the eigenvalue analysis which indicates damping improvement of nearly all modes. Furthermore, the voltage at all buses in the Region 2 are well regulated to be within ± 1% after the removal of the fault as seen from Fig. 5.6(b). The voltage at TTK bus is oscillatory because of the damping control at TTK SVC. The overall results confirm that the application of SVC at KK bus is very

Table 5.13 : System eigenvalues and paticipations of all machines with damping control at TTK SVC and an additional SVC at KK.

Mode			Machine														SVC		
No	ω_n	ζ	UD1	NNG	SRD	UR	SK	BB	MM3	NR1	LKB	CLB	KHL	SNR	TN	NB	TTK	CP	KK
1	5.1690	.0704	.0064	.0245	.0021	.0376	.1670	.0153	.0217	.7209	.0068	.0017	.0004	.0004	-	-	.0022	-	-.0001
2	4.7738	.0718	.0257	.0925	.0058	.1042	.2993	.0450	.0787	.2799	.0279	.0086	.0010	.0012	-	-	.0245	-	.0015
3	6.0222	.0292	.C201	.0909	.0028	.5605	.2996	.0061	.0061	.0032	.0008	.0020	.0004	.0004	-	-	.0030	-	-.0002
4	6.6649	.0601	-	-.0004	-	-.0010	.0110	.0038	.0008	-	-	-	.5602	.4225	.0120	-	-.0001	-	-
5	6.9966	.0264	.0774	.5474	.0084	.2893	.0558	.0032	.0013	.0014	.0023	.0054	.0019	.0012	-	-	-.0008	-	.0002
6	7.4217	.0677	.0033	.0462	-.0006	-.0044	.1046	.7393	.0731	-	.0157	-.0002	.0061	.0030	-	-	.0056	-	-
7	8.6949	.1262	-.0003	.0285	-.0222	.0018	.0580	.1760	.3549	-	.4038	-.0062	.0002	-	-	-	.0236	-	.0007
8	8.9648	.0594	-	-	-	-	-	-	-.0002	-	-	-	.4331	.5698	.0024	-	-	-	-
9	9.3839	.0416	-.0466	.0497	.9690	.0034	-.0012	-.0036	-.0099	-	-.0049	.0316	-	-	-	-	.0026	-	-.0003
10	9.5105	.0153	.9077	.1094	-.0132	.0002	-	-	.0014	-	.0016	-.0071	-	-	-	-	-	-	-
11	9.5603	.1600	.0002	-.0002	.0008	-	.0054	.0246	.4087	-	.5216	.0004	-	-	-	-	.0425	-	-.0004
12	10.0410	.0743	.0041	.0022	.0282	.0006	-	-.0004	-.0037	-	.0010	.9740	-	-	-	-	.0005	-	.0003
13	12.6433	.2338	-	-	-	-	-	-	-	-	-	-	.0030	.0125	1.0597	-.0004	-	-	-
14	12.9461	.0988	-	-	-	-	-	-	-.0004	-	-	-	-	-	-.0004	1.0134	.0005	-	-
15	28.0233	.0791	-	-	-	.0001	-.0034	.0063	.0152	.0004	-	-	-	-	-	.0004	.9655	-.0001	.0160
16	70.1752	.5290	-	-	-	-	-	-	-	-	-	-	-	.0006	-	-	-.0003	.9995	-
17	48.9227	.5307	.0005	.0100	.0072	.0109	.0096	.0033	-.0037	.0134	-.0002	.0048	-	-	-	-	-	.0426	.9022

desirable.

5.8.3 Damping improvement through KK SVC

The damping performance of the system can be further improved by employing supplementary controls at KK SVC. From Fig.5.6(a), the oscillation modes that can be refined are the modes corresponding to

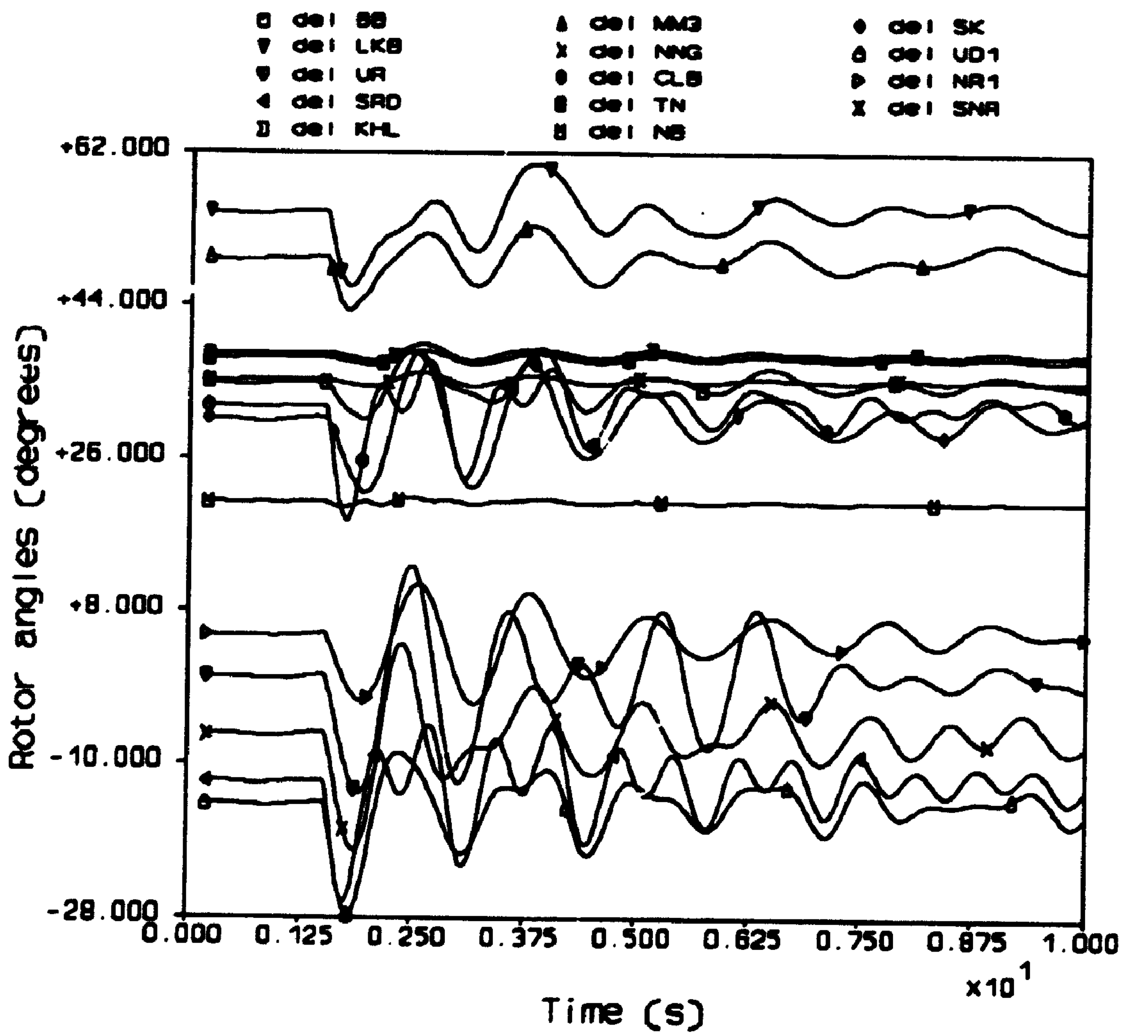

Fig. 5.6(a) : Rotor angle responses of the EGAT system to a temporary increase in local load (0.1 pu resistance) at LS with damping control at TTK SVC and an additional SVC at KK.

NNG, SRD and UD1. Line current signal at KK bus is chosen to be the damping signal. The frequency response of the line currents at KK bus, calculated at complex frequencies of damping 0.1, is shown in Figs. 5.7(a) and 5.7(b). The peaks of the current magnitude response for each line appear at the same frequencies except for the response of the line KK-NR1 where the NR1 mode is present. Since the NR1 mode has already been improved by the damping control at TTK SVC, therefore, the

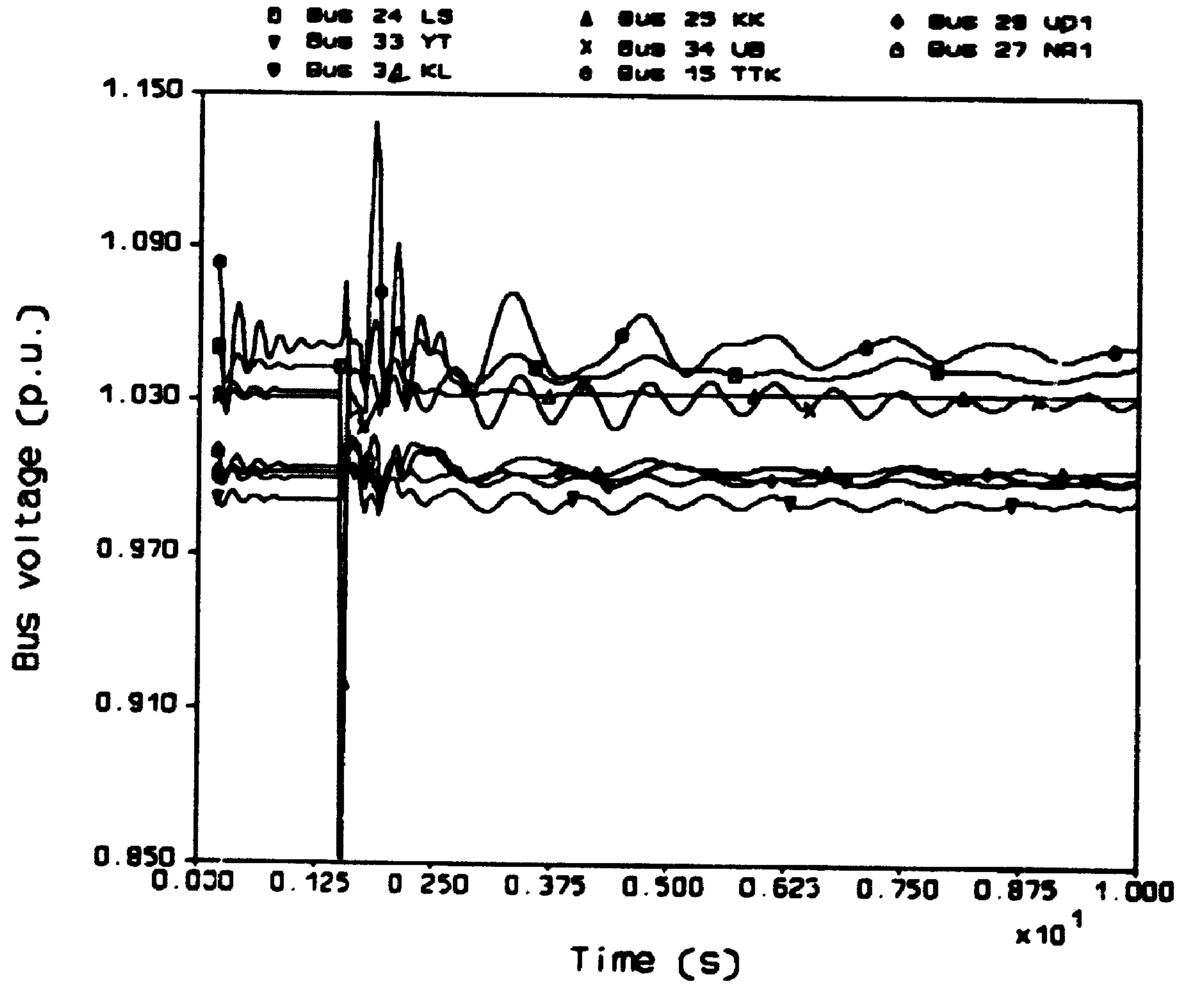

Fig. 5.6(b) : Voltage responses of the EGAT system to a temporary increase in local load (0.1 pu resistance) at LS with damping control at TTK SVC and an additional SVC at KK.

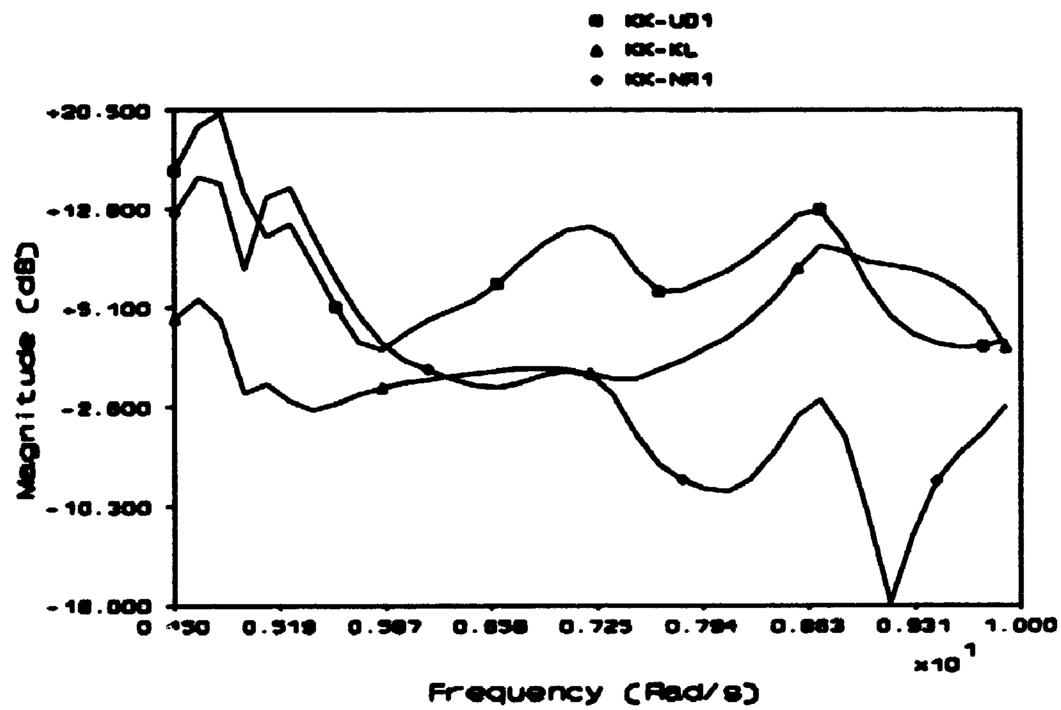

Fig. 5.7(a) : Magnitude response of line currents taken at KK bus of the EGAT system.

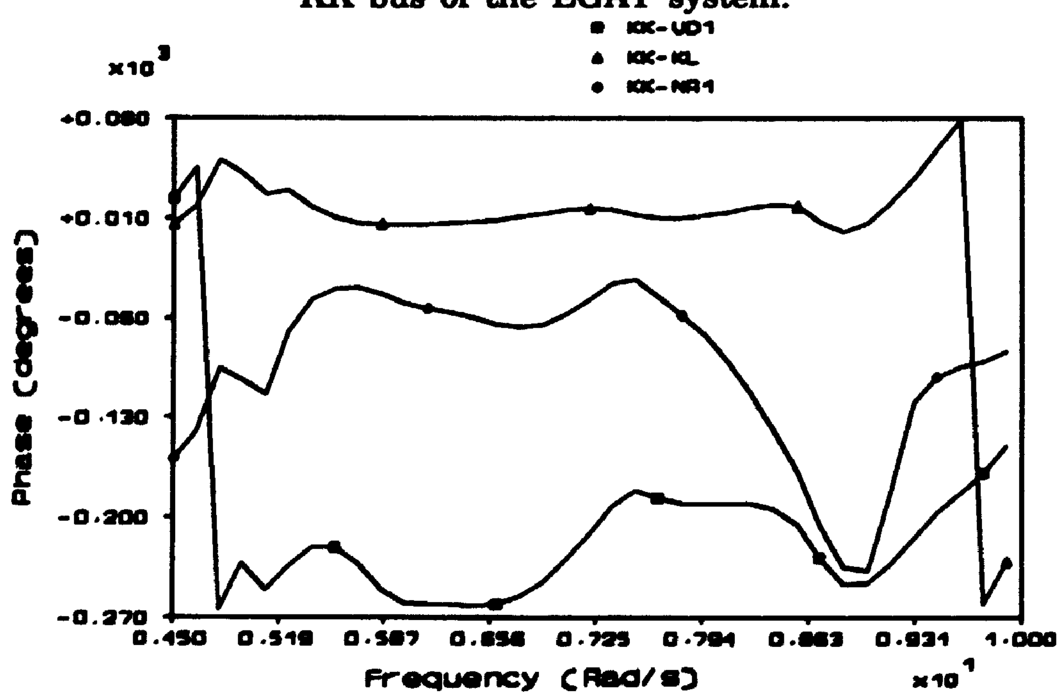

Fig. 5.7(b) : Phase response of line currents taken at KK bus of the EGAT system.

design is focused on the peaks at 4.8, 7.2 and 8.7 rad/s which belong to SK, NNG and LKB machines. It can be seen from the magnitude responses that line KK-UD1 is the most sensitive line and is therefore chosen for the design of the damping control. The numerical values of the magnitudes and phases at the peak frequencies including the required phase compensation for each mode are tabulated in Table 5.14.

Table 5.14 : Frequency response data of line KK-UD1.

Mode	ω_n	Gain(dB)	Phase	Φ_c	Φ_c(adjusted)
2	4.8	20.29	-236.7	236.7	20.0
5	7.2	11.43	-211.8	211.8	15.0
7	8.7	12.78	-228.2	228.2	18.0

The design technique for the supplementary control at KK SVC is similar to that of Section 5.7.4 and is not repeated here. The adjusted phase Φ_c in Table 5.14 is achieved through a phase reversal of -180 degrees or the gain value is negative. Therefore, the transfer function of the auxiliary control at KK SVC assumes the form

$$H(s) = K_c \left[\frac{10s}{1+10s}\right] \cdot \left[\frac{1+.2874s}{1+.1510s}\right] \cdot \left[\frac{1+.1764s}{1+.1093s}\right] \cdot \left[\frac{1+.1533s}{1+.0861s}\right]$$

where K_c is negative and a reset network of time constant 10s is included. The calculated value of the gain K_c is found to be -0.053, -0.106 and -0.07 respectively. By using eigenvalue analysis, the best gain K_c is found to be -0.066. The results of adding damping control at KK SVC obtained from transient stability study are illustrated in Figs. 5.8(a) and 5.8(b).

The eigenvalues of the system and the participations of all machines are shown in Table 5.15. The design is successful in providing additional damping for the specified modes while the voltage regulation of all buses in the Region 2 as seen from Fig. 5.8(b) is attainable. However, the improvement of the desired NNG modes adversely affects the mode corresponding to SRD machine. The damping of SRD machine is lowered

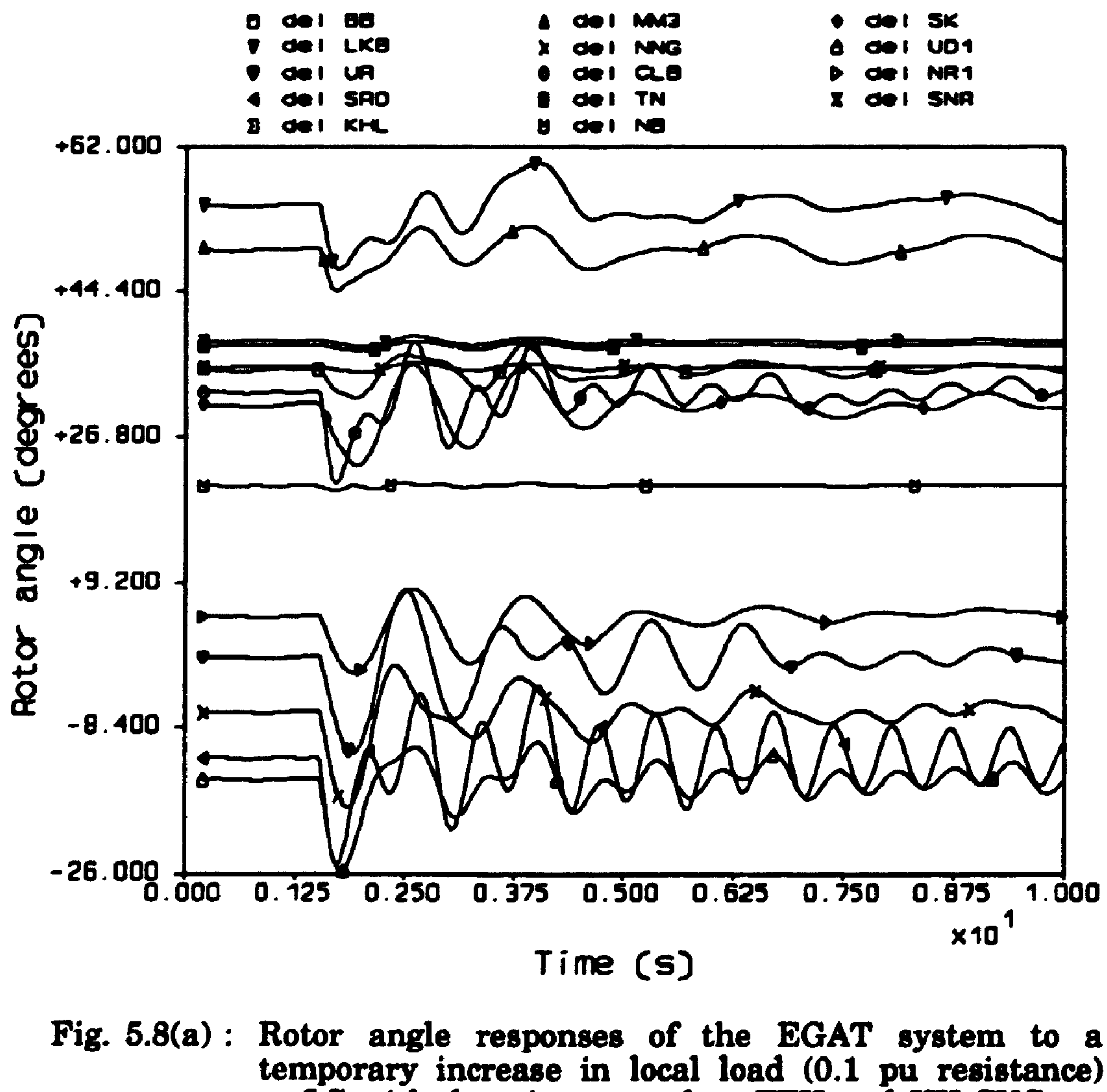

Fig. 5.8(a) : Rotor angle responses of the EGAT system to a temporary increase in local load (0.1 pu resistance) at LS with damping control at TTK and KK SVCs.

which can be seen from the results in Table 5.15 or from Fig. 5.8(a). This phenomenon can be explained through the examination of the eigenvector of that mode. The results in Table 5.5 indicate that for mode 9, the components of the eigenvector corresponding to NNG and SRD machines, are oppositely directed. This means that these machines are oppositely coupled and an improvement of one machine will have an adverse effect on the other. Since the NNG machine lies outside the control of EGAT,

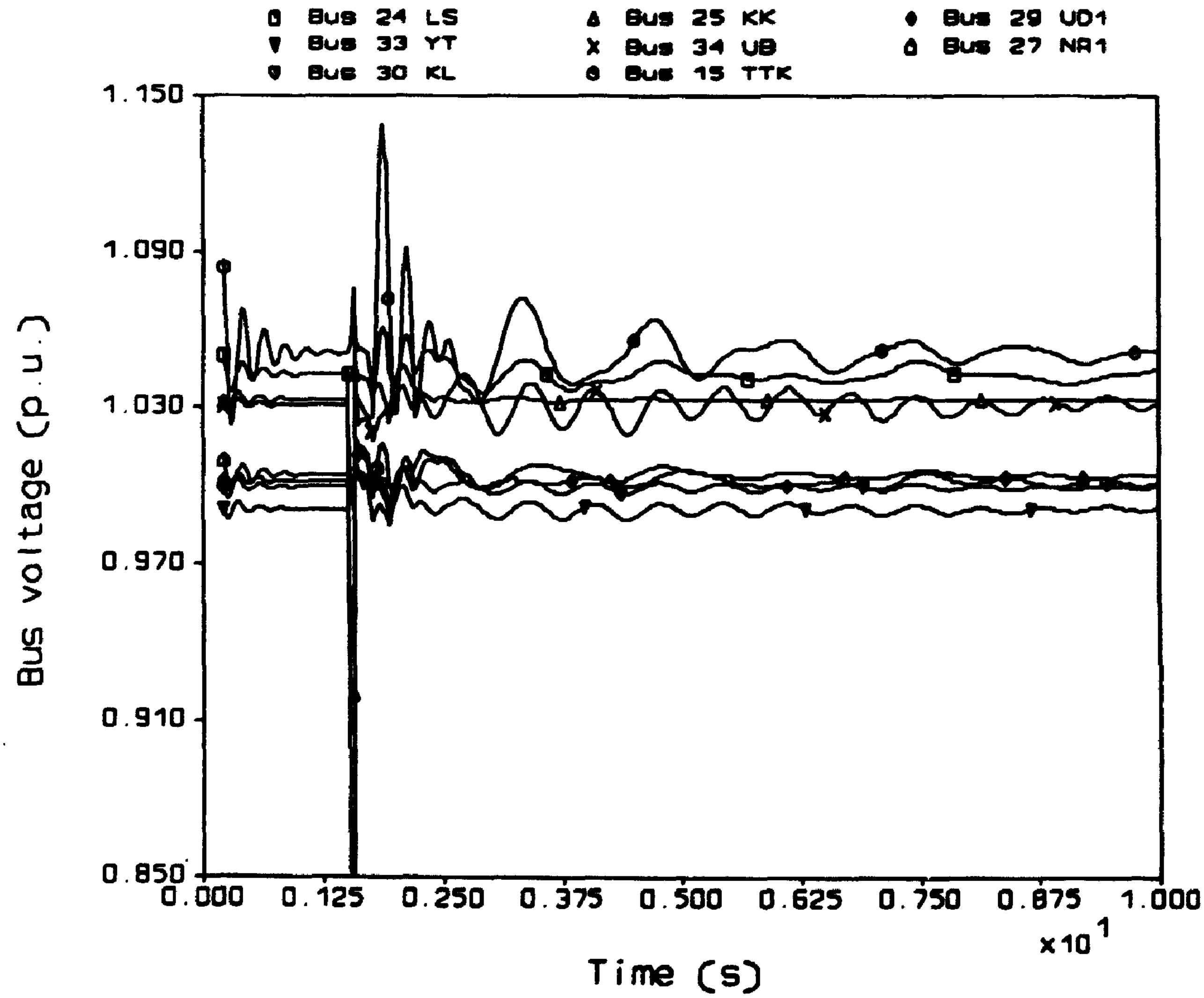

Fig. 5.8(b) : Voltage responses of the EGAT system to a temporary increase in local load (0.1 pu resistance) at LS with damping control at TTK and KK SVCs.

Table 5.15 : System eigenvalues and paticipations of all machines with damping control at TTK and KK SVCs.

Mode			Machine														SVC		
No	ω_s	ζ	UD1	NNG	SRD	UR	SK	BB	MM3	NR1	LKB	CLB	KHL	SNR	TN	NB	TTK	CP	KK
1	5.1443	.0742	.0062	.0234	.0014	.0270	.1032	.0103	.0166	.7999	.0053	.0012	.0002	.0002	-	-	.0039	-	.0075
2	4.6944	.0817	.0372	.1322	.0114	.1188	.2784*	.0436	.0778	.2027	.0276	.0094	.0010	.0012	-	-	.0244	-	.0428
3	6.0122	.0344	.0197	.0881	.0027	.4649*	.3973	.0081	.0092	.0020	.0012	.0020	.0004	.0004	-	-	.0020	-	.0046
4	6.6653	.0600	-.0002	-.0016	-	.0013	.0104	.0035	.0008	-	-	-	.5616	.4232	.0120	-	-.0001	-	-
5	6.8548	.0360	.0615	.3966*	.0065	.3808	.0881	.0109	.0042	.0010	.0027	.0056	.0019	.0013	-	-	-.0003	-	.0396
6	7.4653	.0655	.0062	.0690	-.0008	-.0032	.0744	.7874	.0599	-	.0115	-.0006	.0049	.0022	-	-	.0046	-	-.0099
7	8.8259	.1295	-.0005	.0341	-.0074	-.0004	.0441	.1294	.3569	-	.4754	-.0077	-	-	-	-	.0141	-	-.0283
8	8.9648	.0594	-	-	-	-	-	-	-.0002	-	-	-	.4333	.5697	.0024	-	-	-	-
9	9.3631	.0284	.1795	.1719	.6034	.0046	.0005	.0005	-.0123	.0002	-.0159	.0504	-	-	-	-	.0002	-	.0108
10	9.5379	.0208	.6519*	.0262	.3385	-.0011	-.0002	-.0001	.0056	-	.0036	-.0189	-	-	-	-	-	-	-.0135
11	9.5618	.1619	.0014	-	.0001	-	.0062	.0278	.4486	-	.4738	.0018	-	-	-	-	.0475	-	-.0019
12	10.1077	.0681	.0056	.0062	.0343	.0004	-	-	-.0017	-	-.0029	.9757	-	-	-	-	-.0003	-	-.0107
13	12.6433	.2338	-	-	-	-	-	-	-	-	-	-	.0030	.0125	1.0598	-.0004	-	-	-
14	12.9461	.0988	-	-	-	-	-	-	-.0004	-	-	-	-	-	-.0004	1.0134	.0005	-	-
15	28.0053	.0716	-	.0001	-	-	.0002	.0067	.0144	.0003	.0002	-	-	-	-	.0002	.9474	-.0001	.0319
16	70.1698	.5290	-	-	-	-	-	-	-	-	-	-	-	.0006	-	-	-.0004	.9999	-.0002
17	48.2136	.3622	-.0214	-.0069	.0131	.0023	.0031	.0065	-.0020	.0106	.0039	-.0011	-	-	-	-	.0597	-.0003	.9372

* improved mode

therefore, it is practically reasonable that the damping of this mode should be improved. Further damping improvement on SRD machine, if needed, can be accomplished through the application of power system stabilizer at it.

CHAPTER VI

CONCLUSIONS

6.1 Summary

In this thesis a very brief review of static var compensator, their characteristics and their principal applications have been given in Chapter 2. The major objective of the proposed research was to formulate design procedure for the controllers of SVC. Voltage control is the primarily function of a SVC. However, in this thesis, attention has been primarily focused on the damping contribution of SVCs.

It had been assumed that the design procedure of controllers and supplementary signals can be best handled for two situations :

(a) Parts of a power system which contain long lines which form parts of a radial system can be handled by a single machine infinite bus (SMIB) representation.

(b) Simplified network of power system in which major generation, high voltage transmission lines and loads are represented to form a multi-machine system.

In Chapter 3, models of SVC and their controllers have been developed. Suitable model for steady-state stability studies have been developed. In order to undertake design of stabilizers linear analysis is used.

In Chapter 4, a detailed mathematical model for a single machine infinite bus (SMIB) with a SVC in the mid location of a long line is undertaken. This analysis provides a small signal closed form solution and is a new contribution. The theory is applied to a SMIB test system. Variations of optimal control parameters for the SVC with system load are shown. As well, design of supplementary control is undertaken. For a SVC controller with supplementary damping control, for the test case, the most suitable values are chosen and the system has been studied. Once the effectiveness of the damping contribution for inertial modes of steady-state stability was demonstrated, test for a major disturbance was undertaken. It is shown that the damping signal and the supplementary control developed for a linearized model can provide useful damping for a major disturbance as well.

In order to address the problems of an interconnected multi-machine system, the EGAT system has been used as an example. Identification of poorly damped modes has been done by an eigenvalue analysis. The problem of damping troublesome modes is handled in two ways. In the first case, damping control is added on the existing SVC. Then consideration has been given to the location of a new SVC to further improve the system performance. For the second phase, in addition to the design procedures, a systematic procedure to determine the best location is also undertaken. For a complex system (EGAT), unlike the use of modal analysis for the SMIB system, placement of poles and zeroes is employed. The study of the EGAT system establishes the validity of the procedures. The entire development of Chapter 5 is also a new contribution. Table 6.1 summarizes the inertial modes of the EGAT system under different cases. The damping of most electromechanical modes is improved with the application of damping control at SVCs. The

Table 6.1 : System damping improvement of the EGAT system.

Mode	Machine	case 1		case 2		case 3		case 4	
		ω_n	ζ	ω_n	ζ	ω_n	ζ	ω_n	ζ
		Electromechanical modes							
1	NR	5.0236	.0827	5.0040	.0827	5.1609	.0704	5.1443	.0742
2	SK	5.1012	.0438	5.0738	.0535	4.7736	.0718	4.6944	.0817
3	UR	6.0525	.0247	6.0482	.0251	6.0222	.0292	6.0122	.0344
4	KHL	6.6640	.0604	6.6645	.0603	6.6649	.0601	6.6653	.0600
5	NNG	7.0391	.0248	7.0388	.0253	6.9966	.0264	6.8548	.0360
6	BB	7.4395	.0623	7.4134	.0642	7.4217	.0677	7.4653	.0655
7	LKB	8.8514	.1136	8.7020	.1172	8.6949	.1262	8.8259	.1295
8	SNR	8.9647	.0594	8.9648	.0594	8.9648	.0594	8.9648	.0594
9	SRD	9.4461	.0388	9.4460	.0379	9.3839	.0416	9.3631	.0284
10	UD1	9.5096	.0145	9.5086	.0145	9.5105	.0153	9.5379	.0208
11	MM3	9.7375	.1257	9.5824	.1433	9.5603	.1600	9.5619	.1619
12	CLB	10.0456	.0772	10.0424	.0766	10.0410	.0743	10.1077	.0681
13	TN	12.6434	.2338	12.6434	.2338	12.6433	.2338	12.9433	.2338
14	NB	12.9518	.0986	12.9483	.0987	12.9461	.0988	12.9461	.0988
		Voltage modes							
15	TTK	26.4137	.6072	32.2527	.2598	28.0233	.0791	28.0053	.0716
16	CP	70.1914	.5289	70.1703	.5288	70.1752	.5290	70.1698	.5290
17	KK	-		-		48.9227	.5307	488.2136	.3622

case 1 : the original simplified system

case 2 : with damping control at TTK SVC

case 3 : with additional KK SVC

case 4 : with damping control at TTK and KK SVCs application however reduces the damping of some other modes but without making these unacceptable.The damping ratio of SVC mode at TTK is seen to grossly reduce in Table 6.1. In fact this is to be expected as a result of the application of damping control on the SVC. Because in order to generate a damping component of torque the voltage at SVC bus must change significantly. This observation is to be by comparing damping factor of TTK from case 1 (0.6072) to case 2 (0.2598). Application of a new SVC at KK reduces this ratio further (0.079). Addition of a damping circuit changes the damping ratio of the SVC at KK from 0.5307 to 0.3622.

6.2 Discussions

Addition of damping to a power system is best provided by the addition of power system stabilizers on generators. In the event that the generators are old and have slow acting excitation systems, it may be more economical to replace the excitation system in preference to adding new subsystems such as a SVC.

SVC applications in a power system must be economically justified. Such justification occurs when voltage control and enhancement of transmission capacity are needed.

The objective of this thesis should therefore not be misunderstood to justify the use of stabilizers and/or addition of new SVCs for the purpose.

The point is that should there be SVCs already in the system and either the generators lie outside the administrative control of the utility which faces lightly damped inertial or inter-area modes of oscillations or that the PSSs on generators are already committed to rectify other problems, how should one design or modify the controls of the existing SVCs to rectify the problem.

Furthermore, when planning studies are undertaken to add SVCs in the system, what will be the size and location of a new SVC strictly from the point of steady-state stability. The outcome of this study will augment the decision process.

Having specified the importance of the study presented in this thesis the use of SMIB system also needs clarification. SMIB is not intended to say that this is the system. Nevertheless it provides a manageable system to obtain a closed form solution. Moreover with a good engineering judgement it is not difficult to employ the results of this simple system to many practical situations.

In a multi-machine system there can not be a definitive procedure. And, each system needs a special solution. Application of the techniques developed in this thesis to the EGAT system does two things.

1 It solves the problem arising from the Region 2 of the system and

2 It explains the types of procedure that should be adopted for a new multi-machine system.

For the EGAT system, IEEE Type 1 exciter is chosen primarily because it was suspected that these are in use in EGAT.

Variation of SVC control and damping parameters with load shows the possibility of using an adaptive/intelligent controller. It may however be unnecessary. A two-valued controller may indeed be sufficient. In the studies presented in this thesis it has been shown that for all practical purposes good performance is secured by fixed parameter controllers.

There has been a concern in power system utilities, whether eigenvalue analysis can be used to describe the behaviour of a complex and non-linear system, especially when it is developed from a small-signal, linear and time-invariant model. Eigenvalue analysis is an application of linear control theory and theoretically it can be used for the design of controllers in the system. However the effectiveness of the design has to be verified by other situations such as transient stability for which time domain simulations on computers or on physical component simulators may be used.

6.3 Conclusions

1. By conducting a systematic study it has been demonstrated that the addition of a supplementary control to the SVC controllers can add damping to a system.
2. A new mathematical model for an SMIB system incorporating a SVC on an intermediate bus of the long line in SMIB has been

developed and tested.

3. Eigenvalue analysis is shown to be a powerful tool for the identification of lightly damped system modes as well as for the design of SVC controllers.
4. For a complex, interconnected multi-machine system a procedure is developed to design the SVC controllers and stabilizers. The effectiveness of the procedure has been demonstrated on the EGAT system.
5. Voltage Participation Factors have been shown to be a valuable design tool for the effective location of SVCs in a system primarily to selectively damp certain modes of oscillations.
6. Line current has been found to be an effective damping signal. However before selecting a line current it is important to conduct a frequency response or observability test on it to ensure that information of the modes to be damped is contained in it.
7. The models and procedure developed in this thesis should be valuable for overall system design where steady-state stability enhancement in undertaken with the help of PSSs and SVCs.

APPENDIX A Optimal proportional controller

The characteristic equation from Eqn.(3.18) is

$$(B_o+S_c)(1+sT_2)(1+sT_y^*)+K_pV_o(1+sT_m) = 0$$

Let $a = B_o+S_c$, $b = K_pV_o$

Thus
$$aT_2T_y^*s^2 + (a(T_2+T_y^*)+bT_1)s + (s+b) = 0$$

$$s^2 + \frac{(a(T_2+T_y^*)+bT_1)s}{aT_2T_y^*} + \frac{(a+b)}{aT_2T_y^*} = 0$$

Hence
$$\omega_n^2 = \frac{a+b}{aT_2T_y^*}$$

$$\zeta = \frac{1}{2}\,\frac{a(T_2+T_y^*)+bT_1}{aT_2T_y^*} \cdot \left[\frac{aT_2T_y^*}{a+b}\right]^{1/2}$$

For a relatively good damping, $\zeta = 1/\sqrt{2}$

thus
$$\frac{1}{2} = \frac{[a(T_2+T_y^*)+bT_1]^2}{4aT_2T_y^*\,(a+b)}$$

or
$$2a(a+b)T_2T_y^* = [a(T_2+T_y^*)+bT_1]^2$$

Hence
$$T_1 = \frac{[2a(a+b)T_2T_y^*]^{1/2}-a(T_2+T_y^*)}{b}$$

$$T_1 = \frac{[2(B_o+S_c)(B_o+S_c+K_pV_o)T_2T_y^*]^{1/2}-(B_o+S_c)(T_2+T_y^*)}{K_pV_o}$$

APPENDIX B Optimal integral controller

The signal flow graph of the control block in Fig. 3.8 is shown below.

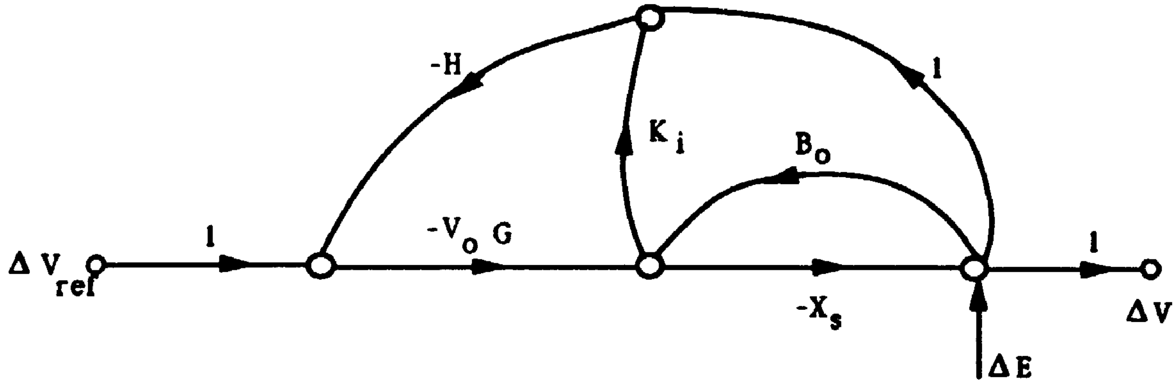

Using Mason's theorem, the output transfer function is of the form

$$\Delta V = \frac{\Delta E + V_o X_s\, G\, \Delta V_{ref}}{1+B_o X_s + V_o(X_s - K_i)GH}$$

and the characteristic equation is

$$1+B_o X_s + V(X_s - K_i)GH = 0$$

let $a = 1+B_o X_s$,

thus $$a+V_o(X_s-K_i)\left(\frac{1}{sT_i}\cdot\frac{1}{1+sT_m}\cdot\frac{1}{1+sT_y}\right) = 0$$

$$aT_iT_y^* s^2 + aT_i s + V_o(X_s-K_i) = 0$$

or $$s^2 + \frac{s}{aT_y^*} + \frac{V_o(X_s-K_i)}{aT_iT_y^*} = 0$$

hence $$\omega_n^2 = \frac{V_o(X_s-K_i)}{aT_iT_y^*}$$

$$\zeta = \frac{1}{2}\cdot\frac{1}{aT_y^*}\left[\frac{aT_iT_y^*}{V_o(X_s-K_i)}\right]^{1/2}$$

for $\zeta = 1/\sqrt{2}$

Hence $$T_i = 2aV_o(X_s-K_i)T_y^*$$

$$= 2(1+B_o X_s)V_o(X_s-K_i)T_y^*$$

APPENDIX C Optimal PI controller

By changing the transfer function of the I-controller, the characteristic equation is

$$1+X_sB_o + V_o(X_s-K_i)GH = 0 \ .$$

Let $a = 1+X_sB_o$ and $b = V_o(X_s-K_i)$ then

$$a + b\,\frac{K_p(1+sT_i)}{sT_i(1+sT_y)}\,\frac{1}{1+sT_m} = 0.$$

Choose $T_i = T_y$ to simplify the derivation, then the above equation becomes

$$a + b\,\frac{K_p}{sT_y(1+sT_m)} = 0.$$

Thus

$$aT_yT_ms^2 + aT_ys + bK_p = 0$$

$$s^2 + \frac{1}{T_m}\,s + \frac{bK_p}{aT_yT_m} = 0$$

Hence

$$\omega_n^2 = \frac{bK_p}{aT_yT_m}$$

$$\zeta = \frac{1}{2}\cdot\frac{1}{T_m}\cdot\left[\frac{aT_yT_m}{bK_p}\right]^{1/2}$$

For $\zeta = 1/\sqrt{2}$,

$$2T_mbK_p = aT_y$$

$$K_p = \frac{aT_y}{2bT_m}$$

$$= \frac{1}{2}\cdot\frac{(1+X_sB_o)}{V_o(X_s-K_i)}\cdot\frac{T_y}{T_m}$$

or with $S_c=1/X_s$

$$K_p = \frac{1}{2}\cdot\frac{(S_c+B_o)}{V_o(1-K_iS_c)}\cdot\frac{T_y}{T_m}$$

APPENDIX D BUS AND LINE DATA OF THE EGAT SYSTEM

BUS DATA

Bus	Name	Type	Volt	Ang	P_L	Q_L	P_G	Q_G	Q_{min}	Q_{max}	CMvar
1	SB+BPK	2	1.000	0.0	1005.2	622.1	2424.7	1167.7	-	-	-
2	BN	0	0.973	-	414.2	310.4	-	-	-	-	-
3	BK	0	0.976	-	537.0	214.2	-	-	-	-	-
4	LPR	0	0.971	-	334.9	183.8	-	-	-	-	94.8
5	NCO	0	0.988	-	0.0	0.0	-	-	-	-	-
6	NB	1	0.970	-	237.6	216.2	160.0	-	-200.0	200.0	82.4
7	RS	0	0.975	-	298.0	161.0	-	-	-	-	-
8	BP2	0	1.003	-	182.0	64.9	-	-	-	-	-
9	SNR	1	1.038	-	-	-	400.0	-	-400.0	400.0	-
10	RB2	0	1.005	-	96.1	27.5	-	-	-	-	-
11	PKK	0	1.024	-	12.4	23.0	-	-	-	-	-
12	CP	1	1.050	-	24.1	14.4	0.0	-	0.0	50.0	-
13	Sgen	0	1.050	-	70.6	-25.0	-	-	-	-	-
14	AT1	0	0.989	-	155.0	68.0	-	-	-	-	-
15	TTK	1	1.050	-	0.0	0.0	0.0	-	-100.0	300.0	-
16	NS	0	1.042	-	65.2	28.6	-	-	-	-	-
17	AT2	0	0.991	-	95.3	52.6	-	-	-	-	-
18	BB	1	1.070	-	58.2	36.5	350.0	-	-300.0	300.0	-
19	PL2	0	1.059	-	-	-	-	-	-	-	-
20	MM3	1	1.050	-	361.7	228.2	825.0	-	-1000.0	1000.0	-
21	SK	1	1.086	-	2.2	2.8	160.0	-	-200.0	200.0	-
22	LKB	1	1.046	-	53.6	26.3	100.0	-	-100.0	100.0	-
23	PE	0	1.035	-	16.6	9.7	-	-	-	-	6.3
24	LS	0	1.043	-	7.2	5.7	-	-	-	-	-
25	KK	0	1.033	-	104.7	2.9	-	-	-	-	-
26	CLB	1	1.063	-	14.8	11.8	40.0	-	-80.0	80.0	-
27	NR1	1	1.004	-	176.7	11.4	12.0	-	-80.0	80.0	70.0
28	UR	1	1.040	-	0.6	1.5	16.0	-	-100.0	100.0	-
29	UD1	1	1.002	-	141.8	41.1	12.0	-	-100.0	100.0	40.0
30	KL	0	1.000	-	17.5	12.5	-	-	-	-	-
31	VT	0	1.018	-	27.3	9.2	-	-	-	-	-
32	NNG	1	1.040	-	-	-	60.0	-	-80.0	80.0	-
33	YT	0	0.991	-	61.1	31.4	-	-	-	-	28.5
34	UB	0	1.031	-	44.7	25.9	-	-	-	-	35.3
35	SRD	1	1.063	-	3.4	2.0	36.0	-	-100.0	100.0	-
36	SR2	0	0.980	-	130.7	64.3	-	-	-	-	20.0
37	TN	1	1.040	-	-	-	40.0	-	-100	100	-
38	KHL	1	1.050	-	-	-	240.0	-	-400.0	400.0	-

LINE DATA

FROM	TO	R %	X %	CLINE(KVA)
1	2	0.11	0.88	6890.00
1	3	0.16	1.20	24000.00
1	5	0.05	0.56	33440.00
2	6	0.18	1.47	2700.00
2	8	0.82	6.11	12450.00
2	17	0.98	7.27	15097.00
3	4	0.05	0.38	3120.00
3	5	0.07	0.71	10600.00
4	6	0.07	0.51	1050.00
4	7	0.17	1.29	2659.00
5	7	0.10	1.07	15900.00
5	15	1.91	17.04	68800.00
6	7	0.19	1.41	2920.00
7	8	0.65	5.63	11960.00
7	14	0.37	2.89	22563.00
7	17	0.82	6.81	14644.70
8	9	0.26	2.05	66460.00
8	10	0.20	1.52	12500.00
8	37	8.84	26.30	5682.00
9	37	3.10	9.24	1994.00
9	38	0.41	3.02	24800.00
10	11	0.96	7.16	59020.00
11	12	8.77	24.91	19000.00
12	13	8.59	21.50	18580.00
14	15	0.81	5.47	42400.00
15	16	0.25	1.78	14440.00
15	20	1.91	17.04	68800.00
16	17	0.49	3.81	30072.00
16	18	0.72	5.55	97600.00
16	19	1.07	5.39	39640.00
17	36	0.41	3.03	24800.00
19	20	0.80	5.94	48500.00
19	21	0.90	4.54	33412.00
19	22	6.20	19.80	2550.00
19	24	0.60	4.50	36800.00
22	23	14.19	42.50	5260.00
23	24	5.40	16.12	2040.00
24	25	0.91	6.82	55750.00
25	26	13.78	41.10	5200.00
25	27	9.23	27.12	20700.00
25	28	14.51	17.81	1900.00
25	29	5.68	16.60	8700.00
25	30	4.15	11.82	6200.00
27	36	6.51	19.28	9400.00
28	29	31.99	39.09	4200.00
29	31	2.67	7.46	8460.00
30	33	4.96	14.17	8845.00
31	32	2.19	7.26	8600.00
33	34	25.40	30.88	3362.00
34	35	7.72	8.77	5300.00

APPENDIX E MACHINE PARAMETERS

No	x_l%	x_d%	x_q%	x_d'%	x_d''%	x_q''%	T_{do}'	T_{do}''	T_{qo}''	MVA	H	D
6	5.0	145.79	87.47	14.32	10.37	0.0	5.5	0.01	0.01	270	2.05	0.1
9	5.0	113.0	74.0	29.0	12.66	15.13	6.5	0.02	0.01	500	3.38	0.1
18	5.0	85.68	60.77	26.81	18.03	0.0	7.5	0.03	0.03	400	3.839	0.1
20	5.0	152.08	91.2	26.0	15.0	0.0	5.4	0.035	0.01	900	2.0	0.1
21	5.0	101.0	60.6	27.8	22.2	0.0	9.3	0.03	0.01	200	7.49	0.1
22	5.0	210.0	126.0	19.0	12.2	0.0	3.1	0.032	0.01	100	4.98	0.1
26	5.0	118.0	76.9	29.7	21.7	0.0	6.5	0.02	0.01	25	3.64	0.1
27	5.0	198.4	119.0	22.9	16.9	0.0	5.5	0.02	0.01	20	7.97	0.1
28	5.0	78.69	47.2	25.1	19.7	0.0	5.0	0.02	0.01	24	8.45	0.1
29	5.0	23.5	21.15	20.1	14.8	0.0	4.5	0.02	0.01	20	7.96	0.1
32	5.0	65.0	39.0	26.0	14.0	0.0	5.0	0.02	0.01	100	4.5	0.1
35	5.0	91.16	54.7	37.3	26.5	0.0	5.5	0.02	0.01	42	2.45	0.1
37	5.0	107.96	70.45	27.2	19.9	0.0	3.0	0.02	0.01	45	3.64	0.1
38	5.0	107.9	73.9	32.5	21.4	0.0	6.5	0.02	0.01	330	3.5	0.1

Note : Machine parameters are % per unit values on its own rating.

REFERENCES

[1] Reactive Power : Basic, Problems and Resolutions, IEEE Tutorial Course Text, 87EH0262-6-PWR, 1987.

[2] CIGRÉ Working Group 31-01, "Static Shunt Devices for Reactive Power Control", CIGRE 31-08,1974.

[3] R.L. Hauth, S.A. Miske and F. Nozari, "The Role and Benefits of Static Var Systems in High Voltage Power System Applications", IEEE Trans. PAS, Vol. PAS-101, pp. 3761-3770, October 1982.

[4] R.T. Byerly, D.T. Poznaniak and E.R. Taylor, "Static Reactive Compensation for Power Transmission Systems", IEEE Trans. PAS, Vol. PAS-101, pp. 3997-4005, October 1982.

[5] R.L. Hauth and R. Moran, "Introduction to Static Var Systems for Voltage and Var Control", IEEE Tutorial Course Text 78EH135-4-PWR, IEEE PES Summer Meeting, Los Angeles, California, July 1978.

[6] R.L. Hauth and R. Moran, "The Performance of Thyristor-Controlled Static Var Systems in HVAC Applications", IEEE Tutorial Text 78EH135-4-PWR, IEEE PES 1978 Summer Meeting, Los Angeles, California, July 1978.

[7] F.P. DeMello, B.K. Johnson, L.N. Hannett, D. Birfet and J. Toulemonde, "Thyristor-Controlled Reactors Analysis of Fundamental Frequency and Harmonic Effects", IEEE PES 1978 Winter Power Meeting, New York, January 29 - February 3, 1978.

[8] L. Gyugyi, R.A. Otto and T.H. Putman, "Principles and Applications of Static, Thyristor-Controlled Shunt Compensators", IEEE Trans. PAS, Vol. PAS-97, pp. 1935-1945, September/October 1978.

[9] CIGRÉ Working Group 31-01, "Model of Static Shunt Var Systems (SVS) for System Analysis", ELECTRA, Vol. 51, March 1977.

[10] CIGRE Working Group 38-01, Task Force No. 2, "Report on Static Var Compensator", CIGRE, Paris, 1986.

[11] H. Frank and T. Petterson, "Thyristor-Switched Shunt Capacitors and their Modelling for Transmission Applications", IEEE 1978 PES Winter Meeting, New York, January 29 - February 3, 1978.

[12] T.J.E. Miller, Editor, REACTIVE POWER CONTROL IN ELECTRIC POWER SYSTEMS, John Wiley & Sons, New York, 1982.

[13] R.M. Mathur, Editor, STATIC COMPENSATORS FOR REACTIVE POWER CONTROL, Canadian Electrical Association, Montreal, 1984.

[14] Å. Ölwegård, K. Walve, G. Wåglund, H. Frank and S. Torseng, "Improvement of Transmission Capacity by Thyristor Controlled Reactive Power", IEEE Trans. PAS, Vol. PAS-100, No. 8, pp. 3930-3939, August 1981.

[15] W.G. Heffron and R.A. Phillips, "Effect of Modern Amplidyne Voltage Regulators on Underexcited Operation of Large Turbine Generators", AIEE Trans. PAS, pp. 692-697, August 1952.

[16] F.P. DeMello, C. Concordia, "Concepts of Synchronous Machine Stability as Effected by Excitation Control", IEEE Trans. PAS, Vol. PAS-88, pp. 316-329, April 1969.

[17] P.M. Anderson and A.A. Fouad, POWER SYSTEM CONTROL AND STABILITY, Iowa State University Press, Ames, Iowa, 1977.

[18] Y.N. Yu, ELECTRIC POWER SYSTEM DYNAMICS, Academic Press, New York, 1983.

[19] M.K. El-Sherbiny and D.M. Mehta, "Dynamic System Stability Part I; Investigation of the Effect of Different Loading and Excitation Systems", IEEE Trans. PAS, Vol. PAS-92, No. 5, pp. 1538-1546, September/October 1973.

[20] IEEE Working Group on Computer Modelling of Excitation System, "Excitation System Models for Power System Stability Studies", IEEE Trans. PAS, Vol. PAS-100, No. 2, pp. 494-509, February 1981.

[21] G. Romegialli and H. Beer. "Problems and Concepts of Static Compensator Control", Proc. IEE, Pt. C, Vol. 128, No. 6, pp. 382-388, November 1981.

[22] H.E. Schweikardt, G. Romegialli and K. Reichert, "Closed Loop Control of Static Var Sources (SVS) on EHV Transmission Lines", IEEE Trans. PAS, Vol. PAS-97, No. 4, July/August 1978.

[23] K. Engverg and S. Ivner, "Static Var Systems for Voltage Control During Steady-State and Transient Conditions", International Symposium on Controlled Reactive Compensation, IREQ, Varennes, Quebec, pp. 252-268, September 1979.

[24] C.F. Chen and L.S. Shieh, "A Novel Approach to Linear Model Simplification", Int. J. Control, Vol. 8, No. 6, pp. 561-570, 1968.

[25] B. Ooi and M.H. Banakar, "Co-ordination of Static Var Compensators with Long Distance Radial Transmission System for Damping Improvement", IEEE Trans. PAS, Vol. PAS-103, No. 2, pp. 256-274, February 1984.

[26] A.E. Hammad and M. El-Sadek, "Application of a Thyristor-Controlled Var Compensator for Damping Subsynchronous Oscillations in Power Systems", IEEE Trans. PAS, Vol. PAS-103, No. 1, pp. 198-212, January 1984.

[27] S.C. Kapoor, "Dynamic Stability of Long Transmission Systems with Static Compensators and Synchronous Machines", IEEE Trans. PAS, Vol. PAS-98, No. 1, pp. 124-134, January/February 1979.

[28] S.C. Kapoor, "Dynamic Stability of Static Compensator-Synchronous Generator Combination", IEEE Trans. PAS, Vol. PAS-100, pp. 1694-1702, April 1981.

[29] A. Chandra, O.P. Malik, G.S. Hope, "A Self-tuning Controller for the Control of Multi-machine Power Systems", IEEE Trans. PS, Vol. 3, No. 3, pp. 1065-1071, August 1988.

[30] P.K. Dash, A.M. Sharaf and E.F. Hill, "An Adaptive Stabilizer for Thyristor Controlled Static Var Compensators for Power Systems", IEEE Trans. PS, Vol. 4, No. 2, pp. 403-410, May 1989.

[31] P.K. Dash, P.C. Panda, A.M. Sharaf and E.F. Hill, "Adaptive Controller for Static Reactive-power Compensators in Power Systems", Proc. IEE, Vol. 134, Pt. C, No. 3, pp. 256-264, May 1987.

[32] J.F. Hauer, "Robust Damping Controls for Large Power Systems", IEEE Control System Magazine, pp 12-18, January 1989.

[33] J.R. Smith, D.A. Pierre, I. Sadighi, M. Nehrir, and J.F. Hauer, "A Supplementary Adaptive Var Unit Controller for Power System Damping", IEEE PES 1989 Winter Meeting, New York, January 29 - February 3, 1989.

[34] K. Bollinger, A. Laha, R. Hamilton and T. Harras, "Power System Stabilizer Design Using Root Locus Methods", IEEE Trans. PAS, Vol. PAS-94, No. 5, pp. 1484-1488, September/October 1975.

[35] A.E. Hammad, "Analysis of Power System Stability Enhancement by Static Var Compensators", IEEE Trans. PAS,Vol. PWRS-1,No. 4, pp. 222-227, November 1986.

[36] D.Q. Mayne and P. Murdoch, "Modal Control of Linear Time Invariant System", Int. J. Control, Vol. 11, No. 2, pp. 223-227, 1970.

[37] Y.Y. Hsu, C.S. Liu, C.J. Lin and C.T. Huang, "Application of Power System Stabilizers and Static Var Compensators on a Longitudinal Power System", IEEE Trans. PS, Vol. 3, No. 4, pp. 1464-1470,

November 1988.

[38] C.L. Chen and Y.Y. Hsu, "Coordinated Synthesis of Multi-machine Power System Stabilizer Using an Efficient Decentralized Modal Control (DMC) Algorithm", IEEE Trans. PS, Vol. PWRS-2, No. 3, pp. 543-551, August 1987.

[39] I.J. Pérez-Arriaga, G.C. Verghese and F.C Schweppe, "Selective Modal Analysis ; Part I : Heuristic Introduction; Part II : The Dynamic Stability Problem", IEEE Trans. PAS, Vol. PAS-101, No. 9, pp. 3117-3134, September 1982.

[40] M. O´ Brien and G. Ledwick, "Placement of Static Compensators for Stability Improvement", Proc. IEE, Pt. C, Vol. 132, No. 1, pp. 30-35, January 1985.

[41] H.H. Happ and K.A. Wirgau, "Static and Dynamic Var Compensator in System Planning", IEEE Trans. PAS, Vol. PAS-97, No. 5, pp. 1564-1578, September/October 1978.

[42] R. Hauth, T. Humann and R.J. Newell, "Application of a Static Var System to Regulate System Voltage in Western Nebraska", IEEE Trans. PAS, Vol. PAS-97, No. 7, pp . 1955-1964, September/October 1978.

[43] R. Elsliger, Y. Hotte and C. Roy, "Optimization of Hydro-Quebec's 735 kV Dynamic-Shunt-Compensated System Using Static Compensators on a Large Scale", IEEE PES 1978 Winter Meeting, New York, January 29 - February 3, 1978.

[44] T. Sawa, Y. Shirai,T. Michigami, Y. Sakanaka and Y. Uemura, "A Field Test of Power Swing Damping by Static Var Compensator", IEEE PES 1989 Winter Meeting, New York, January 29 - February 3, 1989.

[45] A.J.P. Ramos, H. Tyll, "Dynamic Performance of a Radial Weak Power System with Multiple Static var Compensators", IEEE PES 1989 Winter Meeting, New York, January 29 - February 3, 1989.

[46] S. Irokawa, T. Horiuchi, P.K. Muttik and J.C. Smith, "Transmission Line Loss Minimization by SVC", Proc. IEEE/CSEE Joint Conference, Peking, pp. 761-766, October 17-12, 1987.

[47] D.Y. Wong, G.J. Rogers, B. Porretta and P. Kundur, "Eigenvalue Analysis of Very Large Power Systems", IEEE Trans. PS, Vol. PWRS-3, pp. 472-380, May 1988.

[48] A.E. Hammad, "A Fast Stability Programs for Power Systems with Multi-terminal HVDC and Static Var Compensator", IEEE PICA-79, pp. 290-297, May 1979.

[49] C.E.J. Bowler, D.N. Ewart and C. Concordia, "Self-excited Torsional Frequency Oscillations With Series Capacitors", IEEE Trans. PAS, Vol. PAS-92, pp. 1688-1695, September/October 1973.

[50] J.W. Ballance and S. Goldberg, "Subsynchronous Resonance in Series Compensated Transmission Lines", IEEE Trans. PAS, Vol. PAS-92, pp. 1649-1658, September/October 1973.

[51] S. Hungsasutra, R.M. Mathur, "Application and Supplementary Control of Static Var Compensator for long lines", CIGRÉ Symposium, Bangkok, Thailand, November 20-22, 1989.

[52] S.M. Moorty, "Generalized design of damping controls in Power systems", M.E.Sc. Thesis, The University of Western Ontario, 1990, Canada.

[53] IEEE Committee Report : " Proposed Terms & Definitions for Power System Stability", IEEE Trans., Vol. PAS-101, No.7, pp 1894-1898, July 1982.